Theses and Dissertations

12-2015

Reservoir Characterization and Depositional System of the Atokan Grant Sand, Fort Worth Basin, Texas

Victoria Wood
University of Arkansas, Fayetteville

Reservoir Characterization and Depositional System of the Atokan Grant
Sand, Fort Worth Basin, Texas

A thesis submitted in partial fulfillment
of the requirements for the degree of
Master of Science in Geology

by

Victoria Wood
University of Arkansas
Bachelor of Science in Geology, 2013

December 2015
University of Arkansas

This thesis is approved for recommendation to the Graduate Council.

_____

Dr. Christopher L. Liner
Thesis Advisor

_____

Dr. Doy L. Zachry
Thesis Committee

_____

Dr. Walter Manger
Thesis Committee

ABSTRACT

The Atokan Grant Sands are a tight gas sand play that would add new reserves to the Fort Worth Basin. The Fort Worth Basin is located in north-central Texas just west of Dallas, Texas. Within the basin, the study area consists of Denton, Wise, Tarrant, and Parker Counties in Texas. The basin is bounded to the north by the Red River Arch, to the west by the Bend Arch, to the south by the Llano uplift, to the east by the Ouachita structural front, and to the northeast by the Muenster Arch. The Grant Sands are approximately 1,500 ft stratigraphically above their source, the Barnett Shale, and were discovered and mapped from early Barnett vertical drilling. This play evolved from a vertical to a horizontal drilling program with Grant wells being drilled alongside Barnett wells. The purpose of this study is to improve the geologic understanding for enhanced exploration potential.

There is disagreement in the previous studies as to the depositional setting and source areas of the Atoka section of the Fort Worth Basin. This study analyzes core data and regional subsurface mapping to determine an interpretation of the depositional setting of the Grant Sands. A reservoir characterization with a conceptual model for depositional setting will contribute to the current geologic understanding of the Grant Sand Formation to enhance exploration potential.

ACKNOWLEDGMENTS

TABLE OF CONTENTS

INTRODUCTION

The Fort Worth Basin is located in north-central Texas just west of Dallas, Texas (Figure 1). The basin is bounded to the north by the Red River Arch, to the west by the Bend Arch, to the south by the Llano uplift, to the east by the Ouachita structural front, and to the northeast by the Muenster Arch. The sedimentary sequence in the Fort Worth Basin includes up to 12,000 ft thicknesses of Cambro-Ordovician, Devonian, Mississippian, and Pennsylvanian strata (Turner, 1957). In the Fort Worth Basin the Pennsylvanian Atokan and Morrowan rocks range in thicknesses from approximately 200 ft to more than 6,000 ft. The Atoka Group, also termed the Boonsville Field, overlies the unconformity at the top of the Morrowan Marble Falls Limestone.

The Atokan Grant Sands are a tight gas sand play that would add new reserves to the Fort Worth Basin. The Grant gas-bearing Sands are approximately 1,500 ft stratigraphically above their hydrocarbon source rock, the Mississippian Barnett Shale (Figure 2). The Barnett Shale is a highly productive play and stands as the prototype for shale plays in North America. Early Barnett exploration lead to the discovery of the Grant Sands. This play has since evolved from a vertical to a horizontal drilling program with wells being drilled alongside Barnett wells. The sands are informally divided into "upper" and "lower" units with a shale unit between the two at depths from 4,000 to 6,000 ft in the study area. Both upper and lower sands have been horizontally drilled and are productive.
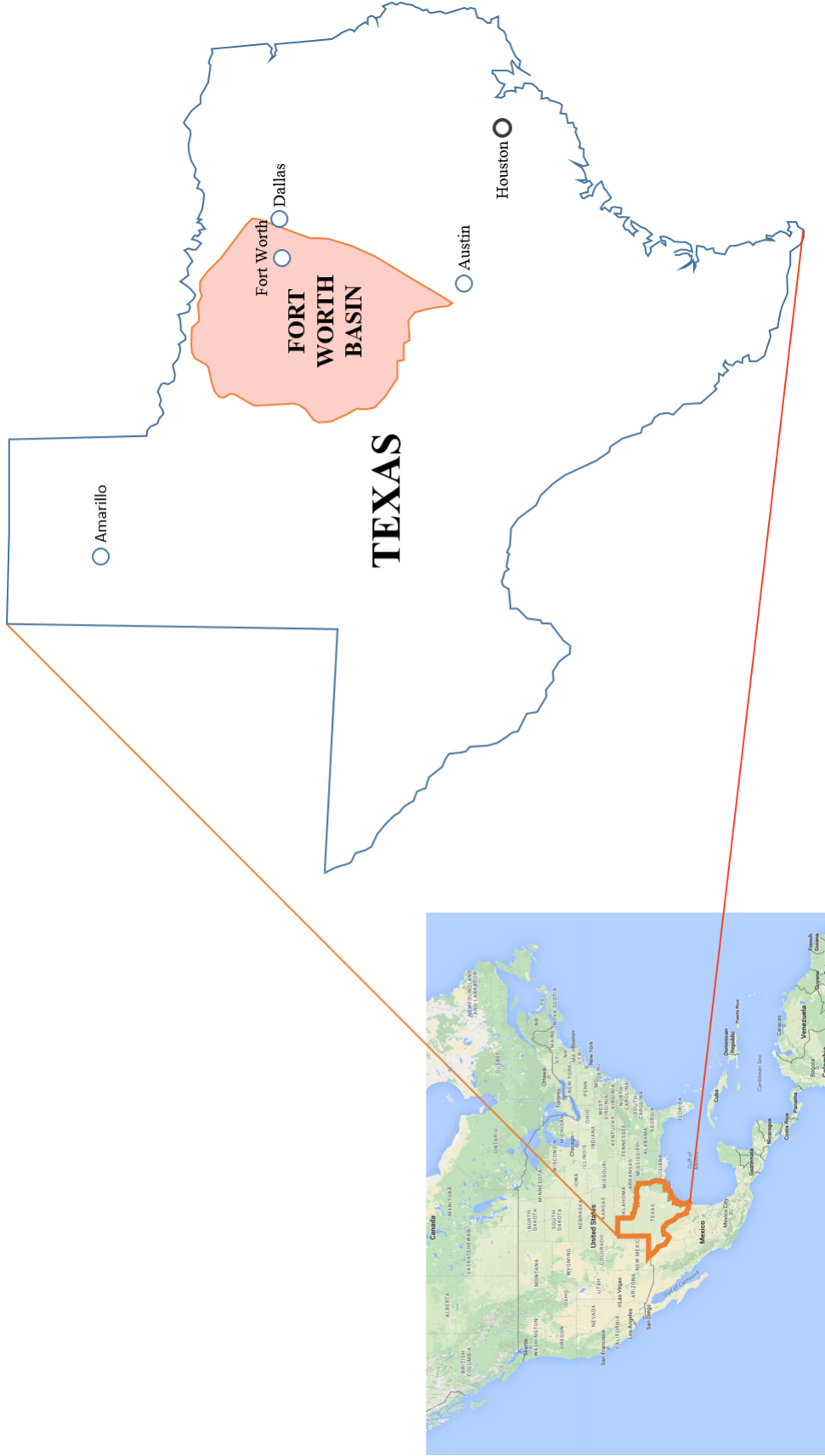
Figure 1. Fort Worth Basin location map. The Fort Worth Basin is located in north-central Texas, just west of Dallas, Texas. The basin is approximately 20,300 square miles in size at 200 miles long and ranging from 10-100+ miles wide.
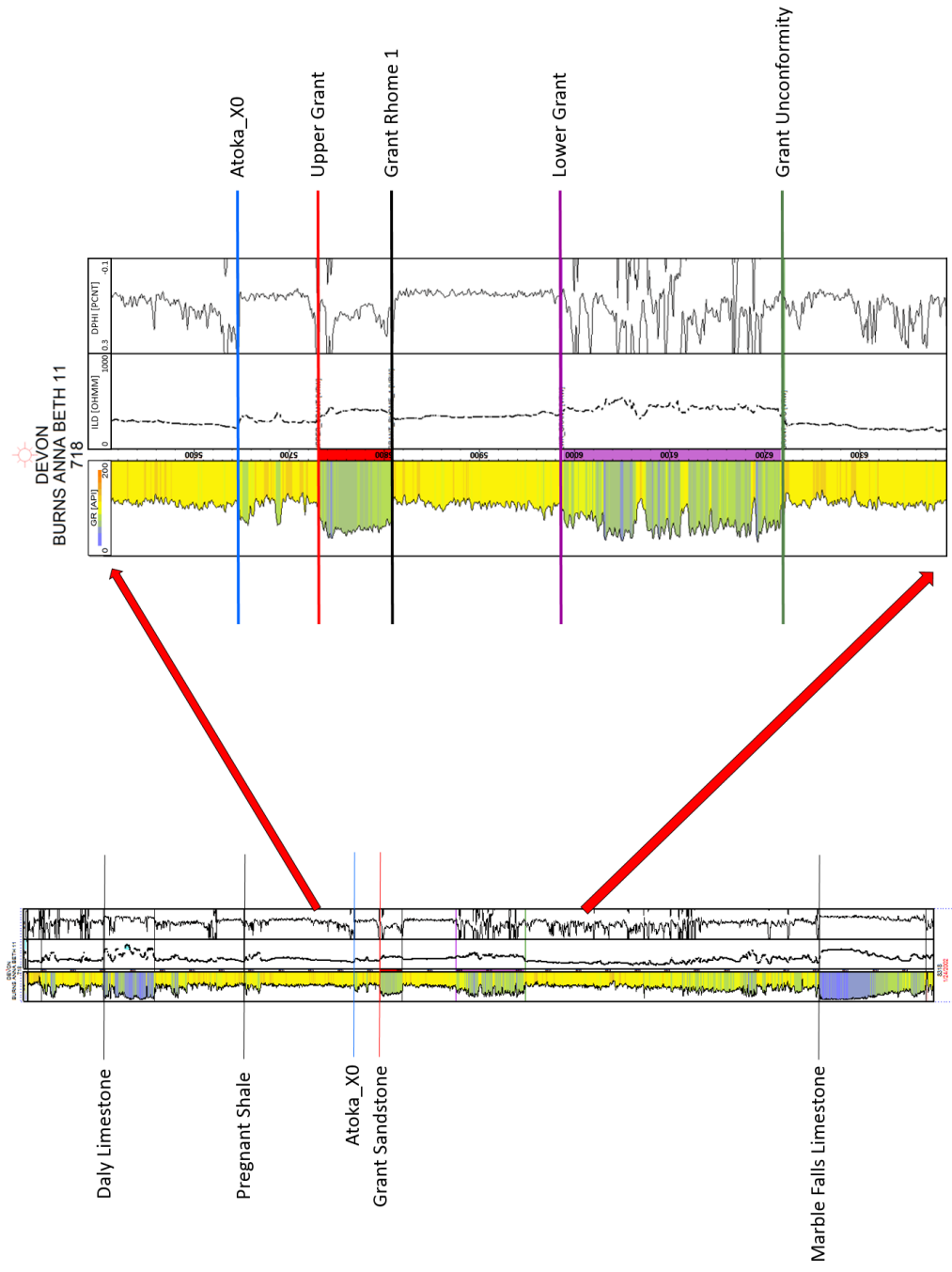
Figure 2. Type log for the Grant Sands with accompanying extended log to show the location of the Grant Sands in relation to the surrounding stratigraphy. The Grant Formation is just below a stratigraphic marker termed the Atoka_X0. The top of the Grant Formation is the top for the Upper Grant Sand. Grant Rhome 1 is the marker for the base of the Upper Grant Sand. A shale unit separates the Upper and Lower Sands of the Grant. The Lower Grant Sand top is marked here with a purple line. The Grant Unconformity is the base of the Lower Grant Sand, and the base of the Grant Formation.

STUDY AREA

The area investigated in this study is located in the north-east section of the Fort Worth Basin (Figure 3). Covering the south-west corner of Denton County, the southern portion of Wise County, the north-east corner of Parker County, and the north-west corner of Tarrant County in Texas. The total area of study is 1,006.4 sq. miles.
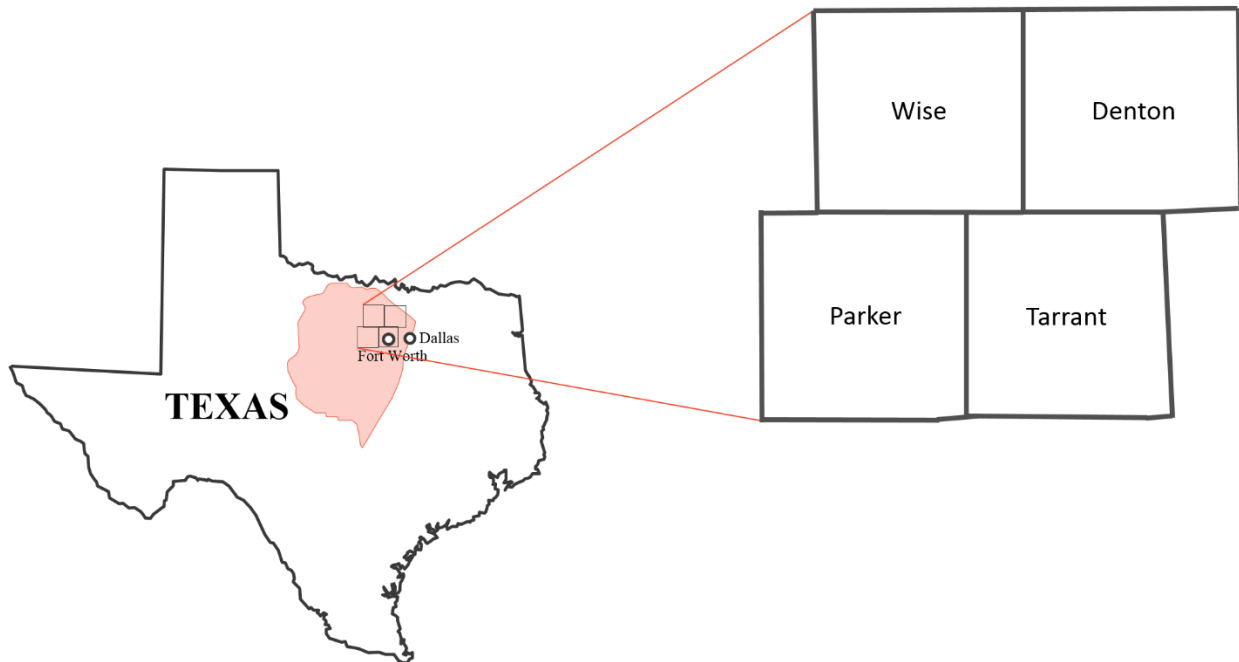
Figure 3. Location of the study area within the Fort Worth Basin. The study area is approximately 1,006 sq. miles with 6,545 wells spread throughout the southwest portion of Denton County, most of the southern part of Wise County, the northeast portion of Parker County, and the northwest corner of Tarrant County.

PURPOSE OF INVESTIGATION

The overall purpose of this study is to improve the geologic understanding for enhanced exploration potential of the Grant Sands. Log data are used to map the regional extents and production variations of the Grant Formation. A petrographic analysis is used to conclude ideal

the ideal completion fluids to avoid damaging the formation. The maps, production data, and completions recommendations of fluids are used collectively as a reservoir characterization for the Grant Formation. A sedimentological examination of core data is used to constrain the lithostratigraphy of the Grant. The lithostratigraphy in conjunction with mapping is used to determine the depositional setting of the Grant Sands. A reservoir characterization with a conceptual model for depositional setting will contribute to the current geologic understanding of the Grant Sand Formation to enhance exploration potential.

REGIONAL SETTING

The Fort Worth Basin is a foreland basin located in north-central Texas, just west of Dallas, TX (Figure 1). The basin is a late Paleozoic structural and depositional feature on the southern margin of North America formed in response to a collision of the North American and proto-South American continental masses (Lovick *et al.*, 1982). Previous to Pennsylvanian time the area that would become the Fort Worth Basin was located on the eastern side of the Texas Arch in the southern section of the Oklahoma Basin.

During the Paleozoic time the Fort Worth Basin area subsided and received Paleozoic carbonates and other marine sediments (Johnson *et al.*, 1989). During the Cambrian and Ordovician, 2,500 to 3,500 ft of sediments were deposited in the basin. Following the deposition, a broad upwarp of the Texas craton occurred in the Middle Ordovician due to the advancing Ouachita structural belt on a continental shelf, making the area a positive feature through the Early Mississippian. Additional subsidence occurred in the Late Mississippian allowing the

Barnett Shale to be deposited. The end of the Mississippian saw uplift to the west and north-northwest, allowing for limited erosion of these features. In the Early Pennsylvanian subsidence resumed along with the deposition of the Atokan and Morrowan series (Blanchard *et al.*, 1968). A change from a passive continental margin to an actively subsiding basin is recorded in the Paleozoic sedimentary sequence. The Fort Worth Basin was emergent during the Triassic and Jurassic times with reverse, gulfward tilting occurring later in the Jurassic. The Jurassic was followed by Cretaceous onlap and Cretaceous carbonates mark the last major geological event in the basin (Lovick *et al.*, 1982).

The basin is an asymmetric wedge-shaped regional feature that was downwarped during the early Pennsylvanian time by the transpression that produced the Ouachita structural belt (Johnson *et al.*, 1989). Striking north-south, the basin is approximately 20,300 square miles in size at 200 miles long and ranging from 10-100+ miles wide (Figure 4). The width ranges from a few miles in the southern end adjacent to the Llano uplift to approximately 100 miles in the north near the city of Fort Worth, TX. The deepest part of the basin is a deep axial trough adjacent to the Ouachita structural belt with a maximum known thickness of 12,000 ft of Paleozoic sedimentary rocks (Thompson, 1982; Johnson *et al.*, 1989). The clastic wedge that filled the trench overlies early to middle Paleozoic shelf carbonates that spread and thin westward onto the margin of the Bend Arch and are unconformably overlain by outcropping Cretaceous strata (Walper, 1982).

The Fort Worth Basin is bounded to the north by the Red River – Electra Arch, to the west by the Bend Arch, to the south by the Llano uplift, to the east by the Ouachita structural

front, and to the northeast by the Muenster Arch (Figure 4). These regional structural elements

were formed in relation to the Ouachita Orogeny.
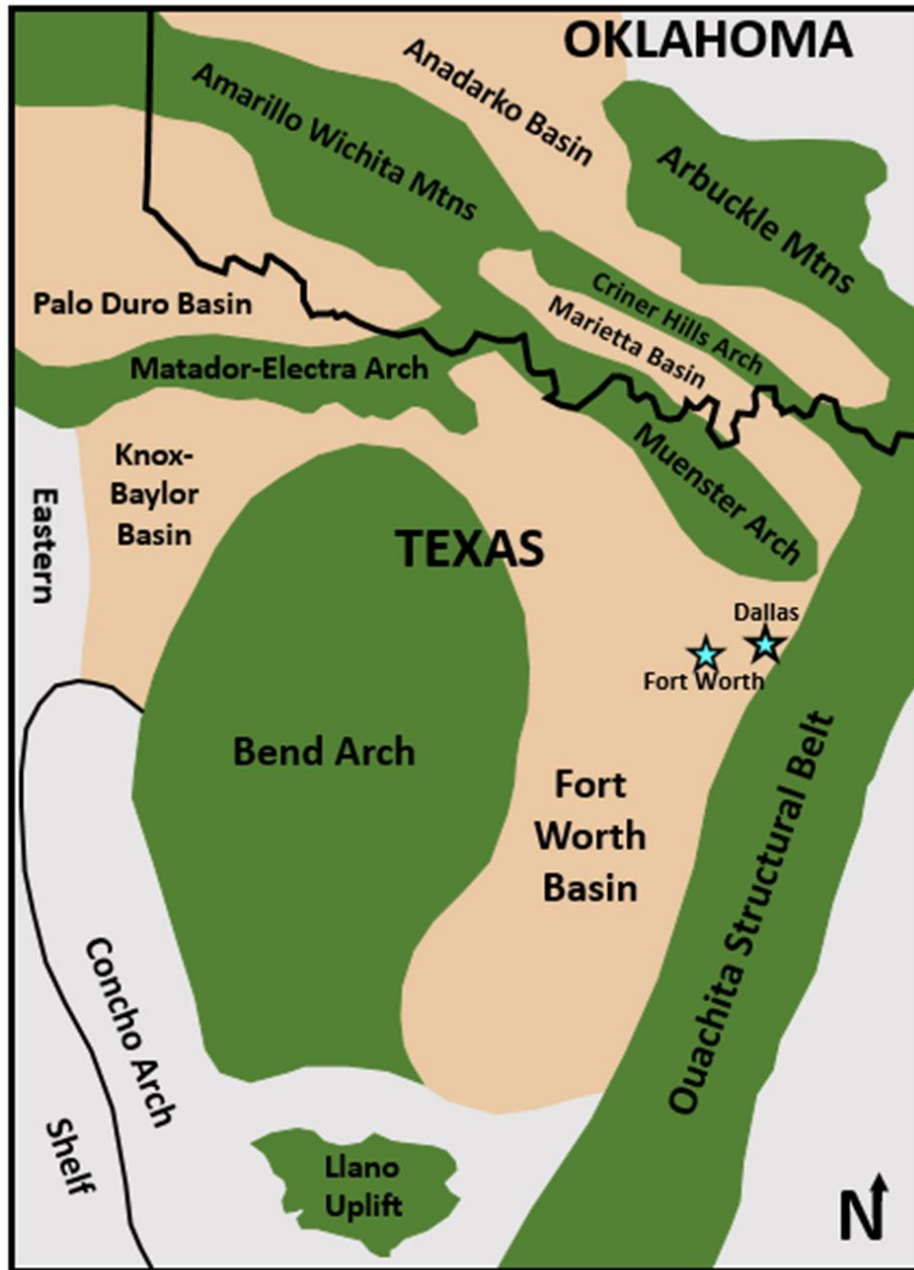
Figure 4. Geologic Setting for the Fort Worth Basin. The basin is a late Paleozoic structural and depositional feature on the southern margin of North America formed in response to a collision of the North American and proto-South American continental masses. The basin is bounded to the north by the Red River Arch, to the west by the Bend Arch, to the south by the Llano uplift, to the east by the Ouachita structural front, and to the northeast by the Muenster Arch.

THE OUACHITA STRUCTURAL BELT

The Ouachita structural front is the eastern boundary of the Fort Worth Basin and represents the southern margin of the North American craton. As the suture zone of the continental-continental collision of the North American and Afro-South American plates that formed Pangea, the structural belt is highly deformed with local metamorphism (Lahti and Huber, 1982). The development of the Ouachita Mountains can be divided into three stages: the first, geosynclinal, from Cambrian to Early Pennsylvanian; the second, orogenic, during the Pennsylvanian; and finally, post orogenic, from the Permian Period to present (Ng, 1982). In relation to the Fort Worth Basin, the Ouachita structural belt was not a significant source area for the basin until at least the middle Atokan Series. With the rise of the Ouachita Mountains, the main source area for the Fort Worth Basin became the Ouachita structural belt from the middle Atokan until the end of the Pennsylvanian time (Lahti and Huber, 1982).

MUENSTER ARCH

Northeast of the Fort Worth Basin is the Muenster Arch. Along the north boundary of the basin near the Muenster uplift, faults trending northwest and west have raised basement rocks approximately 5,000 ft on the northeast (Flawn *et al.*, 1961). The Muenster Arch branches off of the eastern termination of the Red River – Electra Arch and consists of northwest-southeast Precambrian igneous and metamorphic basement rocks (Johnson *et al.*, 1989; Ng, 1979). Although the Muenster Arch branches off of the Red River – Electra Arch, it is part of the Wichita Mountain system (Lahti and Huber, 1982; Ng, 1979). The Fort Worth Basin and

Muenster Arch form a set of paired basins and uplifts in the south Oklahoma-north Texas region. The paired basins and uplifts were formed by the compressional stresses caused by the oncoming continental plate convergence. According to Flawn *et al.* (1961) the uplift of the Muenster Arch occurred in late Mississippian to early Pennsylvanian time. During the uplift period, the arch shed coarse clastic sediments into surrounding basins until the late Pennsylvanian Series, at which time the arch was covered with sediments, effectively ending the period of being a source area (Lahti and Huber, 1982).

RED RIVER – ELECTRA ARCH

The Red River – Electra Arch is the north boundary of the Fort Worth Basin. It is part of the Wichita mountain system and composed of a series of discontinuous fault blocks striking west to northwest that are believed to be controlled by basement fractures reactivated during Ouachita deformation (Lahti and Huber, 1982; Johnson *et al.*, 1989). According to Lovick *et al.* (1982) the Atokan Bend conglomerates of the Fort Worth Basin were sourced from the Muenster and Red River – Electra Arch complex and transported to the basin by prograding, high constructive deltas.

BEND ARCH

The western boundary of the Fort Worth Basin is the Bend Arch. The arch is a flexure and north plunging structural high formed without any uplifting (Ng, 1982). In the subsurface the

arch is observed as an elongate ridge striking north-south. Noting the Fort Worth Basin

subsidence to the east, the Bend Arch represents the hingeline between the Fort Worth Basin and

the Concho Platform to the west. Stresses from the Ouachita structural belt formed the hingeline

in the late Mississippian and early Pennsylvanian Periods (Johnson *et al.*, 1989). In the early

Pennsylvanian Period the Bend arch was the western shelf of the Fort Worth Basin, but after the

filling of the basin in the late Pennsylvanian tilting occurred and it became the eastern shelf of

the Midland Basin (Lahti and Huber, 1982).

LLANO UPLIFT

At the south end of the Bend Arch is a structural dome known as the Llano Uplift that

bounds the southern section of the Fort Worth Basin. The uplift exposes Precambrian and

Paleozoic rocks at the surface (Ng, 1979). The area was uplifted and faulted into a series of

horsts and grabens during the early to middle Pennsylvanian time and acted as a buttress against

the stresses of the Ouachita orogeny (Johnson *et al.*, 1989; Ng, 1979).

STRATIGRAPHY

The stratigraphy of the study area is shown on the stratigraphic column, Figure 5 and

cross section, Figure 6. The Grant sands are Pennsylvanian in age and part of the Bend

Conglomerate Group of the Atokan Boonsville Field (Figure 5). Underlying the Atoka are the

Morrowan strata of the early Pennsylvanian which overlies Mississippian rocks.

The Ordovician-Mississippian boundary is an unconformity at the top of the Viola Limestone. The Mississippian is represented by the Barnett shale and limestones. The Barnett Formation can reach thicknesses over 450 ft and ranges from a dark greyish-brown petroliferous shale in the eastern Llano outcrops to a more calcareous facies with grey to brownish grey crinoidal limestones replacing the shale in the west (Turner, 1957). The Fort Worth Basin Barnett Shale is highly productive and is the North American prototype for shale plays (Tilford and Stewart, 2011).

Overlying the Mississippian Barnett formation is the early Pennsylvanian Morrowan sequence. During that time the Fort Worth Basin was inundated by transgressive seas, which indicated renewed subsidence (Johnson *et al.*, 1989). The resulting carbonates are highly siliceous and exhibit a distinctive variety of sedimentary structures (Gee, 1976). In the study area the Morrowan time encompasses the Marble Falls Limestone formation of more than 150 meters of strata preserved in the subsurface (Johnson *et al.*, 1989).

The Atoka Group, also termed the Boonsville Field, overlies the unconformity at the top of the Morrowan-age Marble Falls Limestone. The Boonsville Field of the Fort Worth Basin thins to the northwest and comprises sandstones, conglomerates, interbedded shales, and thin limestones (Maharaj and Wood, 2009; Johnson *et al.*, 1989). The conglomerates and coarse sandstones are usually composed of subrounded to subangular quartz clasts with feldspars and some chert. Both carbonate and silica cements are commonly found in the sandstones and conglomerates. Dissolution of detrital feldspar grains often creates secondary porosity. The lower portion of the Boonsville Field is the Bend Conglomerate Group. The Bend Conglomerate Group is comprised of sands interbedded by shales with the Upper Grant Sand at the top.

Still in the Boonsville Field of the Atoka, but above the Bend Conglomerate Group, is the Pregnant Shale interval. The Pregnant Shale thickens north to south and eventually pinches out. The interval has a distinct log profile of a coarsening upward sequence that suggests a progradational system from marine shale to delta front to delta plain environments from northwest to southeast.

The Whitehall Sandstone sits above the Pregnant Shale Formation, marking the end of basinal filling by the Pregnant Shale. The Whitehall sands are localized, fluvial in nature, usually developed as a single deposit with flat base and fining upward. The formation varies with thicknesses up to 30 ft trending northeast to southwest.

Above the Whitehall Sandstone is the Caddo Pool Formation. The sequence of limestones, conglomerates, and very fine to coarse grained sands represents a shallow marine prograding delta environment. The Daly Limestone caps the middle section of the Caddo section with thicknesses over 150 ft. The Daly Limestone develops northeast to southwest and pinches out to the northwest. Overall the Caddo Pool Formation exceeds 200 ft. The top of the Caddo Pool Formation is a major unconformity and marks the end of Atoka deposition.
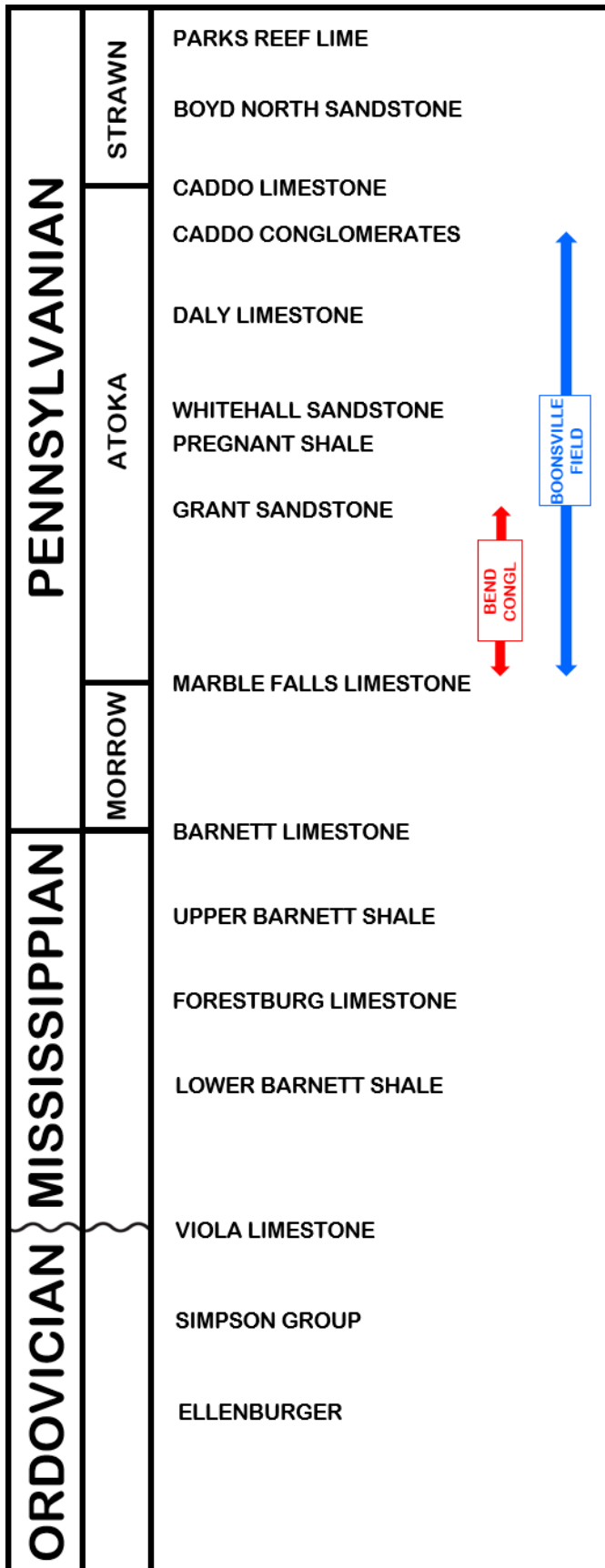
Figure 5. Stratigraphic column for the study area within the Fort Worth Basin. The Ordovician-Mississippian boundary is marked by an unconformity at the top of the Viola Limestone. The Atoka Group, also termed the Boonsville Field, overlies the unconformity at the top of the Morrowan Marble Falls Limestone.
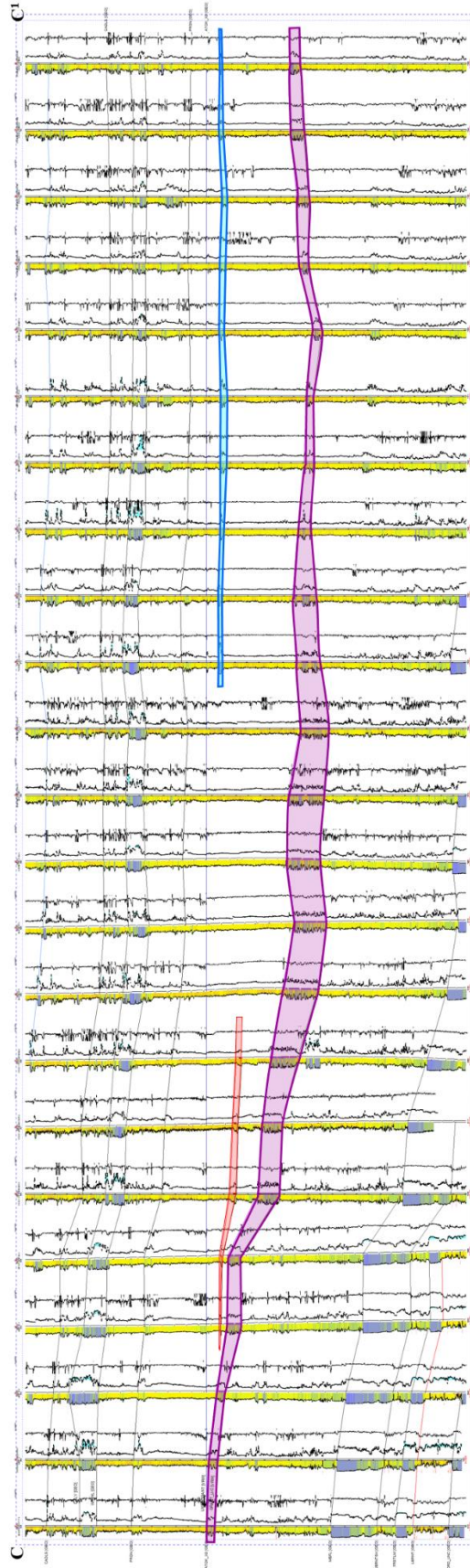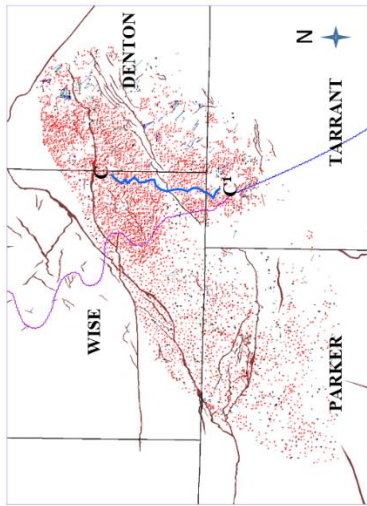
Cross-Section C-C¹ (N-S)

Figure 6. Stratigraphic cross-section hung on the ATOK_X0 marker with 23 wells totaling 16.96 miles north to south. The Upper Grant Sand is depicted in red, the Lower Grant Sand in purple, and the Upper Grant South Sand in blue.

PREVIOUS INVESTIGATIONS

Studies of the Atokan age strata in the Fort Worth Basin date back to the early 1900's. One of the earliest studies with concentration on the Pennsylvanian strata of the Fort Worth Basin was Plummer (1919), who proposed a new classification for the Pennsylvanian strata of Texas.

While some studies focus on the Boonsville Field of the Atoka, others are more specific such as addressing the Bend Conglomerate Group of the Boonsville Field. Two earlier papers of note specifically investigated the Boonsville Field: Blanchard (1968) and Gardner (1968). Gardner (1968) reviewed the discovery, history, geology, and production of the section within Wise County. Blanchard (1968) characterized the geology and production history for not only Wise County, but also Jack County and the Toto Field of Parker County.

Turner (1957) completed a study of Paleozoic stratigraphy of the Fort Worth Basin. The study dissects the Paleozoic age to discuss the depositional environments that progressed throughout time. According to Turner (1957), the Marble Falls, Big Saline, and Caddo are components of a single, inclusive carbonate facies with a black shale environment developing basinward. Thompson (1982) suggested that the Atoka depositional environment is comprised of a series of fan-delta and wave dominated delta systems.

P. T. Flawn completed several studies that are relevant to the Fort Worth Basin area, focusing on the Ouachita structural belt and its sourcing of basins. Flawn (1956) used well cores and cuttings from oil companies to describe the geology of the Precambrian basement rocks of Texas and southeast New Mexico. Flawn (1959) presented preliminary results for a study

15

investigating the stratigraphy and petrography of the strata of the Ouachita structural belt and adjacent foreland. The data were collected from wells that penetrated the rock in those areas, and also investigated structures in the deformed rocks to determine age of deformation of the Ouachita structural belt, which he concluded that the final orogenic pulses were late Pennsylvanian and early Permian for the United States and that in Mexico there was late Permian orogenic activity.

David T. W. Ng studied the Atoka clastic rocks of north-central Texas. Ng (1979) focused on the Atoka clastics of Jack, Palo Pinto, Parker, and Wise Counties. The study was designed to give an interpretation of Atokan depositional environment and determine the most favorable areas for production of hydrocarbons. Ng (1982) concluded that the Ouachita fold belt and regional westward tilting is responsible for the formation of the Atoka clastics wedge. The study also concluded that while structure played a minor role in the accumulation of hydrocarbons, updip porosity and permeability pinchouts (thinning) are the most important factors.

In 1982, several researchers from the Dallas Geological Society studied the Atoka Group. Lovick *et al.* (1982) concluded that the source area for the Bend conglomerates is to the north. Lahti and Huber (1982), also of the Dallas Geological Society, concluded that the source areas for the Atoka are the Wichita mountain system to the north and the Ouachita structural belt to the east. Lahti and Huber (1982) determined that the gas in the Boonsville conglomerates is trapped by the loss of permeability through cementation within the rocks or by "shaling-out" from channel shifting.

More recently, Hentz *et al.* (2012) determined that the source area for the lower Atoka is from the Ouachita fold belt to the southeast and from the Muenster Arch to the northeast. Hentz *et al.* (2012) also suggested that the depositional environment for the lower Atoka was comprised of a combination of braided fluvial systems, braided-plain deposits, and river-dominated deltas. Maharaj and Wood (2009) concluded that river deltas were most likely the depositional environment for the Atoka interval.

There are inconsistencies among authors about the interpretations of the depositional environment for the Atoka age strata. This study analyzes core data to determine sedimentary structures and other characteristics to interpret depositional environment specifically for the Atokan Grant Sand interval.

METHODOLOGY

The workflow (Figure 7) for conducting this subsurface study began with an extensive literature review of the Bend Conglomerates in the Fort Worth Basin. After a comprehensive study of the previous investigations, the next objective was to become familiar with the data supplied by Devon Energy. The study area is highly developed with a large quantity of well log data. Figure 8 depicts the study area and the location of the 6,545 wells within it. Well log formation identifications were initially based on previous formation top picks by industry geologists, in particular Gayle Riggs, at Devon Energy. A set of criteria based on the log characteristics [Gamma Ray (GR), Resistivity (ILD), and Porosity (DPHI)] was established for

consistent formation top picks for this study. The type log (Figure 2) shows the formation top picks for the Grant that were established for this study.

An organized grid system was set up to consistently map the area by correlating well logs (Figure 6). Cross-sections of the well log correlations are hung on the ATOK_X0, a regional marker proximal to the Grant Formation. The ATOK_X0 is easily recognized on logs (low, but uniform, resistivity over a thick interval and a featureless gamma ray) and is consistently picked throughout the area. While completing well log correlations, pay intervals were selected based on a visual interpretation of log curves for "clean" sands. The pay intervals can be seen in the middle track of the type log (Figure 2) as a red marker to designate Upper Grant pay and a purple marker to designate Lower Grant pay. The well log correlations and the pay intervals were then used to produce maps of the Grant Sands.

Structure and gross sand isopach maps for the Lower Grant Sand were created from the well log correlations as shown in Figures 9 and 10. Structure and gross sand isopach for Upper Grant Sand is given in Figures 11 and 12. These maps also depict the regional extent of the Grant Sands in the basin. The Lower Grant is more widespread regionally and ranges in thickness from 20 - 650 ft in the southern portion of the study area as can be seen in Figure 10. The Upper Grant Sand is more regionally constrained, and is up to 100 ft thick in the center of the elongate body oriented northeast-southwest in Figure 12. Both sands are dipping to the north-northeast.

There is a major fault complex that runs through the study area, the Mineral Wells Fault System. The Mineral Wells Fault System runs northeast - southwest throughout the study area (Figure 8). It was nearly parallel with the shoreline during Grant deposition. The faults were deep-seated basement faults that have been reactivated and inverted as high angle thrust faults by

18

the Ouachita Thrust Front. At the time of early/middle Atoka deposition, the basin was to the south and sediment supply from the north with the Marble Falls Limestone Formation dipping southward. The block between the Mineral Wells and the Muenster Arch was being downthrown from the reactivated faults. By late Atoka, the basin fill slowed due to inversion. By the time of Daley Limestone deposition, the basin has been inverted and the sea is to the north. The sediment supply is to the south from the upthrown block on the opposite side of the Mineral Wells. With post Daly Limestone deposition, the inversion continues and the strata from the south sea are inverted to dip to the north (Figures 9 and 11).

The pay intervals were used to produce net sand isopach maps (Figures 13 and 14) for both the Upper and Lower Sands because many boreholes were too washed out (meaning that the readings were inaccurate due to borehole rugosity) to use cut-off parameters for a traditional net sand map. Bubble maps of initial production (Figures 15 and 16) and cumulative gas (Figure 17 and Figure 18) overlain on the respective net sand maps show the production for each sand. The bubble maps and other production data only encompass the 48 "stand alone" wells of the total 64 Grant producers. The 48 wells used for production data are significant because the other Grant producers are wells that have been perforated in the Grant and additional targets. Although the Lower Grant is thicker and more widespread than the Upper, the production data indicates that the Upper Sand is the better reservoir.

While mapping, another "upper" sand unit was discovered. The new sand is similar to the Upper Grant but does not correlate with it. The sand was partially mapped (not shown) and is named the Upper Grant South. The Upper Grant South Sand begins just south of the Upper Grant Sand and continues into Tarrant County (Figure 6).

19

During the mapping phase of this study, other relevant data were located in the well database, such as conventional and sidewall cores of the Grant section. Two of the conventional cores were located at Oklahoma Petroleum Information Center (OPIC) in Norman, Oklahoma. Viewing the core provided hands-on inspection of the rock. OMNI/Weatherford Laboratories completed an examination of a conventional core of the Gordon F. Moore Gas Unit No. 19. The examination analyzed petrography and sedimentology of the cored interval. A report was compiled by OMNI/Weatherford Laboratories. Data from the core report in conjunction with observations from the recent core viewings (June, August, and September 2015 by the author) were used in this study for a sedimentological examination. The summaries of the lithologic description in the core report were very thorough, therefore the sedimentological examination in this study is based upon those findings.

The petrographic analysis by OMNI/Weatherford Laboratories was conducted using 36 thin sections. Detailed thin section descriptions, including modal point count analysis, were compiled for 10 of the 36 thin sections. All 36 samples were examined by X-ray diffraction (XRD) analysis and by scanning electron microscopy (SEM). The sample depths and analyses performed on the core samples are listed in Table 1. Table 2 summarizes the results of the detailed petrographic modal analyses of the core samples, and Table 3 lists the XRD analysis results. A summary of core analysis results, including permeability, porosity, and grain density are outlined in Table 4. Along with Table 4, the core report includes a written summary of the petrographic examination. The results and summary of the petrographic examination are included in this study with the purpose of determining the optimal drilling fluids to be used in completions of Grant wells.

Conventional core can commonly have an offset of the core depths versus the measured depths of the wireline log, especially in wells with shales. The core gamma was compared to the measured depths on the wireline gamma curve and the offset was determined to be approximately 15 ft deeper on the recorded core depths than that of the measured log depths. The offset is used throughout the study to accurately describe and correlate the data.

To determine the stratigraphy of the Grant for this study, a compilation of data was used. The Grant stratigraphy is based on the Gordon F. Moore No. 19 well. Divisions were made based on the wireline log curves Gamma Ray (GR), Resistivity (ILD), and Porosity (DPHI) (Figure 19). The division of units is supported by the conventional core for the Upper Grant and by the formation image interpretation by Fronterra Geosciences for both the Upper and Lower Grant.

The formation image data by Fronterra Geosciences, an FMI type of log, were also used to look for borehole breakout to determine maximum horizontal stress direction. Maximum horizontal stress is an important factor for reservoir rocks as it determines the optimal drilling direction for horizontal wells. Horizontal wells should be drilled perpendicular to the maximum horizontal stress to take advantage of the natural fractures. There were no examples of borehole breakout in the image log; therefore, a definitive conclusion for the maximum horizontal stress direction could not be determined. Using other data and knowledge, it is believed that the maximum horizontal stress direction is the same as the Barnett Shale, oriented northeast - southwest. The Barnett Shale is approximately 1,500 ft stratigraphically below the Grant Formation and with no thrust faults or a zone of decoupling between the Barnett and the Grant, it can be inferred that the maximum horizontal stress is the same.

The OMNI/Weatherford petrographic analysis of the Gordon F. Moore No. 19 cored interval was evaluated to determine the ideal drilling fluid to use in completions of Grant wells. The type of drilling fluid used is important because formation damage can occur if the petrography is not taken into account. Rock with high clay content, specifically smectite, can potentially swell if a fresh water system is used. "Swelling clays" damage the formation by decreasing the porosity and permeability which hinders production. The mineralogy of the cored interval is examined to determine what potential formation damage could occur and a drilling fluid is then recommended on that basis with the prospect of preventing formation damage and generating optimal production rates.

Well logs, maps, previous investigations, and core data were used to determine a model for depositional environment of the Grant Sands. Well logs and maps indicate that the Upper Grant is in a confined elongate body, while the Lower Grant is more widespread, generally thickening to the south. From the core descriptions, it was determined that the Upper Grant Sand was deposited in a fluvial setting. The image log data confirmed that the Upper Grant is fluvial in nature and cross bedding (79 cross beds) indicates that the sand is most likely sourced from the north-northeast. The image log data also indicate that the Lower Grant exhibited slumping, scour surfaces, and soft sediment deformation that could represent a mass transport system. There is also the shale interval between the sands and the Upper Grant South sand that was taken into account when determining a depositional setting. The conceptual model of deposition during a lowstand is consistent with all parts of the Grant Formation.
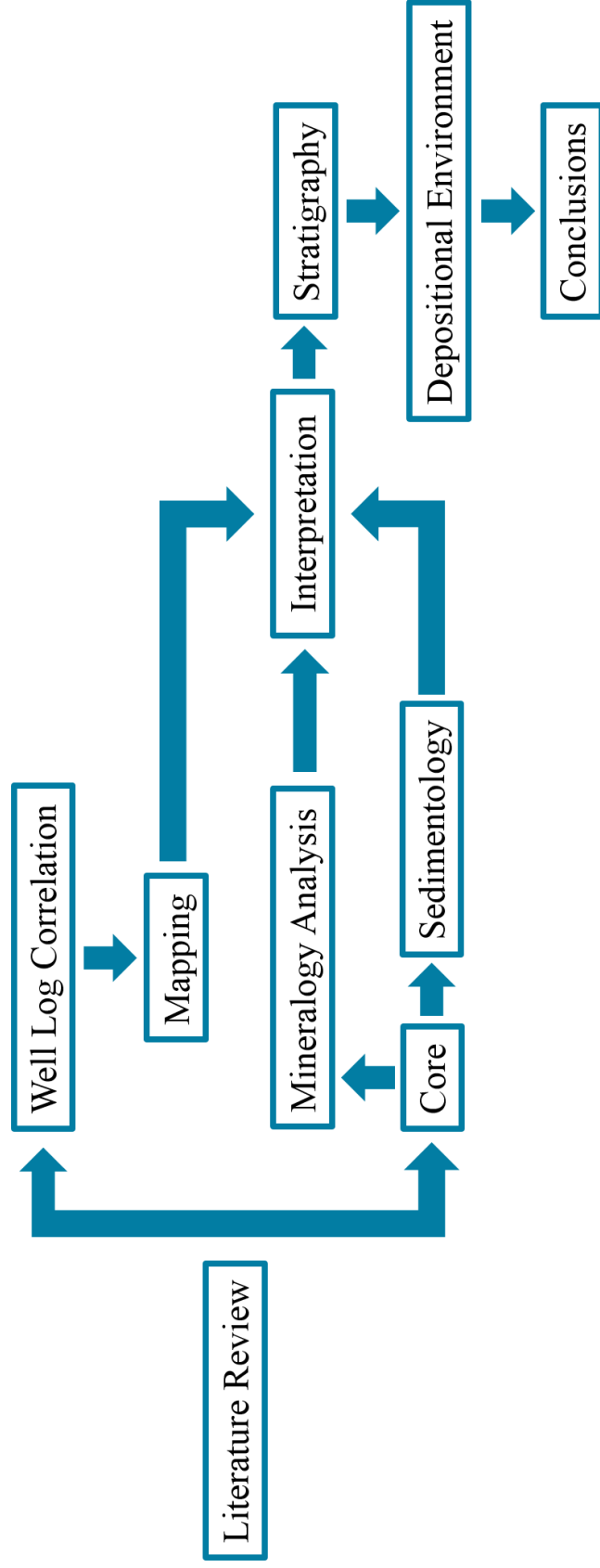
Figure 7. Work flow chart for this study. The purpose of this study is to improve the geologic understanding of the Grant Sands for enhanced exploration potential. That is attained through a reservoir characterization and a conceptual model for the depositional setting of the Grant Sands. The reservoir characterization is composed of maps of the regional extents and production variations as well as recommendations for completions fluids based on the petrographic analysis. The conceptual model for depositional setting is based on the well log correlations, maps, lithostratigraphic analysis of the slabbed core, and the image log data of the cored well.
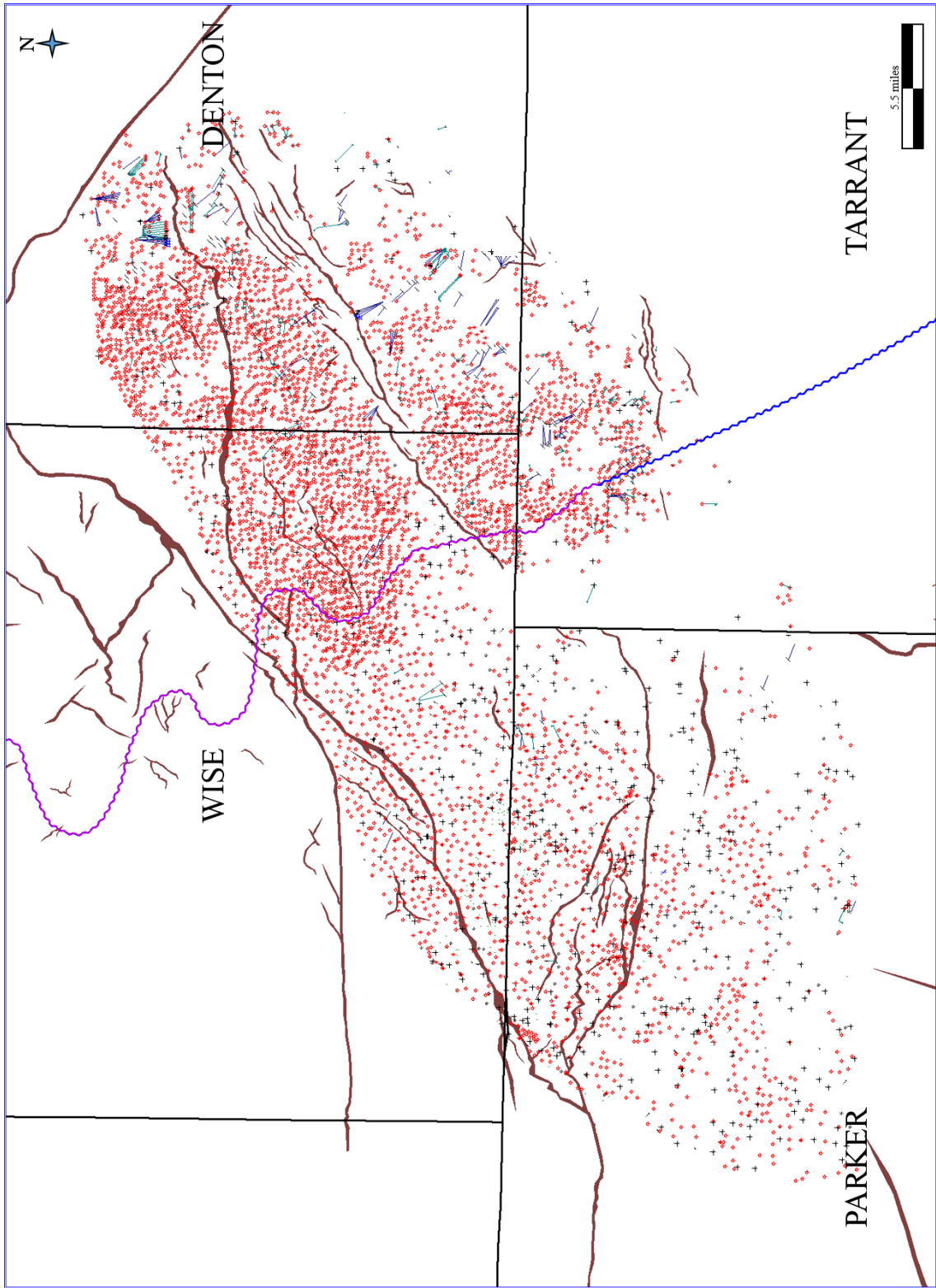
Figure 8. The study area of 1,006.4 sq. miles stretching across Denton, Wise, Parker, and Tarrant Counties with 6,545 wells. The faults shown on the map are the Mineral Wells Fault System.
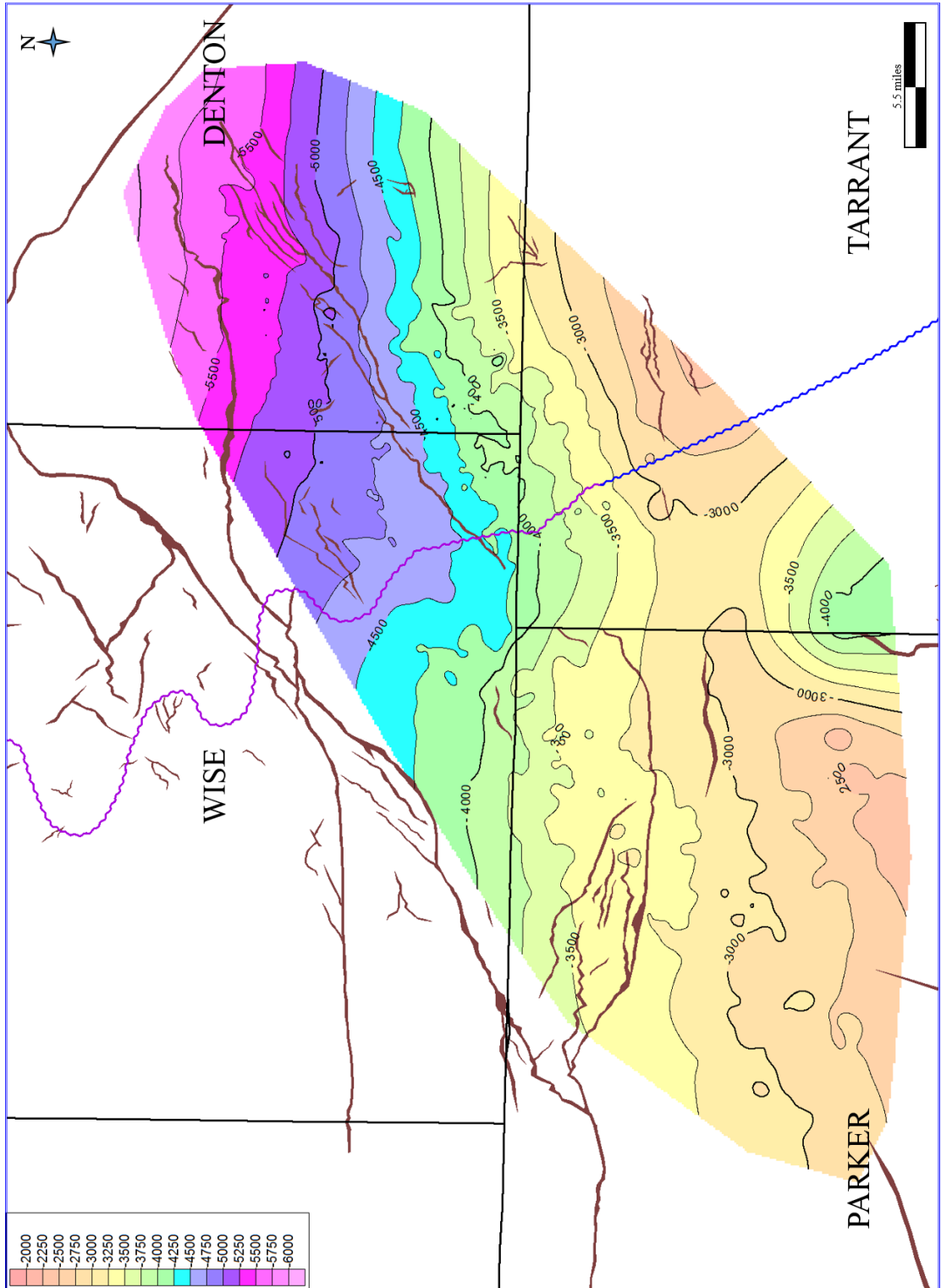
Figure 9. Structure map of Lower Grant Sand, dipping to the north. Contour interval of 250 ft.
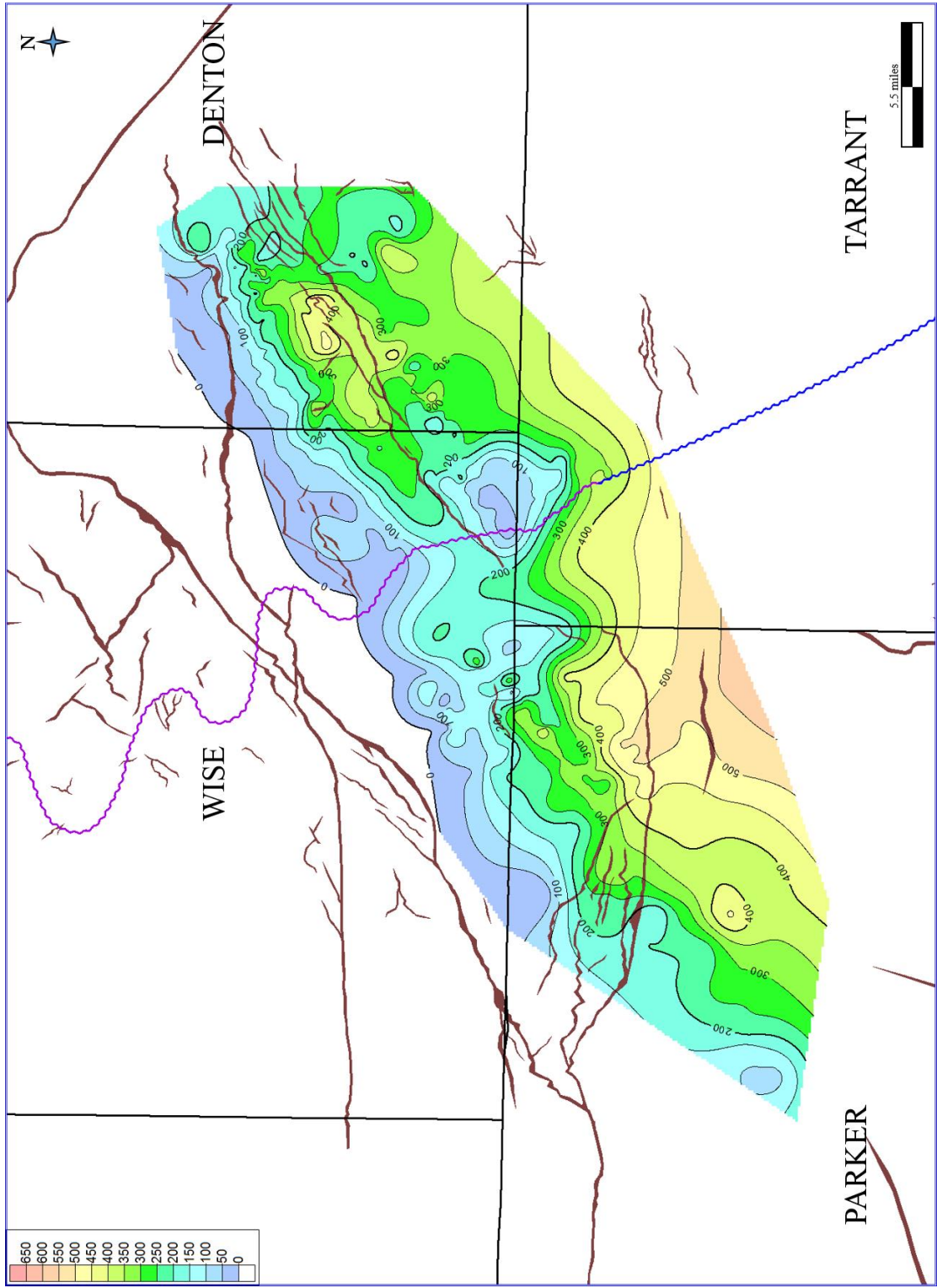
Figure 10. Gross sand isopach map of Lower Grant Sand, pinching out to the north and thickening to the south. Contour interval of 50 ft.

26
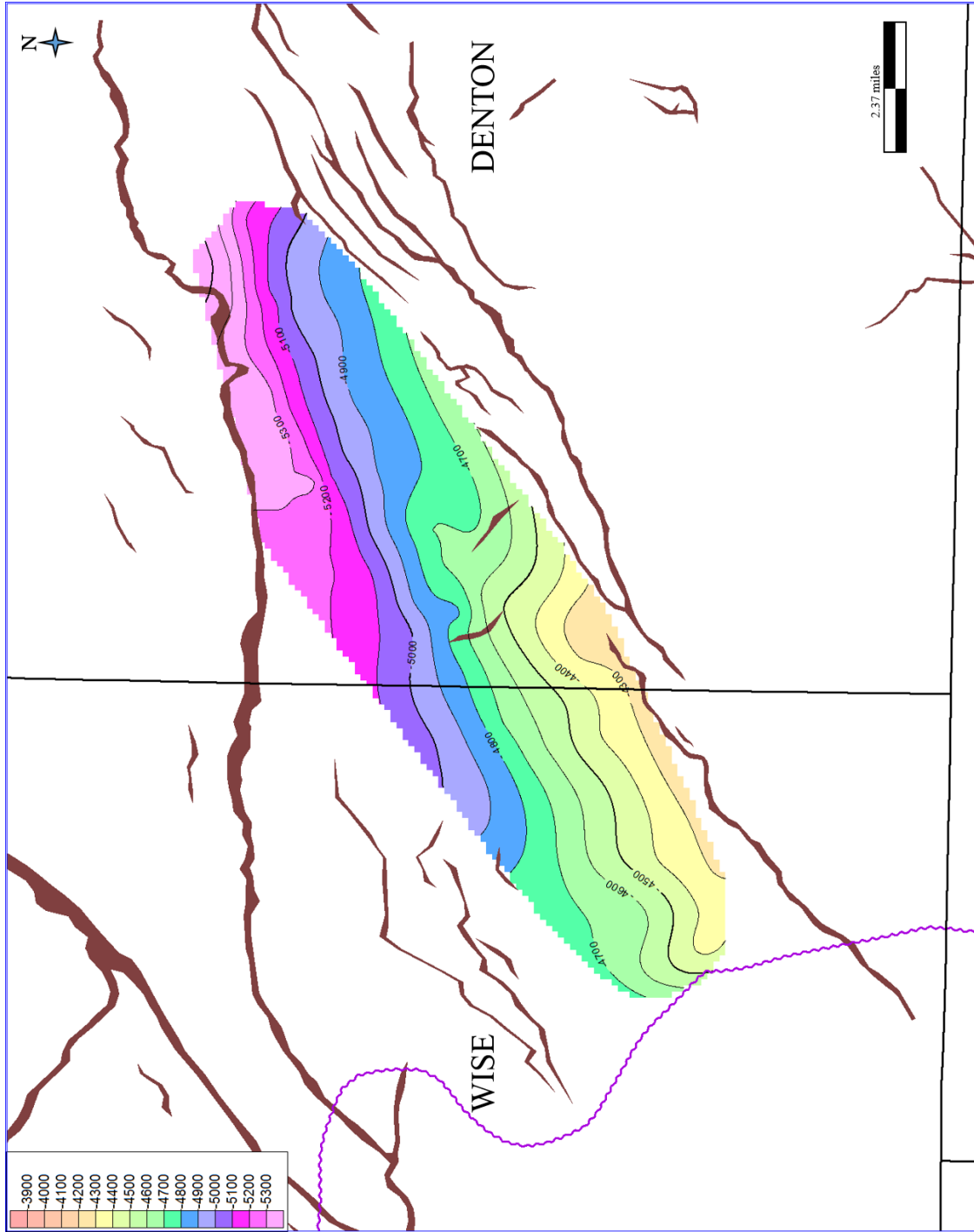
Figure 11. Structure map of Upper Grant Sand, dipping to the north. Contour interval of 100 ft.
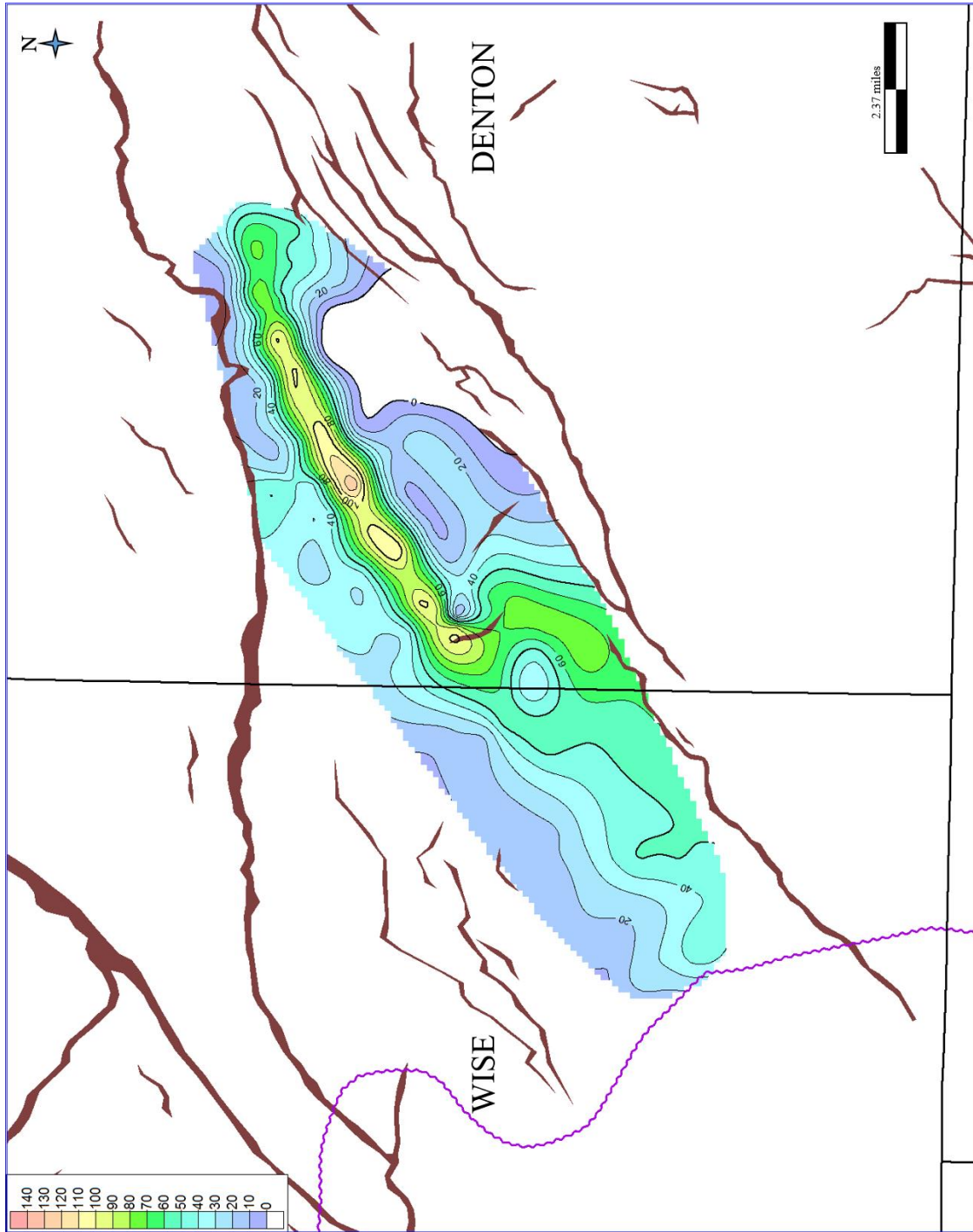
Figure 12. Gross sand isopach map of Upper Grant Sand. Contour interval of 10 ft.
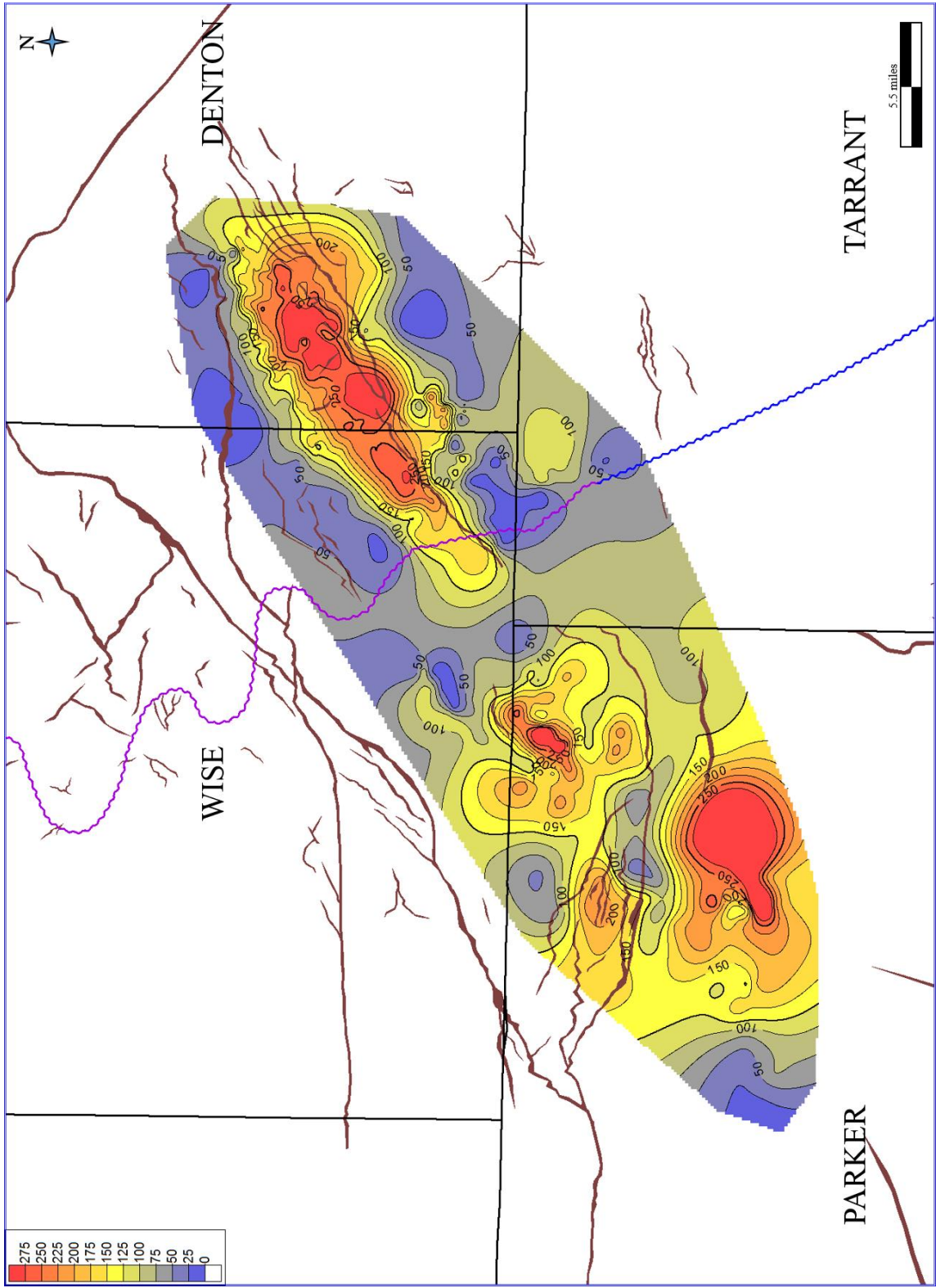
Figure 13. Net sand isopach map of Lower Grant Sand. Contour interval of 25 ft.
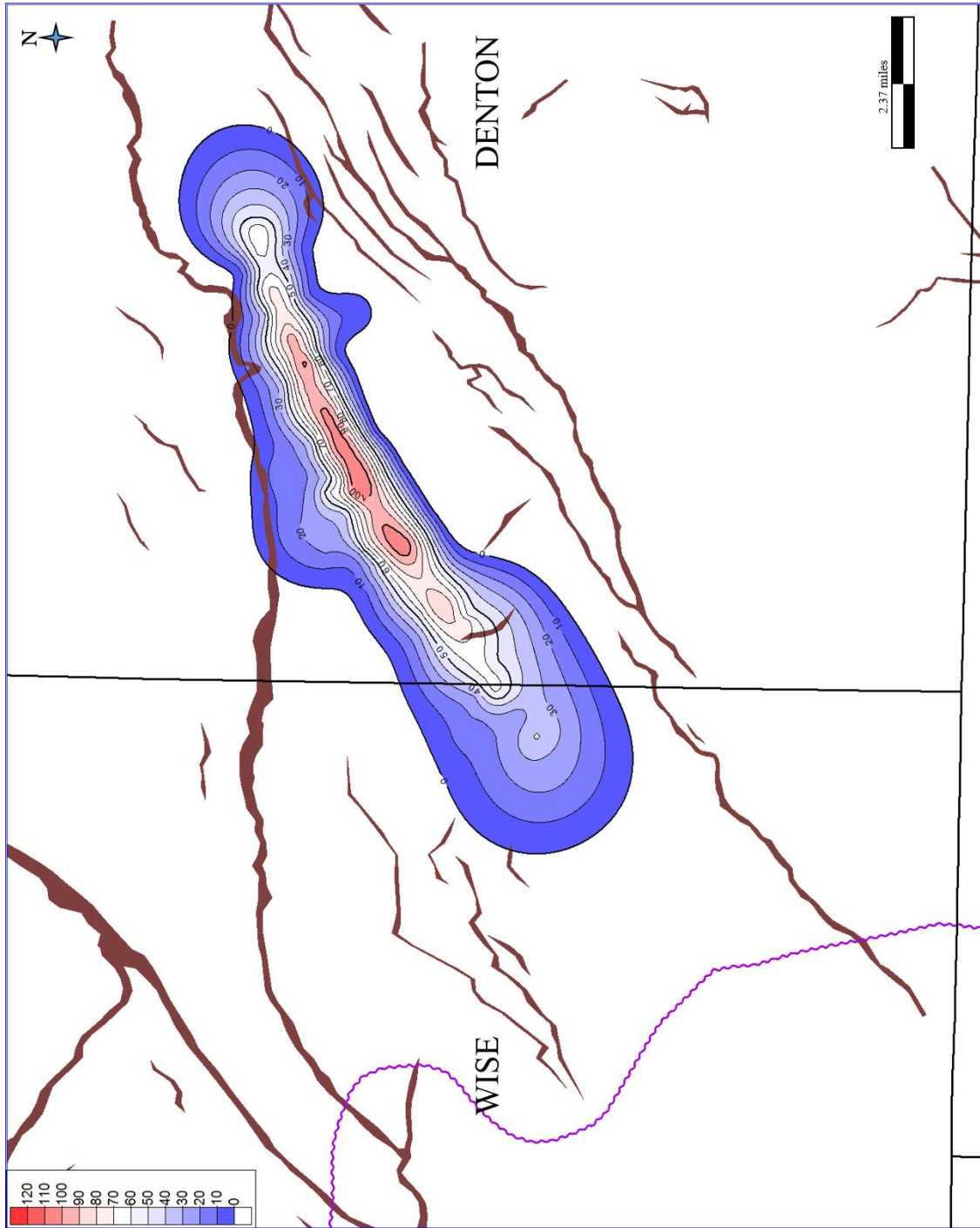
Figure 14. Net sand isopach map of Upper Grant Sand. Contour interval of 10 ft.

30
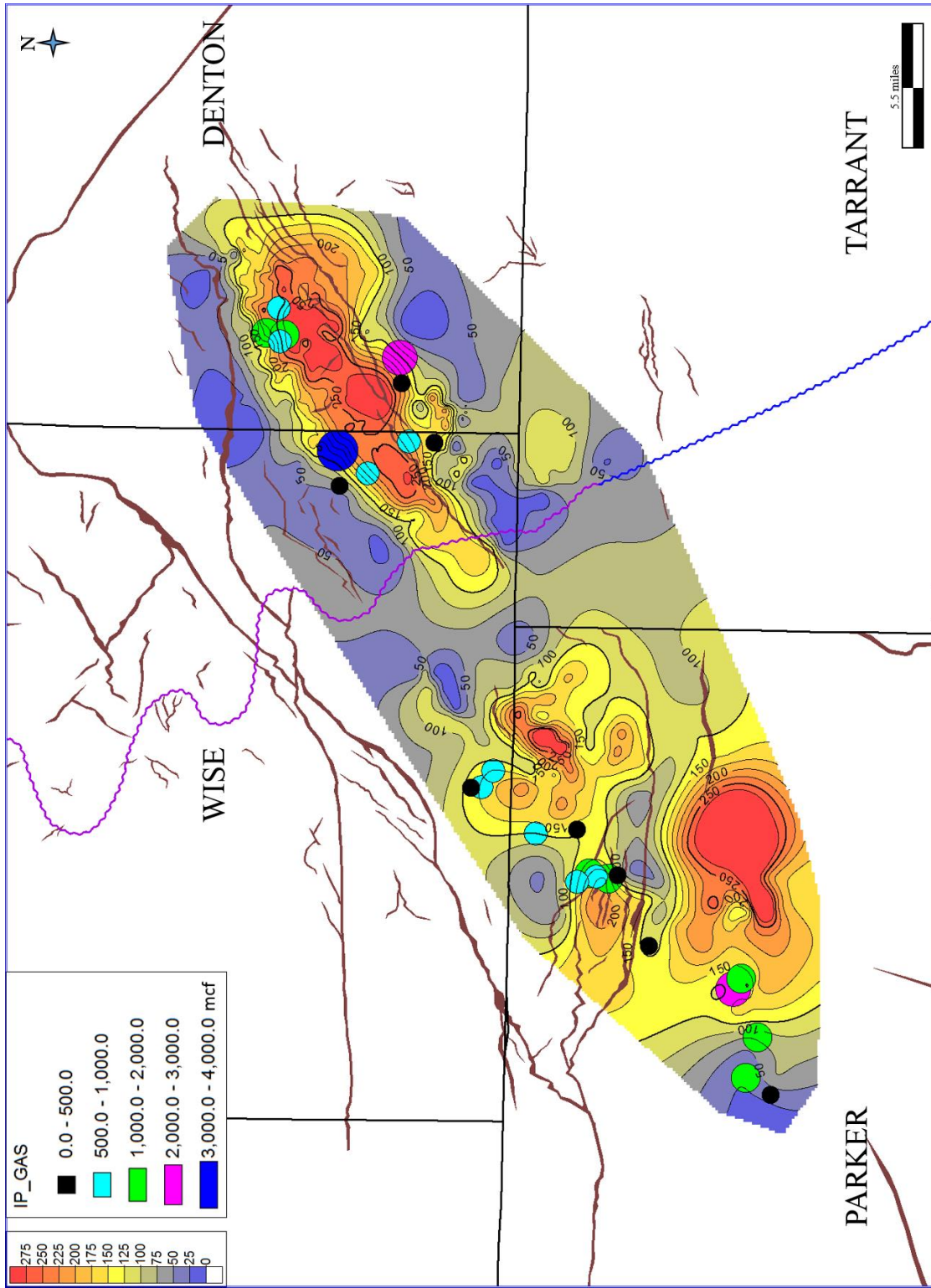
Figure 15. Net sand isopach map of Lower Grant Sand with IP Bubbles. An average Lower Grant horizontal well came on at 1.2 million a day with an EUR of 1.6 BCF.

31
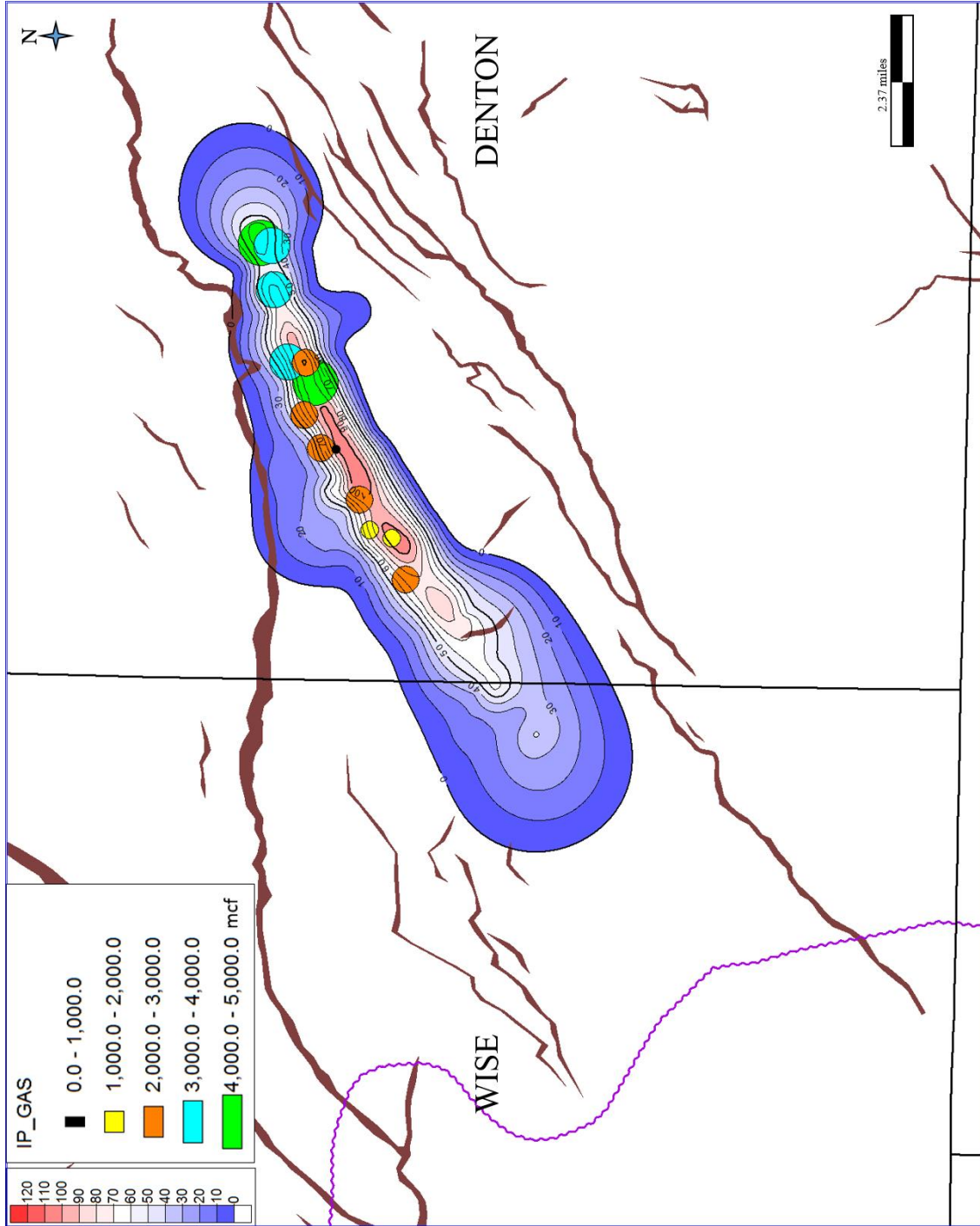
Figure 16. Net sand isopach map of Upper Grant Sand with IP Bubbles. An average Upper Grant horizontal well came on at 2.7 million a day with an EUR of 1.6 BCF.
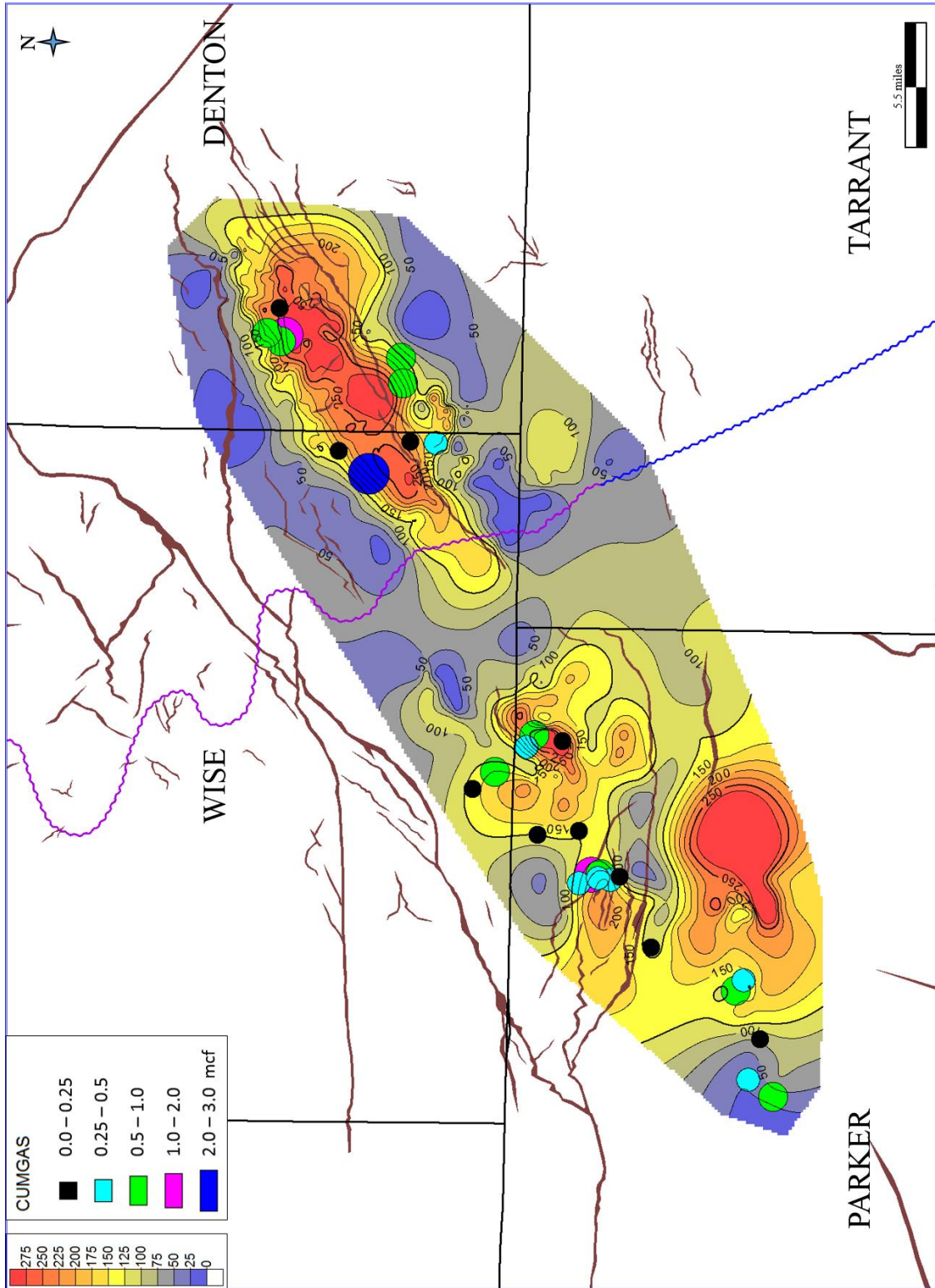
Figure 17. Net sand isopach map of Lower Grant Sand with Cumulative Gas Bubbles. The majority of the Lower Grant wells have less than a 1.0 mcf of cumulative gas.
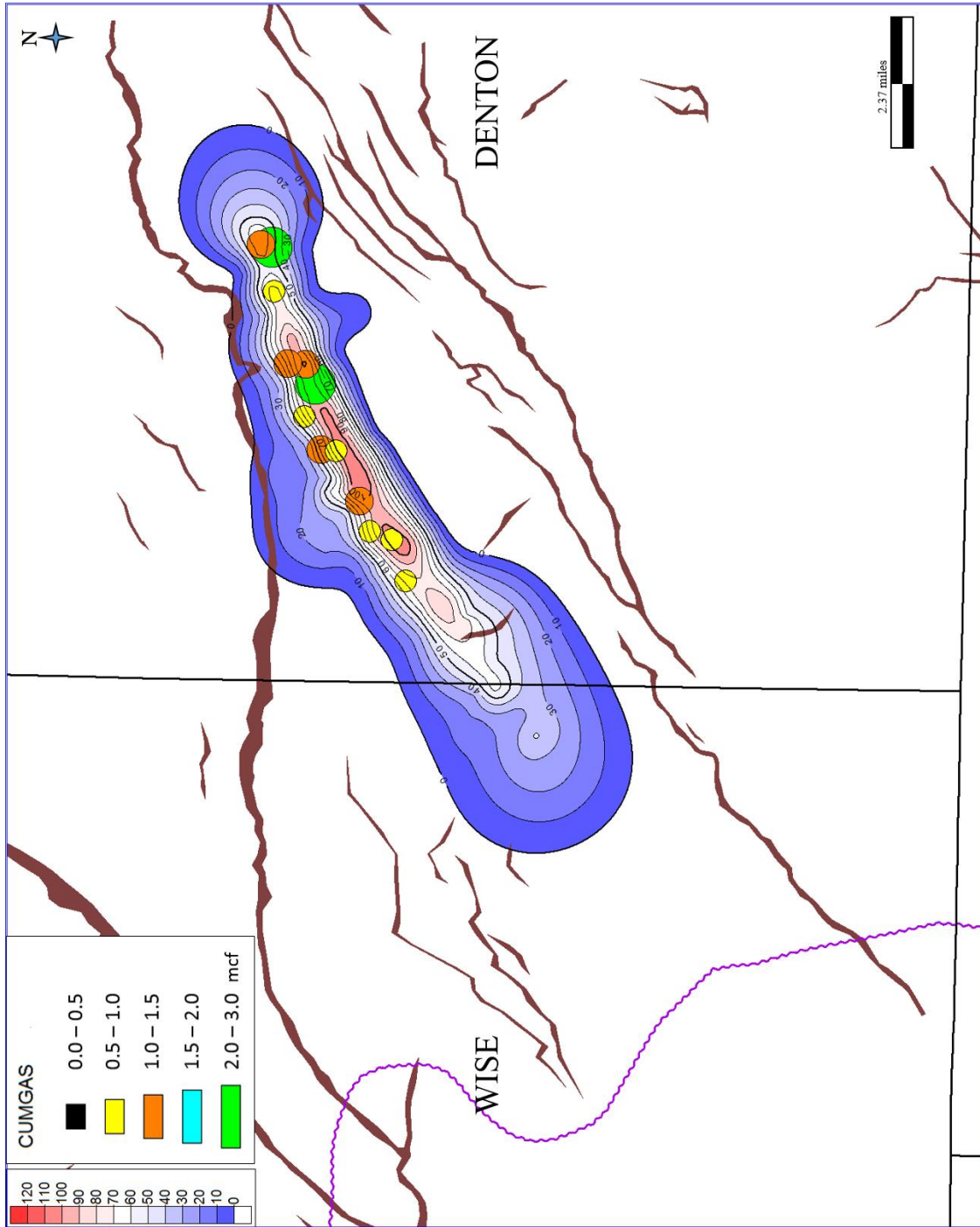
33

Figure 18. Net sand isopach map of Upper Grant Sand with Cumulative Gas Bubbles. The majority of Upper Grant wells have between a 0.5 and 1.5 mcf of cumulative gas.

SAMPLE DEPTHS AND ANALYSES CONDUCTED

Sample Number	Sample Depth (ft.)	Thin Section Preparation	Detailed Thin Section (Modal) Analysis	X-Ray Diffraction Analysis	SEM Analysis
3-21	5970.50	X	X	X	X
3-22	5971.55	X		X	X
3-23	5972.50	X		X	X
3-24	5973.00	X	X	X	X
4-2	5974.20	X		X	X
4-3	5975.50	X		X	X
4-4	5976.15	X	X	X	X
4-5	5977.60	X		X	X
4-6	5978.30	X		X	X
5-1	5979.85	X		X	X
5-2	5980.80	X	X	X	X
5-3	5981.50	X		X	X
5-4	5982.50	X		X	X
5-5	5983.25	X		X	X
5-6	5984.50	X		X	X
5-7	5985.40	X		X	X
5-8	5986.80	X		X	X
5-9	5987.25	X	X	X	X
5-10	5988.75	X		X	X
5-11	5989.60	X		X	X
5-12	5990.60	X	X	X	X
5-13	5991.05	X		X	X
5-14	5992.50	X		X	X
5-15	5993.80	X		X	X
5-16	5994.50	X		X	X
5-17	5995.30	X		X	X
5-18	5996.80	X	X	X	X
5-19	5997.50	X		X	X
5-20	5998.50	X		X	X
5-21	5999.40	X	X	X	X
5-22	6000.30	X		X	X
5-23	6001.25	X		X	X
5-24	6002.65	X	X	X	X
5-25	6003.60	X		X	X
5-26	6004.05	X		X	X
6-1	6005.00	X	X	X	X

Table 1. Modified from the OMNI/Weatherford Laboratories Gordon F. Moore 19 Core Report. Table of the sample depths and the analysis conducted on each of the 36 thin sections from the slabbed core of the Gordon F. Moore No. 19. 10 of the 36 thin sections were used for detailed thin section (modal) analysis. Summaries and photomicrographs of those 10 samples are in Appendix C.

SUMMARY OF THIN SECTION PETROGRAPHIC RESULTS

Sample Number	Sample Depth (Ft.)	Lithology	Total Porosity (% volume)	Secondary Porosity (% volume)	Micro-Porosity (% volume)	Quartz Overgrowth Cement (% volume)	XRD Total Clay (% by wgt)	XRD Chlorite Clay (% by wgt)	Texture / Composition
3-21	5970.50	Sublitharenite	9	3	4	7	8	4	Moderately well sorted fine-grained
3-24	5973.00	Sublitharenite	8	3	3	18	10	4	Moderately well sorted medium-grained
4-4	5976.15	Sublitharenite	7	5	tr	16	8	4	Moderately well sorted medium-grained
5-2	5980.80	Sublitharenite	7	3	2	19	6	3	Moderately well sorted medium-grained
5-9	5987.25	Sublitharenite	7	2	1	17	8	4	Moderately well sorted fine-grained
5-12	5990.60	Sublitharenite	7	5	1	19	7	4	Moderately well sorted fine-grained
5-18	5996.80	Sublitharenite	7	3	2	18	7	4	Moderately well sorted medium-grained
5-21	5999.40	Litharenite	6	3	1	9	11	5	Moderately sorted fine-grained
5-24	6002.65	Sublitharenite	6	3	2	20	9	4	Moderately well sorted medium-grained
6-1	6005.00	Sublitharenite	7	4	1	18	10	4	Moderately well sorted fine-grained

Inner Shelf / Offshore Bioturbated SS

Transgressed Fluvial/Deltaic SS

Fluvial/Deltaic Channel Sandstone
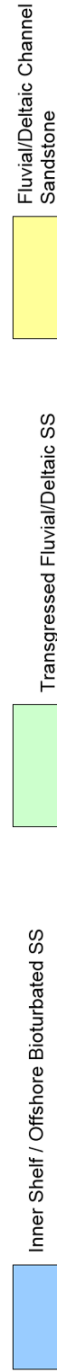
Table 2. Modified from the OMNI/Weatherford Laboratories Gordon F. Moore 19 Core Report. Summary of the results of the detailed thin section (modal) analysis of the 10 thin sections described in Appendix C.

Plug Number	Sample Depth (ft)	Clays				Carbonates			Quartz	K-spar	Other Minerals				Clays	Totals	
		Chlorite	Kaolinite	Illite	Mx I/S*	Calcite	Dol/Ank	Siderite			Plag.	Pyrite	Zeolite	Barite		Carb.	Other
3/21	5970.5	3	2	2	Tr	0	0	Tr	83	2	7	1	0	0	7	Tr	93
3/22	5971.55	5	3	3	Tr	0	0	Tr	79	1	8	1	0	0	11	Tr	89
3/23	5972.5	4	2	2	Tr	0	0	Tr	79	1	11	1	0	0	8	Tr	92
3/24	5973	4	3	3	Tr	0	0	Tr	78	1	10	1	0	0	10	Tr	90
4/2	5974.2	4	2	3	Tr	0	0	Tr	84	1	6	Tr	0	0	9	Tr	91
4/3	5975.5	5	2	3	Tr	0	0	Tr	84	1	5	Tr	0	0	10	Tr	90
4/4	5976.15	4	2	2	Tr	0	0	Tr	86	1	5	Tr	0	0	8	Tr	92
4/5	5977.6	5	3	5	Tr	0	0	Tr	78	1	7	1	0	0	13	Tr	87
4/6	5978.3	5	1	2	Tr	0	0	Tr	86	1	5	Tr	0	0	8	Tr	92
5/1	5979.85	3	2	2	Tr	0	0	Tr	87	1	5	Tr	0	0	7	Tr	93
5/2	5980.8	3	1	2	Tr	0	0	Tr	87	1	5	1	0	0	6	Tr	94
5/3	5981.5	2	1	2	Tr	0	0	Tr	90	1	4	Tr	0	0	5	Tr	95
5/4	5982.5	3	1	2	Tr	0	0	Tr	88	1	5	Tr	0	0	6	Tr	94
5/5	5983.25	3	2	2	Tr	0	0	Tr	86	1	6	Tr	0	0	7	Tr	93
5/6	5984.5	3	1	2	Tr	0	0	Tr	87	1	6	Tr	0	0	6	Tr	94
5/7	5985.4	3	2	2	Tr	0	0	Tr	85	1	6	1	0	0	7	Tr	93
5/8	5986.8	4	1	2	Tr	0	0	Tr	87	1	5	Tr	0	0	7	Tr	93
5/9	5987.25	4	2	2	Tr	0	0	Tr	86	1	5	Tr	0	0	8	Tr	92
5/10	5988.75	4	2	3	Tr	0	0	Tr	85	1	5	Tr	0	0	9	Tr	91
5/11	5989.6	4	1	2	Tr	0	0	Tr	86	1	6	Tr	0	0	7	Tr	93
5/12	5990.6	4	1	2	Tr	0	0	Tr	87	1	5	Tr	0	0	7	Tr	93
5/13	5991.05	4	2	2	Tr	0	0	Tr	87	1	4	Tr	0	0	8	Tr	92
5/14	5992.5	4	1	3	Tr	0	0	Tr	86	1	5	Tr	0	0	8	Tr	92
5/15	5993.8	5	2	3	Tr	0	0	Tr	83	1	6	Tr	0	0	10	Tr	90
5/16	5994.5	5	3	3	Tr	0	0	Tr	82	1	6	Tr	0	0	11	Tr	89
5/17	5995.3	5	3	3	Tr	0	0	Tr	82	1	6	Tr	0	0	11	Tr	89
5/18	5996.8	4	1	2	Tr	0	0	Tr	85	1	6	1	0	0	7	Tr	93
5/19	5997.5	4	2	3	Tr	0	0	Tr	84	1	6	Tr	0	0	9	Tr	91
5/20	5998.5	3	2	2	Tr	0	0	Tr	83	1	7	Tr	0	0	9	Tr	91
5/21	5999.4	5	3	3	Tr	0	0	Tr	80	1	7	1	0	0	11	Tr	89
5/22	6000.3	4	2	2	Tr	0	0	Tr	84	1	6	1	0	0	8	Tr	92
5/23	6001.25	4	2	3	Tr	0	0	Tr	83	1	6	1	0	0	9	Tr	91
5/24	6002.65	4	1	4	Tr	0	0	Tr	83	1	7	Tr	0	0	9	Tr	91
5/25	6003.6	5	2	6	Tr	0	0	Tr	79	1	7	Tr	0	0	13	Tr	87
5/26	6004.05	4	1	5	Tr	0	0	Tr	83	1	6	Tr	0	0	10	Tr	90
6/1	6005	4	1	5	Tr	0	0	Tr	83	1	5	1	0	0	10	Tr	90
Average		4	2	3	Tr	0	0	Tr	84	1	6	Tr	0	0	9	Tr	91

Inner Shelf / Offshore Bioturbated SS   Transgressed Fluvial / Deltaic SS   Fluvial / Deltaic Channel SS

Fluvial / Deltaic SS

Table 3. Modified from OMNI/Weatherford Laboratories Gordon F. Moore 19 Core Report. X-Ray Diffraction Results for the 36 thin sections from the slabbed core of the Gordon F. Moore No. 19.

OMNI
Laboratories, Inc.

SUMMARY OF ROUTINE CORE ANALYSES RESULTS
Vacuum Dried at 180°F   Net Confining Stress: 800 psi

Devon Energy Corporation
Gordon F. Moore GU No. 19 Well
Boonsville Field

Denton County, Texas
File: HH-36703

Core Number	Sample Number	Sample Depth, feet	Permeability, millidarcys		Porosity, percent		Grain Density, gm/cc
			to Air	Klinkenberg	Ambient	800 psi	
3	3-21	5970.50	0.023	0.010	9.1	9.1	2.66
3	3-22	5971.55	0.021	0.0088	8.9	8.9	2.66
3	3-23	5972.50	0.019	0.0077	8.8	8.8	2.66
3	3-24	5973.00	0.011	0.0039	9.2	9.2	2.68
4	4-2	5974.20	0.025	0.011	7.1	7.1	2.66
4	4-3	5975.50		+	6.7	6.7	2.66
4	4-4	5976.15	0.0077	0.0026	6.0	6.0	2.65
4	4-5	5977.60	0.034	0.016	7.5	7.4	2.66
4	4-6	5978.30	0.011	0.0039	5.4	5.4	2.65
5	5-1	5979.85	0.011	0.0040	6.7	6.7	2.65
5	5-2	5980.80	0.0089	0.0030	5.6	5.6	2.65
5	5-3	5981.50	0.020	0.0084	5.9	5.9	2.64
5	5-4	5982.50	0.0094	0.0033	4.5	4.5	2.64
5	5-5	5983.25	0.010	0.0037	5.6	5.5	2.65
5	5-6	5984.50	0.0091	0.0032	5.4	5.3	2.65
5	5-7	5985.40	0.0085	0.0029	6.2	6.2	2.66
5	5-8	5986.80	0.0090	0.0031	4.5	4.5	2.65
5	5-9	5987.25	0.0075	0.0025	3.8	3.7	2.65
5	5-10	5988.75	0.021	0.0088	5.9	5.9	2.65
5	5-11	5989.60	0.013	0.0048	5.9	5.9	2.65
5	5-12	5990.60	0.046	0.023	6.9	6.8	2.65
5	5-13	5991.05	0.0097	0.0034	5.7	5.7	2.65
5	5-14	5992.50		+	6.3	6.2	2.65
5	5-15	5993.80	0.015	0.0059	5.6	5.6	2.66
5	5-16	5994.50	0.012	0.0046	5.8	5.8	2.65
5	5-17	5995.30	0.0081	0.0027	5.7	5.6	2.65
5	5-18	5996.80	0.026	0.012	5.3	5.3	2.65
5	5-19	5997.50	0.015	0.0059	5.8	5.8	2.65
5	5-20	5998.50	0.0082	0.0028	5.5	5.5	2.65
5	5-21	5999.40	0.030	0.014	6.1	6.1	2.66
5	5-22	6000.30	0.021	0.0088	5.8	5.7	2.66
5	5-23	6001.25	0.010	0.0036	5.1	5.1	2.65
5	5-24	6002.65	0.0095	0.0033	5.1	5.0	2.65
5	5-25	6003.60	0.0085	0.0029	6.8	6.8	2.66
5	5-26	6004.05	0.010	0.0036	6.1	6.1	2.65
6	6-1	6005.00	0.051	0.026	6.2	6.1	2.65
	Average values:		0.016	0.0070	6.2	6.2	2.65

+ Indicates sample is unsuitable for this type of measurement

Table 4. Modified from OMNI/Weatherford Laboratories Gordon F. Moore 19 Core Report. Summary of Core Analyses Results of the 36 thin sections from slabbed core of the Gordon F. Moore No. 19.
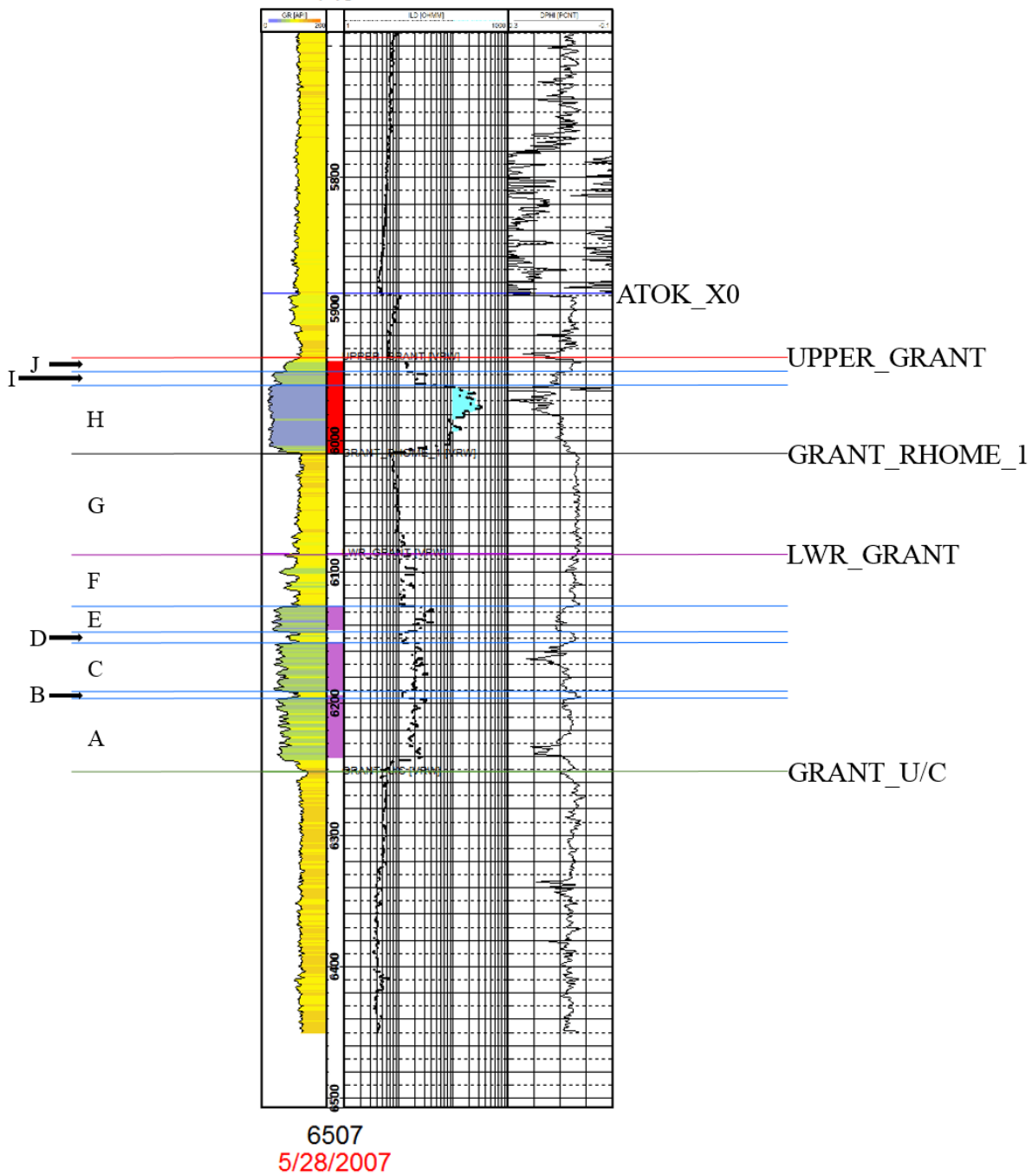
Figure 19. Stratigraphy of the Grant Formation. The Grant Formation is subdivided into 10 units. The base of the Grant Formation is marked by the Grant Unconformity (GRANT_U/C). The Lower Grant is subdivided into 6 units: the base sand (A), the bottom shale unit (B), the middle sand (C), the middle shale unit (D), the top sand (E), and the thinly bedded sands (F). Subunit G marks the shale unit dividing the Lower Grant from the Upper Grant. The Upper Grant is subdivided into 3 units: the base sand (H), the middle sand (I), and the top sand (J).

GRANT CORE

The better quality of the two Grant Sand conventional cores is the Gordon F. Moore Gas

Unit No. 19, Boonsville Field, Denton County, Texas (Figure 20). The cored interval is from

5850-5850.6 ft and 5897-6005.1 ft. The cored interval of 5897-6005.1 ft starts approximately 40

ft above the top of the Upper Grant Sand interval and cored almost the entirety of the Upper

Grant, lacking approximately 15 ft of sand prior to the base of the Upper Grant. A report by

OMNI/Weatherford Laboratories completed a petrologic analysis and a lithologic core

description from the slabbed conventional core with the purpose of characterizing the lithology

of the cored sequence and evaluating the sedimentology.
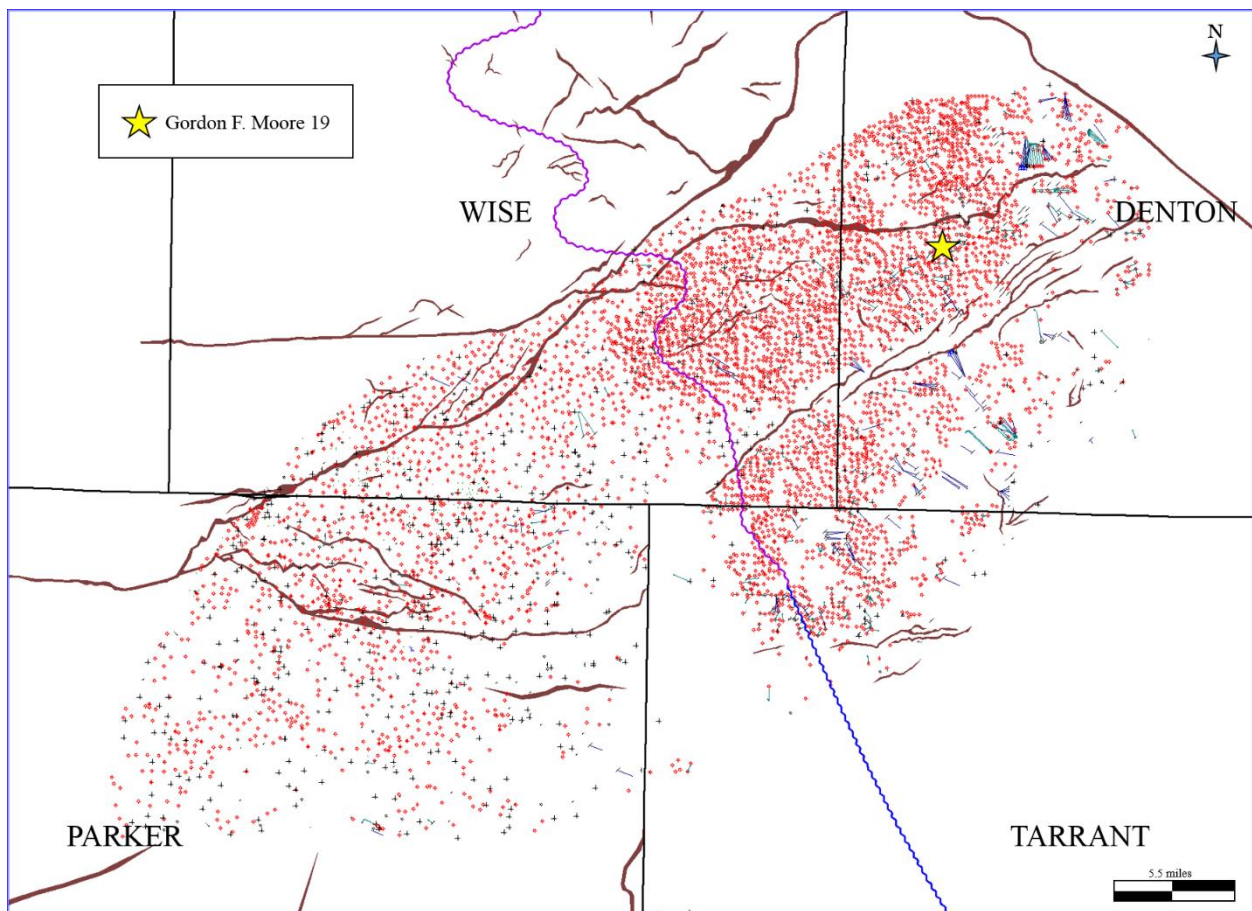
Figure 20. Location of the well Gordon F. Moore No. 19 used in this study for the cored
interval, the sedimentology and petrology from the core, and the FMI type of log of the well.

SEDIMENTOLOGICAL EXAMINATION

OMNI/Weatherford Laboratories generated a lithologic core description from examination of the slabbed core. There were nine depositional/lithologic units determined within the core based on grain size and sedimentary structures. A summary for each of the lithologic units was compiled in the OMNI/Weatherford report with photographs of the slabbed core (Appendix B).

o   *Outer Shelf – Slope Shale/Claystone*

The sections 5850-5850.6 ft and 5897-5903.7 ft consist of featureless, dark grey shale and/or claystone. Both pyrite and siderite are present in the rock. Silt laminations and lenticular ripple bedding is present from 5902.3-5903.7 ft. Due to the lack of wave formed sedimentary structures with coarse grained layers or storm lag deposits, the report interprets the units to have accumulated below storm wave-base and is categorized as an outer shelf – slope setting.

o   *Outer Shelf Bioturbated Shale/Mudstone*

From 5903.7-5906.2 ft, the unit consists of bioturbated silty shale and/or mudstone with Helminthoida, which is a 2D trace fossil represented by tightly packed meanders or spiral trails. The high abundance of burrows indicates a decrease in the sediment input in relation to the biogenic activity. The report identifies the unit from an outer shelf setting.

o   *Outer Shelf Shale/Mudstone*

The section from 5906.2-5926.4 ft is composed predominantly of laminated and lenticular ripple bedded, silty shale/mudstone with burrows. From 5908.4-5910 ft the trace fossil Helminthoida is abundant. The lenticular bedding and laminations are indicative of a coarser sediment transport most likely with some traction transport along the sea bottom. There is a

scour feature at 5924.4 ft that has been filled with silt or very fine grained sand that has inclined or wave-rippled bedding. At 5926 ft there is a storm deposit bed with abundant shell deposits. There is an abundance of burrowing and traces of <u>Helminthoida</u>, <u>Planolites</u>, and <u>Chondrites</u> in the bioturbated silt-rich beds. Due to the presence of erosional scours and wave-formed features the report interprets the section to have accumulated above storm wave base yet below normal wave base. The coarse silt-rich beds have sharp bases indicative of higher energy events, such as storm lag deposits or debris flows. This unit has been identified as an outer shelf setting.

- o *Outer Shelf – Slope Shale/Mudstone*

From 5926.4-5955.8 ft, the unit consists of slightly laminated, argillaceous mudstones. The majority of the layering is slightly disturbed from soft sediment deformation. There are a few burrow traces of <u>Planolites</u>. At 5928.8 ft there is a thin bed of calcareous skeletal fragments. The unit is interpreted to have accumulated below storm wave base due to the lack of wave formed features. The deformed beds may be due to a down slow creep and subsequent soft sediment deformation. The unit is identified as an outer shelf setting.

- o *Outer to Inner Shelf Fining-Upward Shaley Sandstone to Shaley Siltstone*

The section from 5955.8-5968 ft is a bioturbated sequence gradually fining upward from a shaley, fine grained sandstone to a shaley siltstone. There are bioturbated laminations of sand between 5959-5963.2 ft. Many burrow traces are present including (in order of abundance) <u>Chondrites</u>, <u>Helminthoida</u>, <u>Phanolites</u>, <u>Asterosoma</u>, and <u>Zoophycos</u>. Due to the gradual decreasing grain size, the unit is interpreted to have accumulated within a gradually deepening marine setting. According to Chamberlain (1978), the trace fossil assemblage is indicative of an inner to outer shelf setting.

- o *Inner Shelf/Offshore Bioturbated Sandstone*

From 5968-5973.7 ft is a bioturbated, fine grained sandstone to a shaley siltstone containing numerous burrow traces. Identifiable burrow traces include (in order of abundance) Chondrites, Helminthoida, Asterosoma, Phanolites, Zoophycos, Teichnichnus/Diplocraterion, and Thalassinoides. The base of the unit contains a 0.10 ft thick layer of dark, gray shale. The section is interpreted to have accumulated well above storm wave base, but the lack of preservation of physical sedimentary structures indicates that the setting is below the normal wave base. The trace fossil assemblage is indicative of an offshore/inner shelf setting (Chamberlain, 1978).

- o *Transgressive Fluvial/Deltaic Sandstone*

The section from 5973.7-5979.15 ft consists of a fining upward sequence of cross-bedded and sub-horizontally laminated stacked beds of fine to medium grained sandstone. There is some contoured layering from soft sediment deformation present due to slumping or contortion during high depositional flow velocities. The sandstone beds from 5973.7-5974.2 ft are well burrowed with identifiable traces consisting of numerous Chrondrites, Planolites, and Terebellina. There is a fine grained sandstone bed from 5974.2-5975.7 ft containing subhorizontal laminations, contorted bedding, and some Planolites traces. There are not burrow traces found near the base of the unit. The unit is interpreted to have accumulated within an abruptly transgressive fluvial/deltaic system. The grain size of the unit is smaller than the sandstones below, possibly due to a decreasing channel gradient due to rising sea level.

- o *Fluvial/Deltaic Channel Sandstone*

From 5979.15-6005.1 ft is a unit comprised of sandstone and shale. The top of the unit consists of dark, gray shale from 5979.15-5979.5 ft. The sandstone portion of the unit consists of

stacked beds of fine to medium grained sand that predominantly contains large scale trough cross-bedding. Ripple-bedded sandstones are also present. Soft sediment deformation is the form of slumping and contorted beds is common. There is a fluid escape feature at 5983.6 ft. That feature attests to the rapid rates of deposition. There are roots present from 5993.8-5996.9 ft. The presence of roots indicates subaerial exposure of the system. The unit is interpreted to have accumulated within a fluvial/deltaic system of a relatively coarse grained meandering system. The meander system would contain chute bars versus the strictly fining upward point bars.

PETROGRAPHIC ANALYSIS

OMNI/Weatherford Laboratories performed a petrographic analyses on samples from 3 sandstone lithologic/depositional units: the inner shelf/offshore bioturbated sandstone (5968-5973.7 ft), the transgressive fluvial/deltaic sandstone (5973.7-5979.15 ft), and the fluvial/deltaic channel sandstone (5979.15-6005.1 ft). Detail thin sections descriptions were conducted on 10 of the 36 thin sections produced (Appendix C). All 36 samples were examined by x-ray diffraction (XRD) analysis and by scanning electron microscopy (SEM). The petrographic examination summary is divided into sections. The sections of the examination are sedimentary fabric and texture, framework grain mineralogy, cementation, and pore networks/reservoir quality.

There were 7 thin sections examined from the fluvial/deltaic channel sandstone unit ranging from moderate to moderately well sorted and fine to medium grained. Stylolites are common in the unit below 5987 ft. Within the fluvial/deltaic channel sandstone there is an almost vertical fracture infilled with a maximum thickness of 1.00 mm of calcite cement from 5992.5-5994 ft. The only thin section analyzed from the transgressive fluvial/deltaic sandstone unit

consists of a moderately well sorted, medium grained sandstone. The inner shelf/offshore

bioturbated sandstone unit is made up of 7 to 11% (by weight) of the sandstone based on XRD

analysis of 4 samples. The average measured porosity for the inner shelf/offshore bioturbated

sandstone unit is 9%. The transgressive fluvial/deltaic sandstone unit has an average measured

porosity of 6.5% versus a 5.7% for the fluvial/deltaic channel sandstone unit.

The sandstones within the cored intervals are primarily sublitharenites with only one

sample being a litharenite (Table 2 and Figure 21). The most common lithic fragments are

metamorphic rock fragments (MRF). The MRF average 5% by volume per model analysis and

range in abundance from 2 to 8%. The second most abundant lithic fragments are volcanic rock

fragments (VRF), which average 2% and range from 1 to 3% by volume. Mudstone and chert

fragments are also present, but less common, ranging from trace to 2% by volume. There is a low

amount of feldspar of approximately 3% by volume based on modal thin section analysis. The

low abundance of feldspar is due to extensive leaching of feldspar grains and the formation of

secondary intragranular porosity.

Quartz overgrowth cement is the most abundant cement in the sandstone unit. Based on

modal analysis of 10 thin sections, the quartz overgrowth cement averages 16% and ranges from

7 to 20% by volume in abundance. The second most abundant cement is pore-lining clay. The

pore-lining clay averages 2% by volume and ranges from 1 to 4% in abundance based on thin

section modal analysis. The most common clay mineral within the rock unit is chlorite clay.

Chlorite clay averages 4%, while Illite averages 3% (by weight). The total clay content averages

9% based on XRD. Based on the SEM examinations, chlorite and illite are present lining pores

throughout the interval (Plates 37B, 37C, 43B, 69D). Some of the pore-lining clays form bands

of microporosity between the framework grains and the quartz overgrowths. Authigenic clay is also present as grain replacement, as can be seen in Plate 33B. Pyrite is the next most abundant replacement mineral, averaging 1% by volume based on modal thin section analysis (Plates 30A, 33A, 40A). Other replacements minerals include carbonate cements, such as Fe-dolomite and Fe-calcite. There are replacement minerals of feldspar grains or feldspathic components of lithic grains such as plutonic rock fragments (Plates 4B, 11B, 33B, 36B).

Of the 10 thin sections (Table 2), only 2% primary intergranular porosity is observed from examination by modal analysis. Most of the intergranular porosity has been reduced by quartz overgrowth cement. The majority of porosity exists as secondary intragranular pores derived from the dissolution of feldspars or the feldspathic components of lithic fragments. The secondary porosity totals about 50% of the average total porosity (7%) observed in the 10 thin sections. An average of less than 2% of the total rock volume based on modal analysis is microporosity occurring within the remnants of framework grains replaced by clay (Plate 33B).
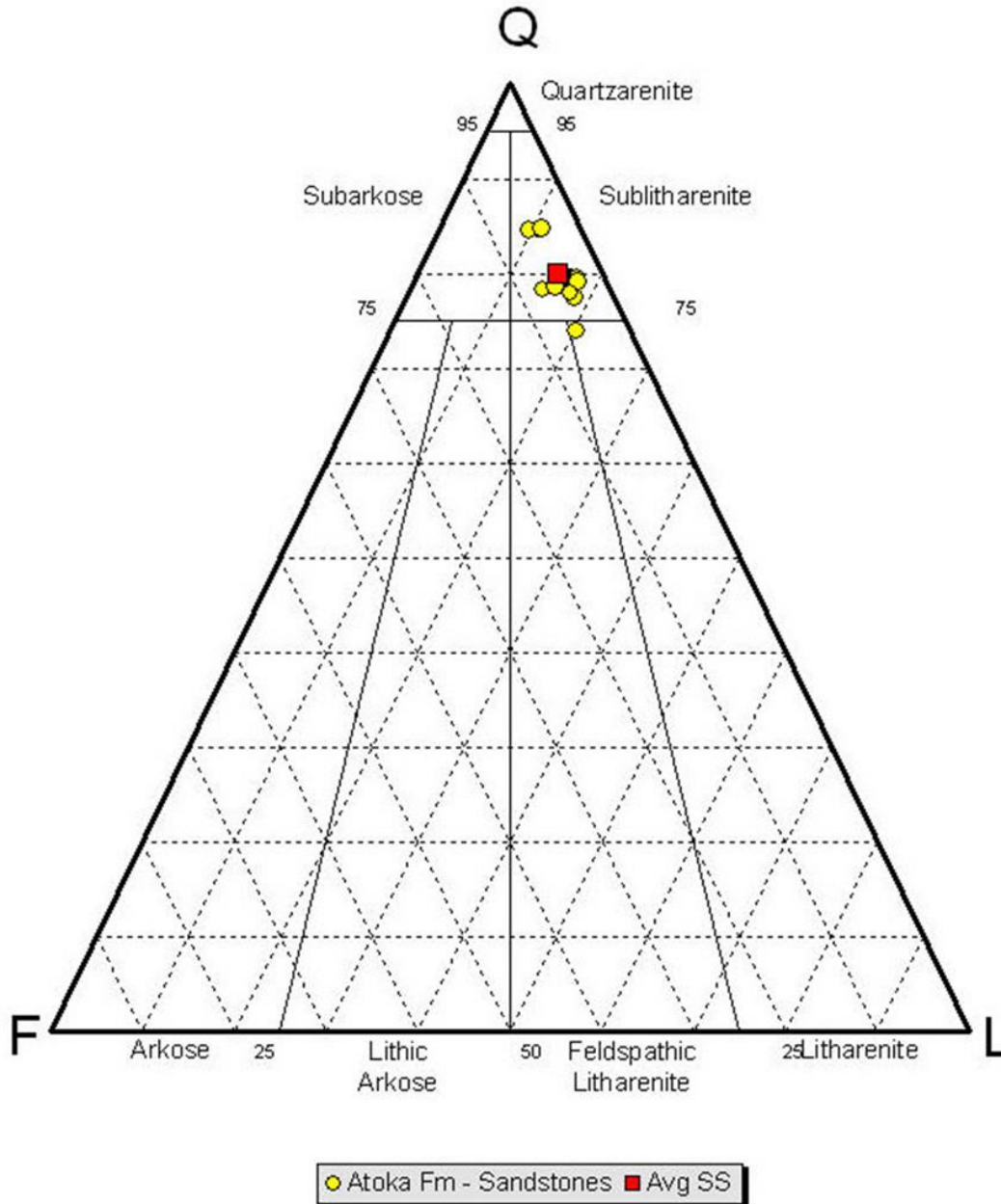
Figure 21. Modified from OMNI/Weatherford Laboratories Gordon F. Moore 19 Core Report. QFL diagram showing composition of Atoka Formation sandstones from the Gordon F. Moore No. 19 cored interval based on classification of Folk (1980). This diagram used the 10 thin sections of the detailed thin section (modal) analysis described in Appendix B. 9 of the 10 samples are sublitharenites with one sample classified as a litharenite.

GRANT STRATIGRAPHY

The stratigraphy of the Grant for this study is based on the Gordon F. Moore No. 19 well. Based on the analysis of the data reported above, this study suggests a subdivision of the Grant Formation into 10 lithostratigraphic units, 6 units in the Lower Grant Sand and 4 units in the Upper Grant Sand (Figure 19). The author is not aware of any previous publication subdividing the Grant Sands. Divisions were made based on the wireline log curves: Gamma Ray, Resistivity (ILD), and Porosity (DPHI). The division of units is supported by the conventional core for the Upper Grant and by the formation image interpretation by Fronterra Geosciences for both the Upper and Lower Grant.

LOWER GRANT

The Lower Grant lithostratigraphy is based on log curves (gamma, resistivity, and porosity) and the formation image interpretation report by Fronterra Geosciences for the Gordon F. Moore No. 19. A conventional core would allow for a more complete analysis of the Lower Grant stratigraphy. The Lower Grant of the Gordon F. Moore No. 19 can be subdivided into 6 units of alternating sandstones and shales (Figure 19).

The base of the Lower Grant is a ripple/irregular bedded sand with a sharp base. The bottom of the Lower Grant has a sharp base and is marked the "Lower Grant Unconformity (GRANT_U/C)". The unit at the base of the Lower Grant (Unit A) is an argillaceous sandstone unit of 45-50 ft thick with ripple/irregular bedding and a couple of very thin siltstone/sandy mudstone layers of 2 ft or less. The gamma ray and resistivity curves show the sands to be

48

separated from interbedded shales. The intervening shales hinder the resistivity, showing an average of roughly 25 OHM•M. Above the base unit (Unit B) is a layer of ripple/irregular bedded mudstone/shale of approximately 6 ft. The middle unit of sand (Unit C) is just over 35 ft of argillaceous sand with a couple thin layers of interbedded larger grain sandstone. Unit C is composed of sands slightly cleaner than those of Unit A, but overall Unit C is also separated with intervening shale layers that hinder the resistivity. Dividing the middle and upper units of sand is a unit of approximately 8 ft of mudstone/shale (Unit D) with a siltstone/sandy mudstone layer of 2-3 ft in the center. The top sandstone unit (Unit E) is about 20 ft thick of a larger grain sandstone with ripple/irregular bedding. Unit E has some shale layers interbedded, but is a cleaner sand package than the sands below. Overall, the sands of the Lower Grant are separated with intervening shales, but become cleaner moving up section. The upper most unit (Unit F) of the section is roughly 40 ft of interbedded mudstone/shale and sandstone. Above the Lower Grant is an interval of mudstone/shale (Unit G) of approximately 75 ft thick dividing the Upper Grant and Lower Grant.

UPPER GRANT

The Upper Grant lithostratigraphy is based on the log curves (gamma, resistivity, and porosity), conventional core, and the formation image interpretation report by Fronterra Geosciences for the Gordon F. Moore No. 19. The Upper Grant of the Gordon F. Moore No. 19 can be subdivided into 4 units shown in Figure 19. The bottom of the Upper Grant has a sharp base with the abrupt change from mudstone/shale to sandstone. The lowest unit (Unit H) of the Upper Grant is 50-55 ft thick, appears "blocky" on the gamma ray, and is composed of clean

sands with crossbeds (>15˚), ripple/irregular bedding, and parallel bedding based on the

Fronterra image log report. With the approximately 15 ft offset of the core considered, the lowest

sand unit correlates to the "fluvial deltaic channel sandstone" section depicted by

OMNI/Weatherford Laboratories in the core report. The resistivity reaches over 300 OHM•M at

its highest peak with an average of about 170 OHM•M. This high resistivity could be due to the

tightness of the sand or from to the presence of gas. The middle unit (Unit I) in the Upper Grant

is a fine sandstone approximately 10 ft thick and slightly fines upward. Unit I reaches a

resistivity of roughly 30 OHM•M. The uppermost unit (Unit J) is just over 10 ft thick that

gradually fines upward. Correlating the log to the core report, unit J is a shaley sandstone to

shaley siltstone. Above the Upper Grant is a large unit of shale and mudstone leading up to the

Pregnant Shale Formation.

MINERALOGY AND COMPLETIONS

Depending on the fluids, contact with specific minerals can damage a formation during

drilling, completion and stimulation. The total clay content average of 9% for the Upper Grant

Sand is not necessarily an issue for completions, but the 4% chlorite pore-lining clay (of the

total) is definitely an issue when completions fluids are being considered. The fluids introduced

into the formation preferentially contact the pore-lining and pore-filling minerals. Chlorite is a

mineral containing iron and is sensitive to HCl acid and oxygen-rich fluids. The iron is released

during acidizing causing the partial to complete dissolution of the minerals. They can rapidly

precipitate, blocking pore throats and can immediately reduce permeability. With the presence of

4% (average) chlorite pore-lining clay and a total average porosity of 7%, acids should not be used in regards to the Grant Sands to avoid formation damage.

DEPOSITIONAL ENVIRONMENT

The Grant Formation was deposited during a lowstand (Figure 22) in a basin with a shelf break of a type 1 sequence (Van Wagoner *et al.*, 1988). The type 1 sequence overlies a type 1 sequence boundary which is "characterized by subaerial exposure and concurrent subaerial erosion, associated with stream rejuvenation, a basinward shift of facies, a downward shift in coastal onlap, and onlap of overlying strata" (Van Wagoner *et al.*, 1988). Due to the basinward shift in facies, deeper water marine rocks can be directly overlain by non-marine or shallow marine rocks. Van Wagoner *et al.* (1988) interprets the type 1 sequence boundary to form when the rate of eustatic fall exceeds the rate of basin subsidence at the depositional shoreline break, producing a relative fall in sea level at that position.

The lowstand systems tract is subdivided into 3 units, the basin-floor fan (lower most unit), slope fan (middle unit), and lowstand wedge (uppermost unit) (Van Wagoner *et al.*, 1988). The Lower Grant Sand is a component of the slope fan and/or the basin-floor fan (Figure 22). The basin-floor fan is characterized of submarine fans associated with the erosion of canyons into the slope and incised fluvial valleys into the shelf. The slope fan unit is characterized by turbidite and debris flow on the middle to base of the slope (Van Wagoner *et al.*, 1988). The Fronterra image log exhibits soft sediment deformation in the Lower Grant possibly representing a mass transport complex. The image log data supports an argument for the slope fan unit over

the basin-floor fan of the lowstand systems tract, but without further information, such as core(s) of the Lower Grant and/or seismic data, a definitive conclusion for slope fan or basin floor fan cannot be made in this study.

I interpret the Upper Grant Sand as a component of the lowstand wedge unit of the lowstand systems tract (Figure 22). The lowstand wedge is bounded above by the transgressive surface (Van Wagoner *et al.*, 1988). The OMNI/Weatherford core report categorizes the Upper Grant to be "from a predominantly fluvial setting to outer shelf/slope marine setting". The Fronterra image log data for the Upper Grant characterizes the sands to be from slope channel complexes sourced from the northeast (determined from 79 cross-beds). Figure 22 depicts an example of a well log response of lowstand wedge from a section illustrated in red to represent fluvial or estuarine sandstones within incised valleys. The well log response is ideally similar to the log response for the Upper Grant Sand.

The lowstand conceptual model (Figure 22) also allows for explanations of the shale unit between the sandstones of the Grant and the additional sand discovered to the south of the Upper Grant. The model depicts a unit of shelf and slope mudstones between the slope fan and shallow marine to fluvial sandstones at the top of the lowstand wedge. The shallow marine sandstones depicted in the model (Figure 22) could be an explanation for the Upper Grant South sand, but without complete mapping of that unit and other additional data, that determination is only conjecture.
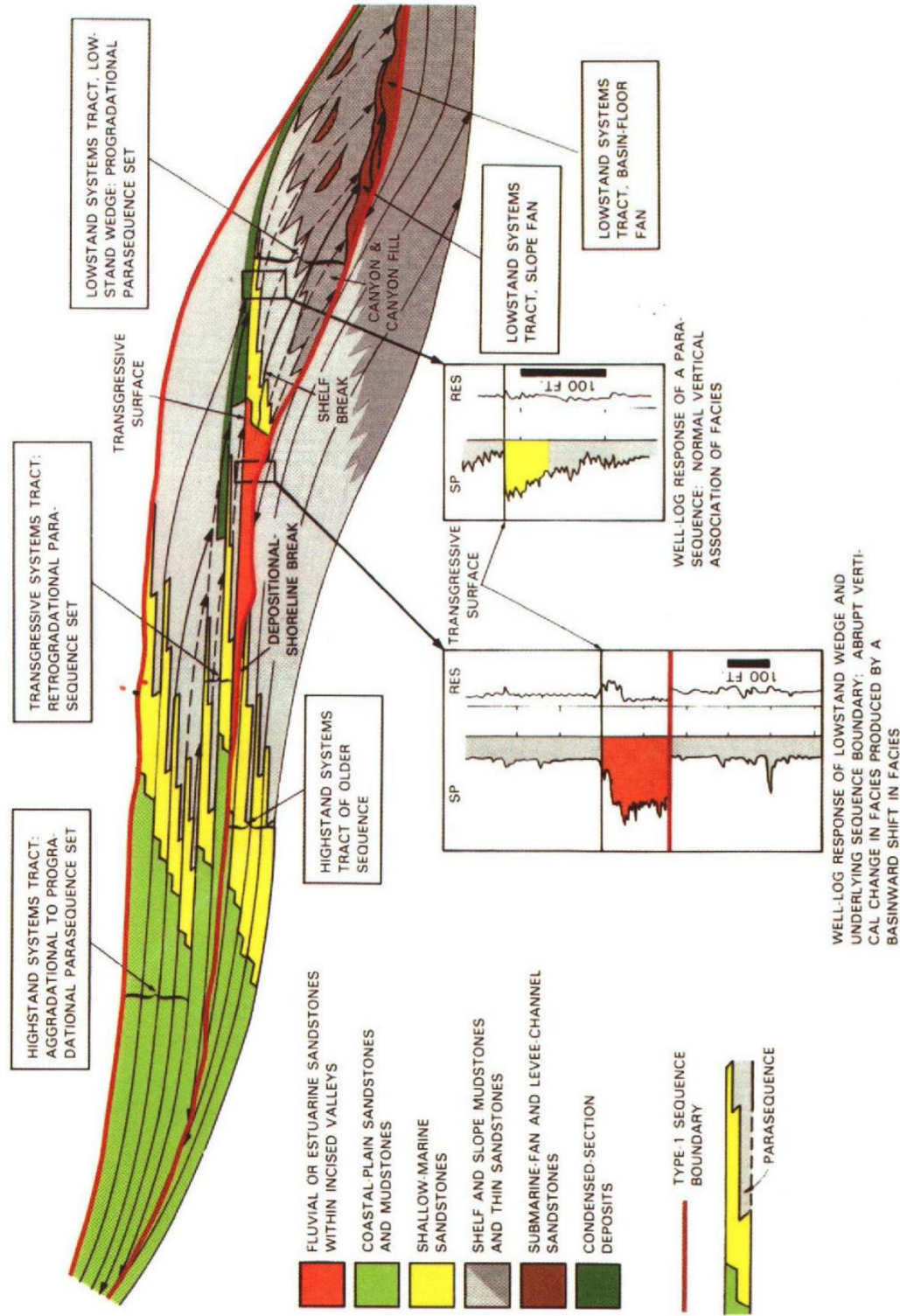
Figure 22. Modified from Van Wagoner *et al.* (1988) as a conceptual model for the depositional setting of the Grant Formation. The Grant Formation was deposited during a lowstand in a basin with a shelf break of a type 1 sequence, as outlined by Van Wagoner *et al.* (1988). During a lowstand there is a basinward shift of facies. The Lower Grant Sand is a component of the slope fan and/or the basin-floor fan. The Upper Grant Sand is a component of the lowstand wedge unit.

CONCLUSIONS

      The Grant Sands are both productive tight gas sand units with future potential for further production. The use of maps from this study, specifically the net sand maps of the Upper and Lower Grant, will assist with the planning of new drills for Grant wells and up-hole recompletions of Barnett Shale wells. The core examinations determined subdivisions of depositional/lithologic units that were used with log curves to construct a detailed stratigraphic analysis of the Grant Formation. The subdivisions can be used with drilling data, such as landing zones, to determine ideal target facies for drilling. The mineralogical analysis concluded that the Grant has an abundance of chlorite as pore lining clay, therefore slickwater would be the optimal completions fluid. Well correlations, maps, image log data, and information from previous investigations were used to collectively conclude that the Grant Formation was deposited during a lowstand in a basin with a shelf break of a type 1 sequence. Determining a conceptual model for deposition is important because it introduces possible new exploration targets, such as the Upper Grant South. In conclusion, the Grant Sands are productive, they can be more productive, and there may be additional reserves in the Grant Sand play.

WORKS CITED

Blanchard, K. S., O. Denman, and A. S. Knight. (1968). Natural gas in Atokan (Bend) section of northern Fort Worth Basin, in B. W. Beebe and B. F. Curtis, eds., Natural gases of North America: AAPG Memoir 9, p. 1446–1454.

Chamberlain, C. K. (1978). Recognition of trace fossils in cores: (in) Trace Fossil Concepts SEPM Short Course No. 5: (Eds. Basan, P.) SEPM, p. 119-166.

Flawn, P. T. (1956). Basement Rocks of Texas and Southeast New Mexico. University of Texas at Austin, Bureau of Economic Geology Publication 5605, p. 261.

Flawn, P. T. (1959). The Ouachita Structural Belt[1]. The University of Texas at Austin, Bureau of Economic Geology. The Geology of Ouachita Mountains Symposium, p. 20-29.

Flawn, P. T., Goldstein, A. Jr., King, P. B., and Weaver, C. E. (1961). The Ouachita System. The University of Texas at Austin, Bureau of Economic Geology Publication 6120.

Folk, Robert L. (1980). Petrology of Sedimentary Rocks. Hemphill Publishing Company. Austin, Texas.

Gardner, R. A. (1960). The Boonsville (Bend Conglomerate Gas) field, Wise County, Texas: Abilene Geological Society, Geological Contributions 1960, p. 7-17.

Hentz, T. F., W. A. Ambrose, and D. L. Carr. (2012). Reservoir systems of the Pennsylvanian lower Atoka Group (Bend Conglomerate), northern Fort Worth Basin, Texas: High-resolution facies distribution, structural controls on sedimentation, and production trends. AAPG Bulletin, V. 96, No. 7 (July 2012), p. 1301–1332. DOI:10.1306/10041111078.

Johnson, K. S., T. W. Amsden, R. E. Denison, S. P. Dutton, A. G. Goldstein, B. Rascoe, P. K. Sutherland, and D. M. Thompson. (1989). Geology of the southern mid-continent: Oklahoma Geological Survey Special Publication 89-2, p. 53.

Lahti, V. R. and W. F. Huber. (1982). The Atoka Group (Pennsylvanian) of the Boonsville field area, north-central Texas, *in* C. A. Martin, ed., Petroleum geology of the Fort Worth Basin and Bend arch area: Dallas Geological Society, p. 377–399.

Lovick, G. P., C. G. Mazzine, and D. A. Kotila. (1982). Atokan clastics: Depositional environments in a foreland basin. C. A. Martin, ed., Petroleum geology of the Fort Worth Basin and Bend arch area: Dallas Geological Society, p. 193–212.

Maharaj, V. and L. Wood. (2009). A quantitative paleo-geomorphic study of the fluvio-deltaic reservoirs in the Atoka interval, Fort Worth Basin, Texas, U.S.A.: Gulf Coast Association of Geological Societies Transactions, v. 59, p. 495-509.

Ng, D. T. W. (1979). Subsurface study of Atoka (Lower Pennsylvanian) clastic rocks in parts of Jack, Palo Pinto, Parker, and Wise counties, north-central Texas. AAPG Bulletin, 63(1), 50-66.

Ng, D. T. W. (1982). Subsurface study of Atoka (Lower Pennsylvanian) clastic rocks, north-central Texas. North Texas Geological Society. Basins of the Southwest – Phase 2, p. 155-191.

OMNI/Weatherford Laboratories Staff. (2008). Final Report: Petrographic and Sedimentological Study of Conventional Cores from the Atoka Formation. Devon Energy Corporation – OKC – Gordon F. Moore Gas Unit No. 19.

Plummer, F. B. (1919). Preliminary paper on the stratigraphy of the Pennsylvanian formations of north-central Texas. AAPG Bulletin, v. 3, no. 1, p. 132-150.

Tilford, M. J. and M. R. Stewart. (2011). Barnett Shale and Atoka Conglomerate: The next horizontal oil and gas play in Oklahoma. Shale Shaker – Oil and Gas Exploration, July-August 2011, p. 10-31.

Turner, G. L. (1957). Paleozoic stratigraphy of the Fort Worth Basin. Abilene and Fort Worth Geological Societies, 1957 Joint Field Trip Guidebook, p. 57-77.

Thompson, D.M. (1982). Atoka Group (Lower to Middle Pennsylvanian), northern Fort Worth Basin, Texas: terrigenous depositional systems, diagenesis, and reservoir distribution and quality. The University of Texas at Austin, Bureau of Economic Geology, Report of investigations No. 125.

Van Wagoner, J. C., H. W. Posamentier, R. M. Mitchum, P. R. Vail, J. F. Sarg, T. S. Loutit, and J. Hardenbol. (1988). An overview of the fundamentals of sequence stratigraphy and key definitions. Sea-level changes – An integrated approach, SEPM Special Publication No. 42, p. 39–45.

Walper, J. L. (1982). Plate tectonic evolution of the Fort Worth Basin, in Martin, C. A., ed., Petroleum Geology of the Fort Worth Basin and Bend Arch area: Dallas Geological Society, p. 237–251.

ADDITIONAL READING

Ball, M.M. and W. J. Perry. (1996). Bend Arch-Fort Worth Basin Province (045), in Gautier, D.L., Dolton, G.L., Takahashi, K.I., and Varnes, K.L., eds., 1995 National assessment of United States oil and gas resources—Results, methodology, and supporting data: U.S. Geological Survey Digital Data Series DDS–30, p. 11.

Clark, F. T. and H. H. Bybee. (1951). Fort Worth Basin and Muenster Arch, North Central Texas. Bull. Amer. Assoc. Petrol. Geol, 35(2), p. 353-56.

Ewing, T. E. (1991). The Tectonic Framework of Texas (Text to accompany "The Tectonic Map of Texas"). University of Texas at Austin, Bureau of Economic Geology of Texas.

Gee, D. E. (1976). The Base of the Pennsylvanian in the Fort Worth Basin — Some regional comparisons above and below. Abilene Geological Society, Geological Contributions 1976, p. 5-10

Herkommer, M. A. and G. W. Denke. (1982). Stratigraphy and hydrocarbons, Parker County, Texas, in C. A. Martin, ed., Petroleum geology of the Fort Worth Basin and Bend arch area: Dallas Geological Society, p. 97–127.

Hill, R. J., D. M. Jarvie, J. Zumberge, M. Henry, and R. M. Pollastro. (2007). Oil and gas geochemistry and petroleum systems of the Fort Worth Basin: AAPG Bulletin, v. 91, p. 445–473.

Homann, Hermann. (2007). Formation Image Report: Facies and Depositional Environments of Atokan Sequences in Wells Gordon F. Moore 19 and S.H. Griffin Estate 19H, Denton County, Texas. Fronterra Geosciences.

McBroom, R. L. (1981). North-Central Texas. AAPG Bulletin, 65(10), p. 1854-1856.

Pollastro, R. M., R. J. Hill, D. M. Jarvie, and M. E. Henry. (2003) Assessing undiscovered
resources of the Barnett–Paleozoic total petroleum system, Bend arch–Fort Worth Basin
province, Texas (abs.): AAPG Southwest Section Convention, Fort Worth, Texas, March
1–5, 2003, 18 p., http://www.searchanddiscovery.com/documents/pollastro/index.htm.

Pollastro, R. M., R. J. Hill, D. M. Jarvie, and C. Adams. (2007). Geologic framework of the
Mississippian Barnett Shale, Barnett-Paleozoic total petroleum system, Bend arch-Fort
Worth Basin, Texas. AAPG Bulletin, v. 91, no. 4, p. 405-436, doi:
10.1306/10300606008.

Williams, L. (1982). The Viola Ordovician of southwest Montague County, in C. A. Martin, ed.,
Petroleum Geology of the Fort Worth Basin and Bend Arch area: Dallas Geological
Society, p. 253–259.

APPENDIX

Cross-Section A-A¹ (N-S)
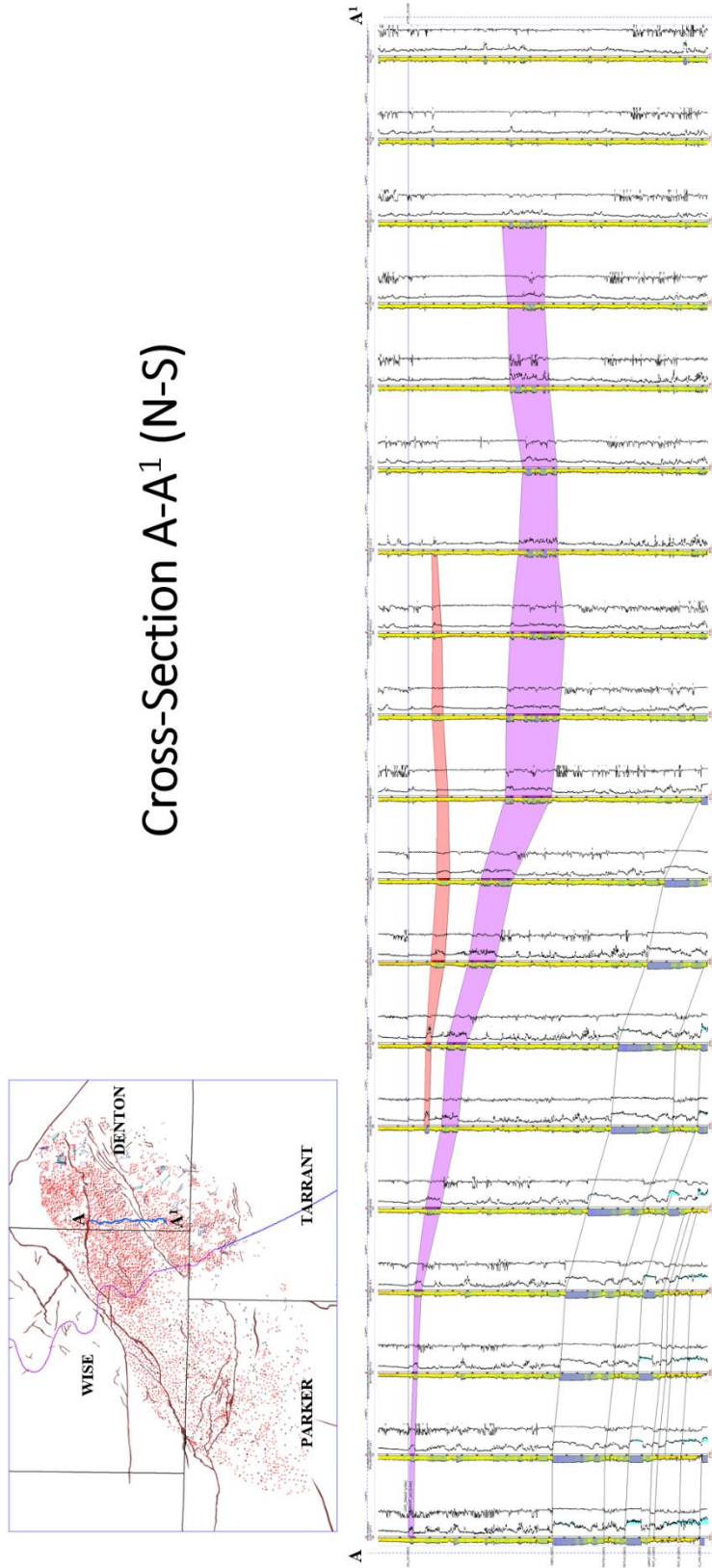
Stratigraphic cross-section hung on the ATOK_X0 marker with 19 wells, totaling a length of 10.2 miles north to south. The Upper Grant Sand is depicted in red and the Lower Grant Sand in purple.
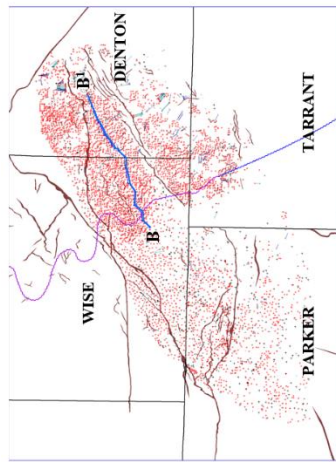
Cross-Section B-B¹ (W-E)
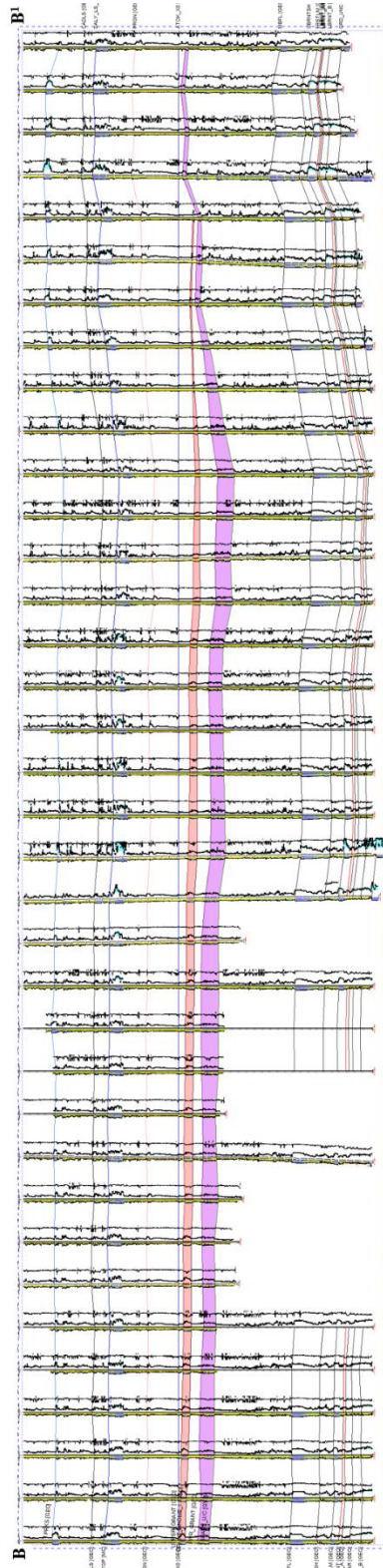
Stratigraphic cross-section hung on the ATOK_X0 marker with 36 wells totaling a distance of 19.48 miles west to east. The Upper Grant Sand is depicted in red and the Lower Grant Sand in purple.

APPENDIX B – Core Photographs
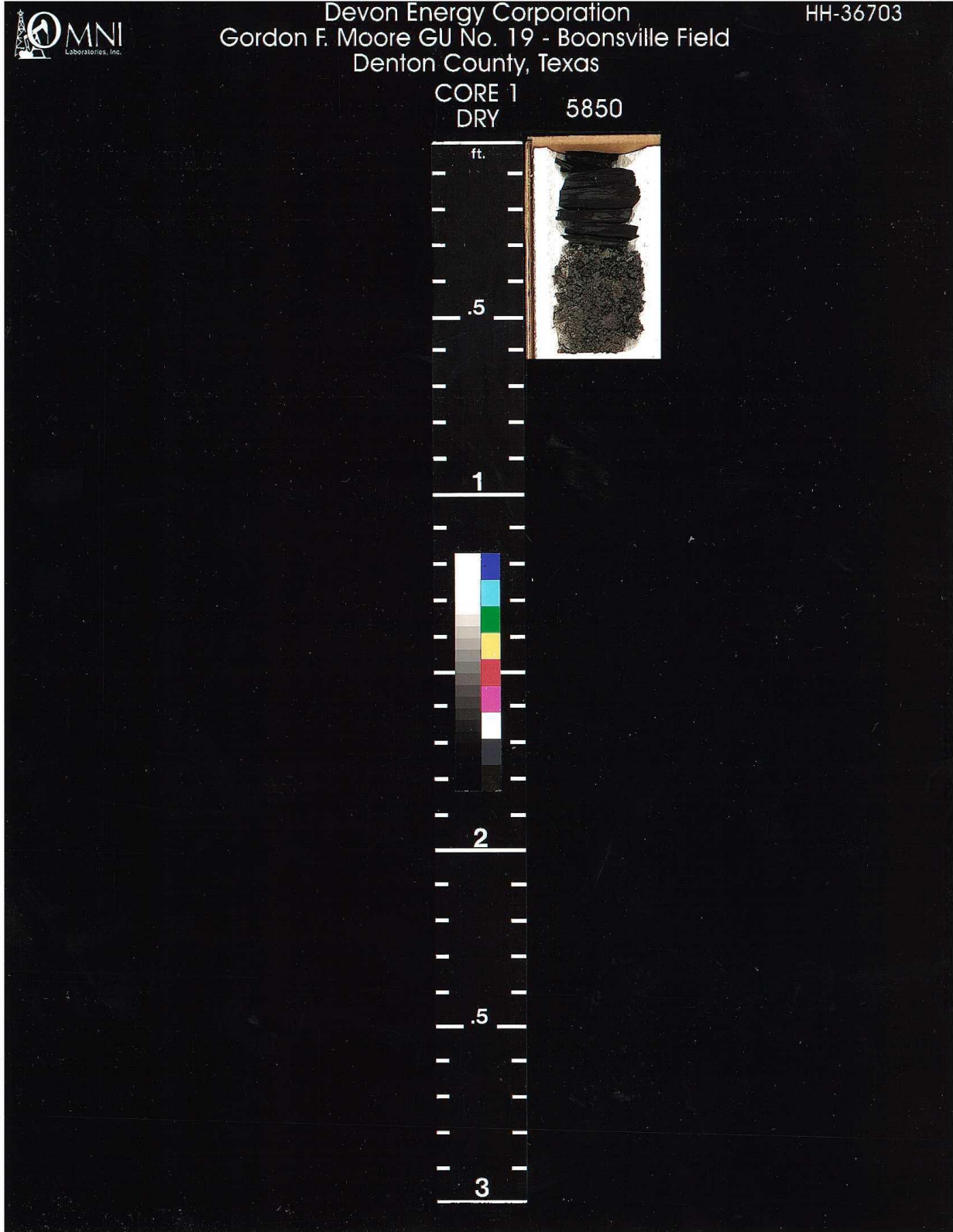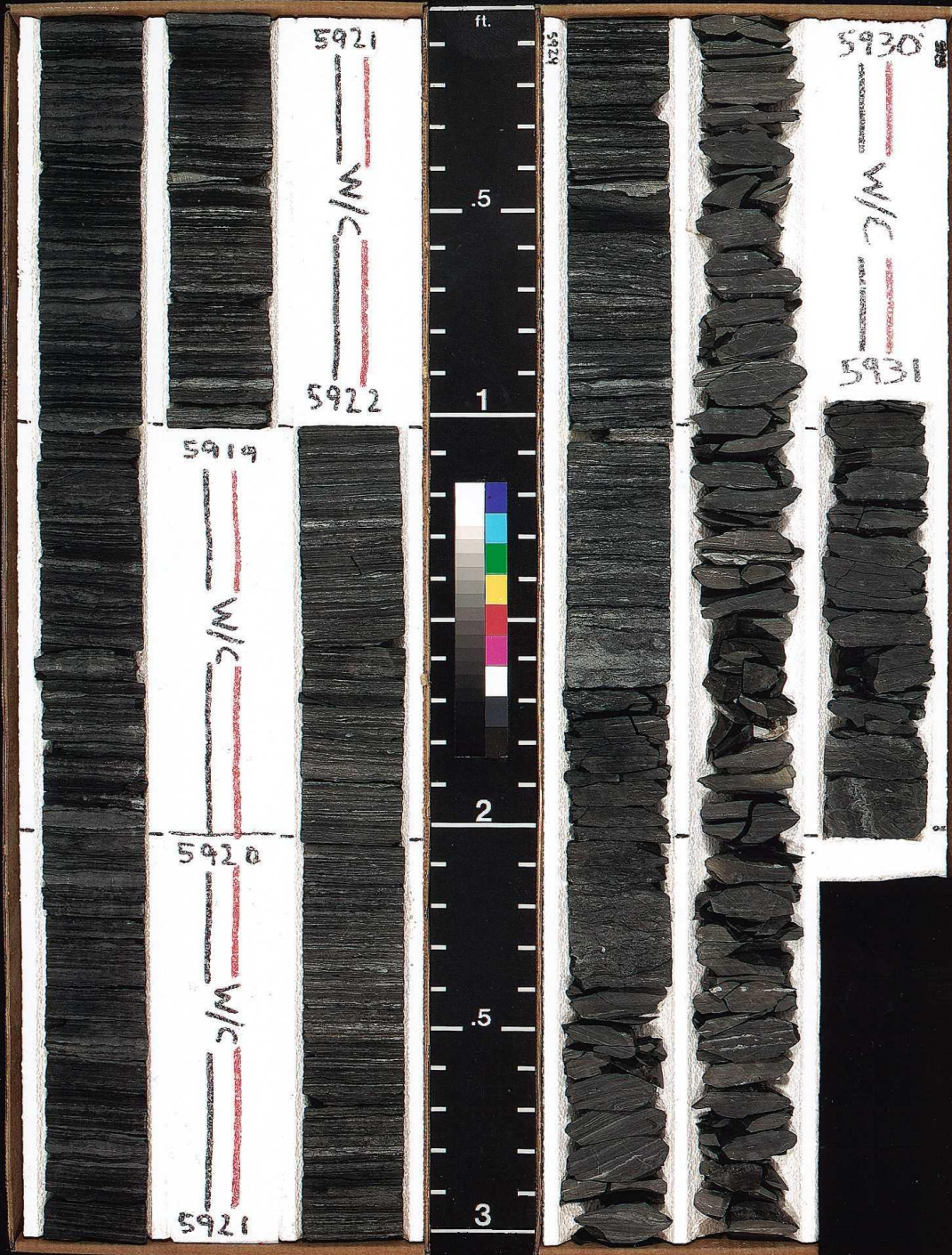
Devon Energy Corporation
Gordon F. Moore GU No. 19 - Boonsville Field
Denton County, Texas
HH-36703

CORE 2
DRY

5897   5900   5903   5906   5909   5912

Devon Energy Corporation
Gordon F. Moore GU No. 19 - Boonsville Field
Denton County, Texas
HH-36703
CORE 2
DRY

5915 5918 5921 5924 5927 5930

CORE 3
DRY

5935   5938   5941   5944   5947   5950

OMNI
Laboratories, Inc.
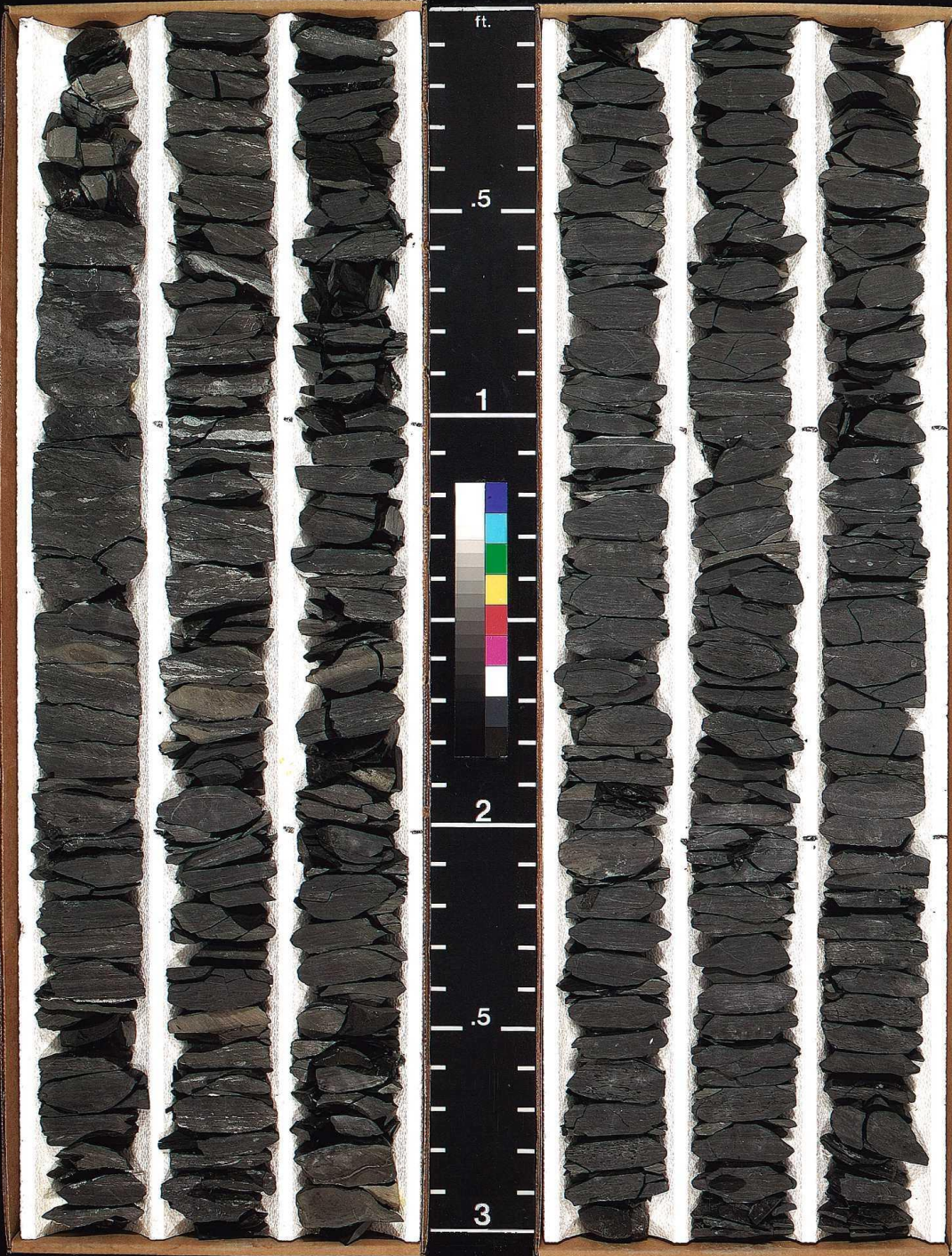
5953   5956   5959   **CORE 3 DRY**   5962   5965   5968
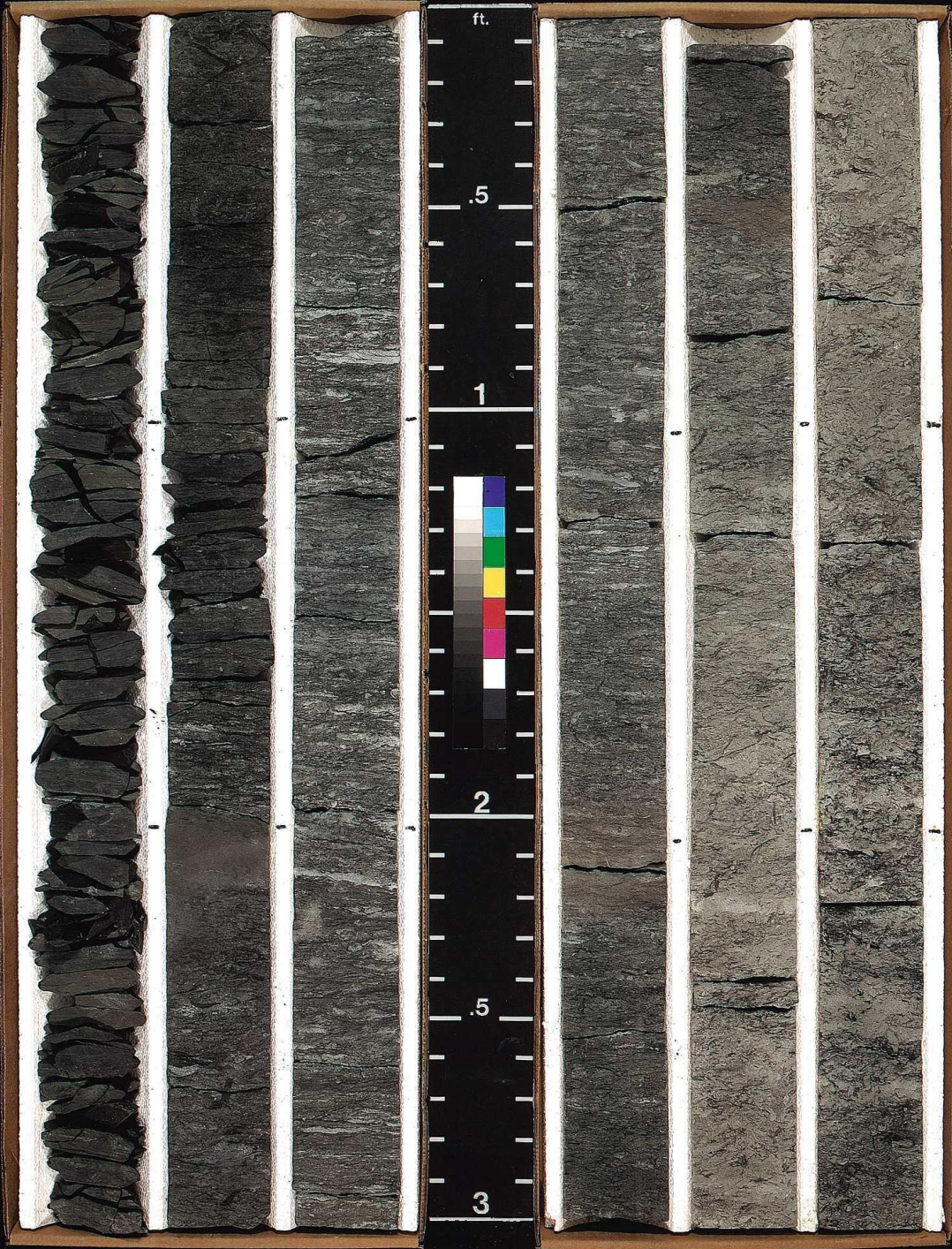
Devon Energy Corporation
Gordon F. Moore GU No. 19 - Boonsville Field
Denton County, Texas

HH-36703

CORE 3
DRY
5971

CORE 4
WET

5973   5976   5979

Devon Energy Corporation
Gordon F. Moore GU No. 19 - Boonsville Field
Denton County, Texas

HH-36703

OMNI
Laboratories, Inc.

CORE 5
WET

5979   5982   5985   5988   5991   5994

ft.

.5

1

2

.5

3

OMNI Laboratories, Inc.

CORE 5
WET

5997   6000   6003

CORE 6
WET

6004

ft.

.5

1

TOP OF
CORE
6

6004.6

6005.1
BOTTOM
CORE
6

6004.6
BOTTOM
CORE
5

2

.5

3
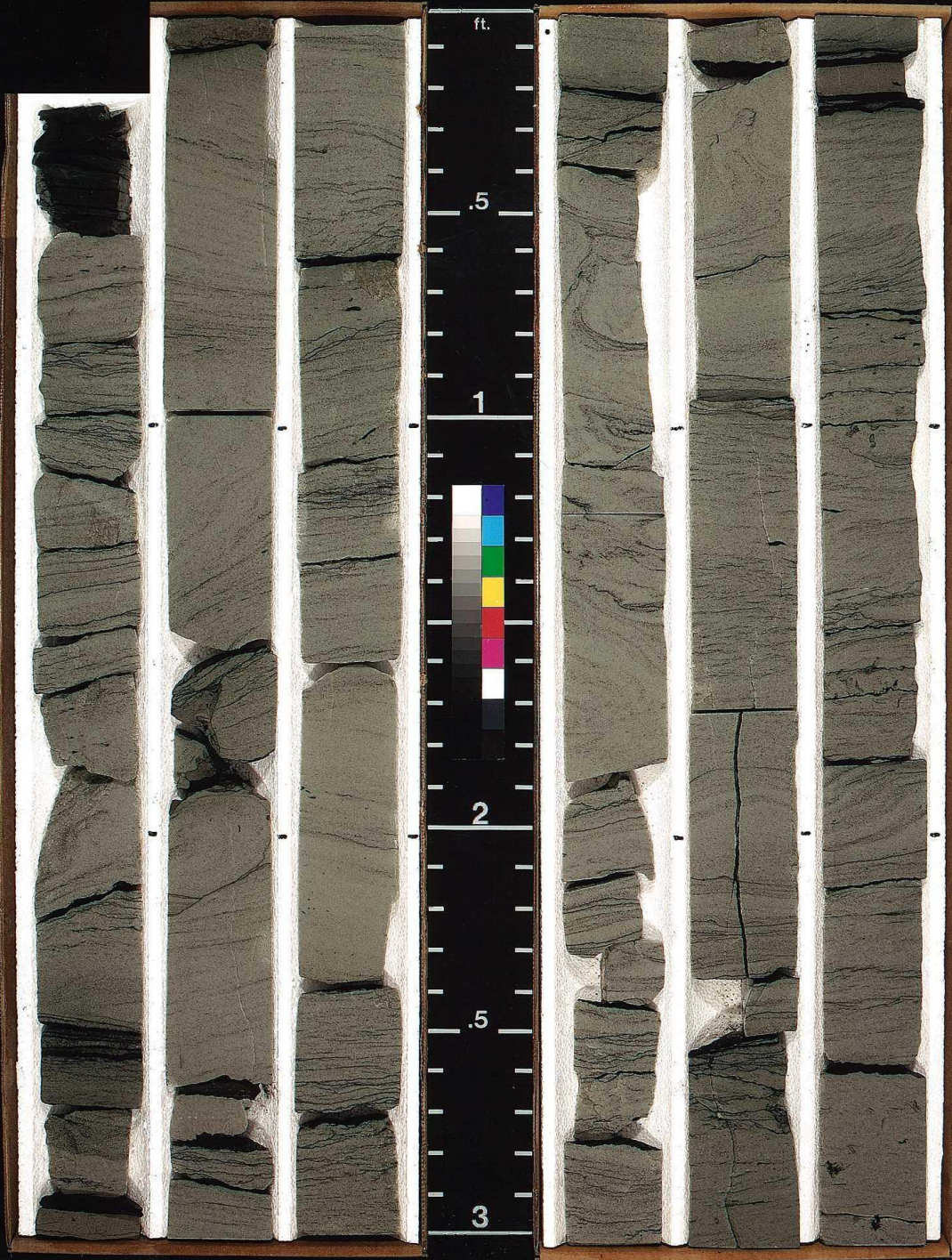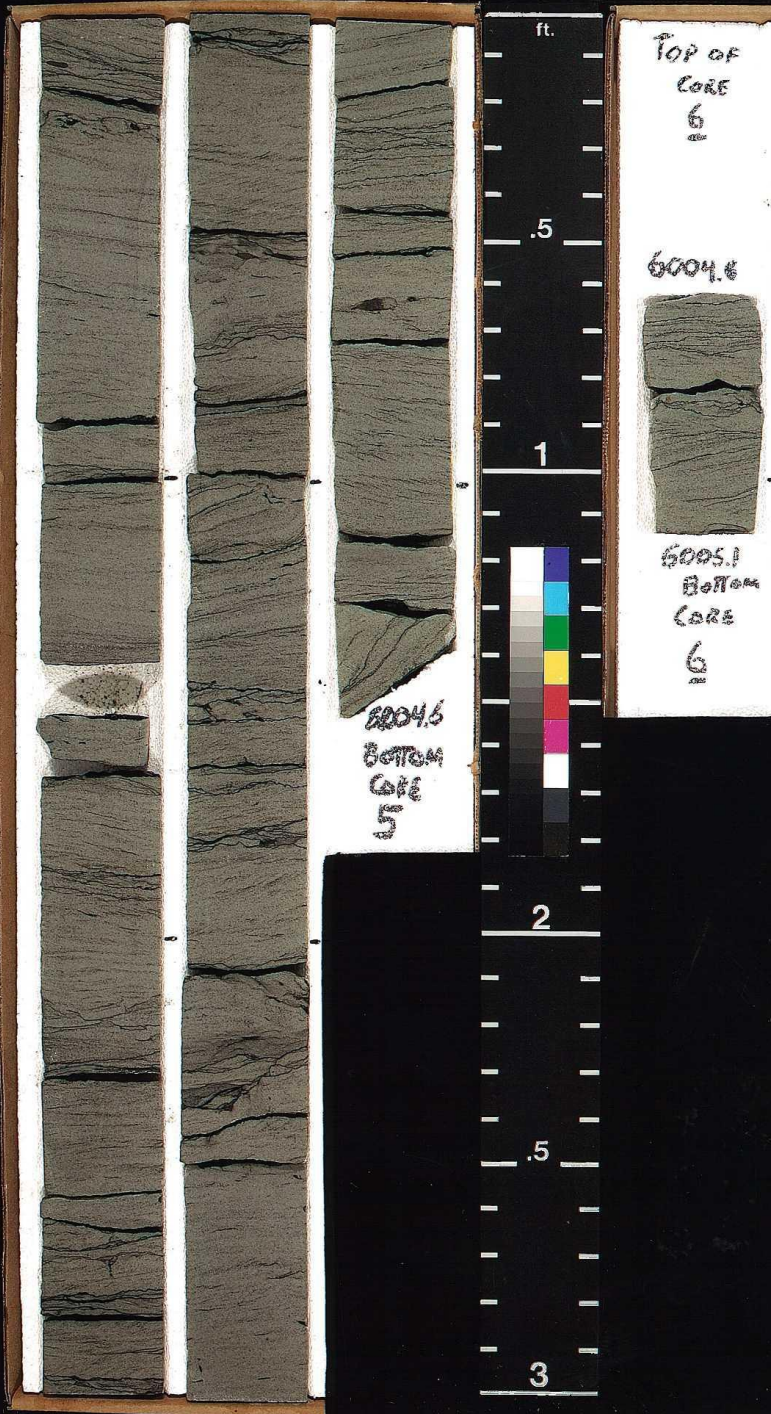
APPENDIX C – Selected Thin Section and SEM Photomicrographs with Descriptions

OMNI/Weatherford Laboratories performed a petrographic analyses on samples from the Gordon F. Moore No. 19 cored interval. A total of 36 thin sections were produced from samples of the core. All of the samples were examined by x-ray diffraction (XRD) analysis and by scanning electron microscopy (SEM). Detail thin sections descriptions were conducted on 10 of the 36 thin sections produced. The following are photomicrographs and descriptions of those 10 thin sections from the OMNI/Weatherford Laboratories.
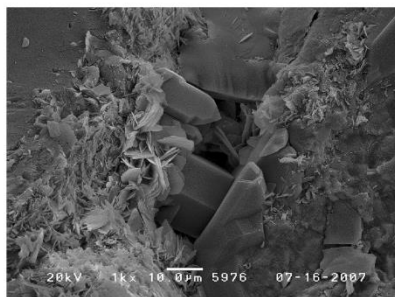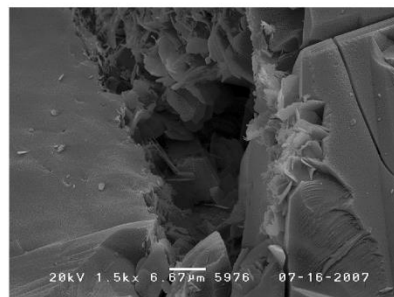
SAMPLE DEPTH: 5970.50 ft
SAMPLE NUMBER: 3-21

Measured Porosity*: 9.1%
Measured Permeability (air)*: 0.023mD
(*Net Confining Stress: 800 psi)
Grain Density: 2.66gni/cc

PLATE 1A
General view is of a fine-grained, well sorted sandstone with mudstone lithoclasts, and porosity consisting of a minimum of primary intergranular or intragranular pores microporosity.
Magnification: 40X
Light: Plane Polarized

PLATE 1B
Detailed view shows intergranular pores infilled with detrital clay and pseudomatrix which coincide with microporosity. Quartz overgrowth cement is abundant. Secondary intragranular pores are present within a partially leached framework grain.
Magnification: 200X
Light: Plane Polarized

PLATE 37
Fine sand-sized quartz (Plates A-D) is the primary detrital grain type in this moderately well sorted sublitharenite. Lithic fragments (Plate C and Plate D) are present in minor amounts. Quartz overgrowth cement (Plates A-D) reduces primary intergranular pore volume. Authigenic chlorite clay (Plate B, Plate C, and Plate D) occurs as grain-coating and pore-filling material. The platelet morphology of the clay (Plate B) has a high associated microporosity and is likely to contain irreducible water.
Magnification: 37A-100X
Magnification: 37B - 1000X
Magnification: 37C - 800X
Magnification: 37D - 1000X
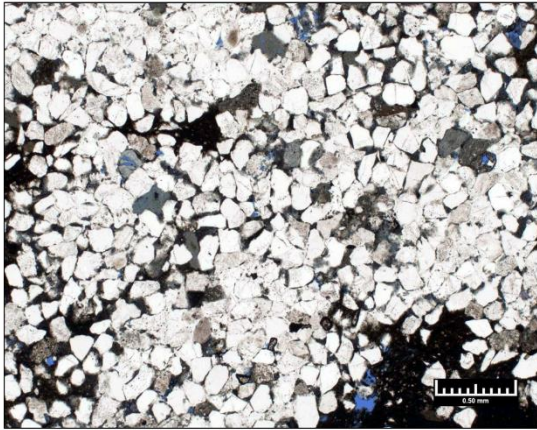
Plate 1A
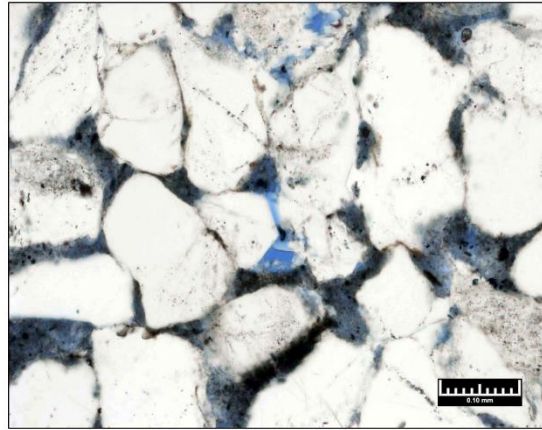
Plate 1B

Plate
37A
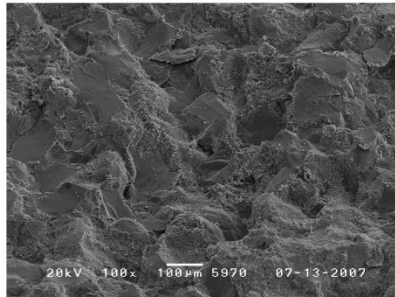
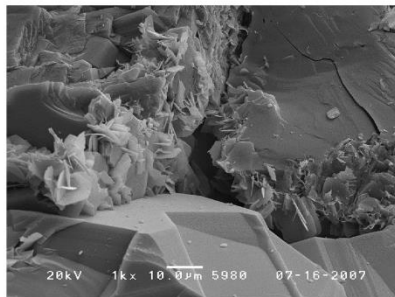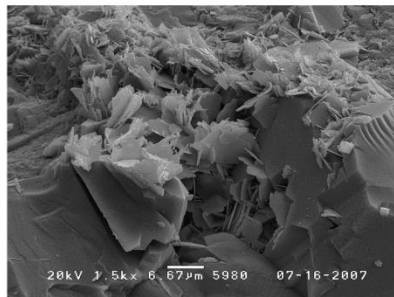

Plate
37B
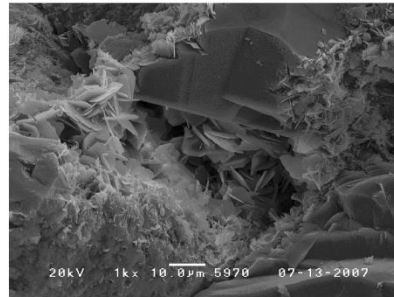
Plate
37C
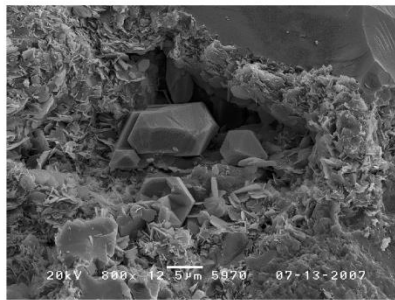
Plate
37D
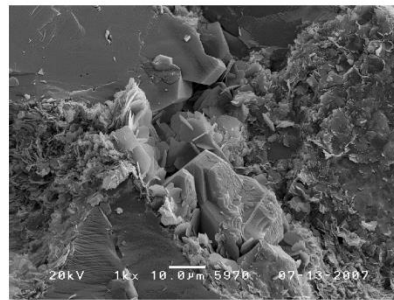
SAMPLE DEPTH: 5973.00 ft
SAMPLE NUMBER: 3-24

Measured Porosity*: 9.2%
Measured Permeability (air)*: 0.011mD
(*Net Confining Stress: 800 psi)
Grain Density: 2.66gm/cc

PLATE 4A
General view is of a medium-grained, moderately well sorted sandstone with
macroporosity restricted predominantly to secondary intragranular pores. Intergranular pores are
predominantly filled with quartz overgrowth cement detrital matrix or pseudomatrix.
Magnification: 40X
Light: Plane Polarized

PLATE 4B
Detailed view shows remnants of primary intergranular pores partially infilled with quartz
overgrowth cement. Ankerite is replacing a grain (stained blue). Detrital matrix or pseudomatrix
is infilling some pores.
Magnification: 200X
Light: Plane Polarized

PLATE 40
This medium-grained sandstone is classified as a sublitharenite. Quartz (Plate A, Plate B, and
Plate C) is the primary detrital grain type with lesser amounts of lithic fragments (Plate A and
Plate C) and feldspar. There is a minor amount of inter-mixed chlorite and illite clay coating
grains (Plate B) and filing pores (Plate C and Plate D). Quartz overgrowth cement (Plate A, Plate
C, and Plate D) is common. Grain-coating microcrystalline pyrite (Plate B) occurs in trace
amounts. Pore types include primary intergranular pores (Plate B and Plate C), secondary
intragranular pores associated with partially dissolved grains (Plate A), and micropores
associated with clays.
Magnification: 40A - 100X
Magnification: 40B - 1000X
Magnification: 40C - 100DX
Magnification: 40D - 1500X
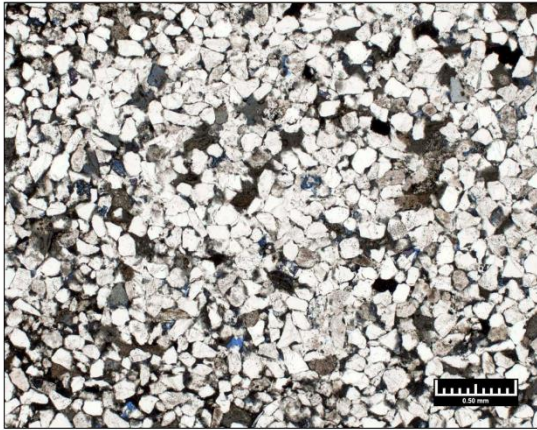
Plate 4A
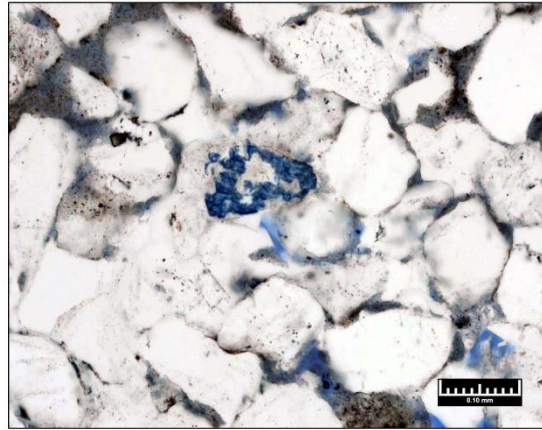
Plate 4B

Plate
40A
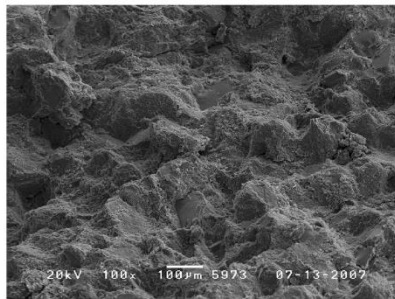
Plate
40B
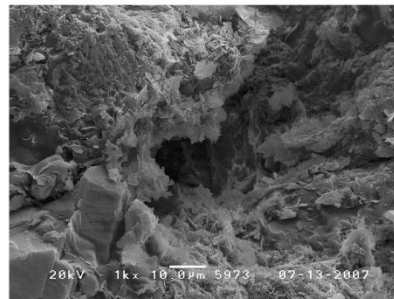
Plate
40C
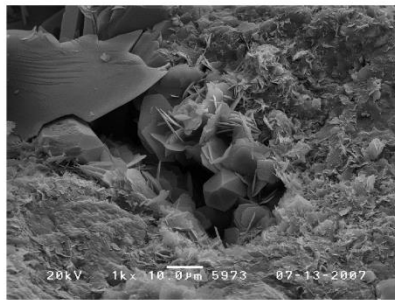
Plate
40D
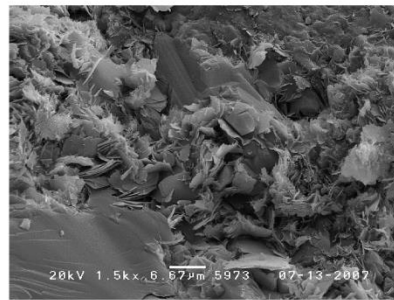
SAMPLE DEPTH: 5976.15 ft
SAMPLE NUMBER: 4-4

Measured Porosity*: 6.0%
Measured Permeability (air)*: 0.077mD
(*Net Confining Stress: 800 psi)
Grain Density: 2.65gm/cc

PLATE 7A
General view is of a medium-grained, moderately well sorted sandstone with relatively common secondary intragranular pores and remnants of primary intergranular pores. Argillaceous mudrock grains are common.
Magnification: 40X
Light: Plane Polarized

PLATE 7B
Detailed view shows remnants of primary intergranular pores partially infilled with quartz overgrowth cement.
Magnification: 200X
Light: Plane Polarized

PLATE 43
This medium-grained sandstone is moderately well sorted. Quartz (Plate A and Plate B) is the primary detrital grain type and the sample is classified as a sublitharenite. Chlorite clays (Plate B, Plate C, and Plate D) occur as grain-coating and pore-filling material. Quartz overgrowth cement (Plate B, Plate C, and Plate D) is common and can surround chlorite clays (Plate B, Plate C, and Plate D). Secondary intragranular pores associated with partially dissolved grains (Plate A) are the primary pore type in this sandstone. Primary intergranular pores (Plates A-D) are present in minor amounts.
Magnification: 43A - 70X
Magnification: 43B - 700X
Magnification: 43C - 1000X
Magnification: 43D - 1500X
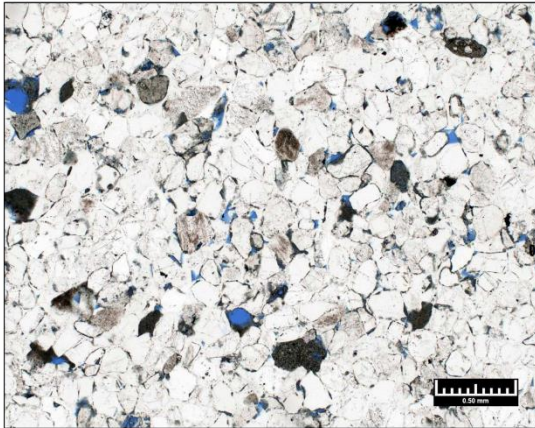
Plate 7A
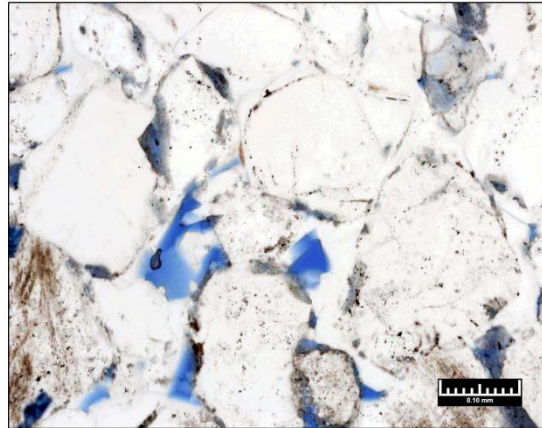
Plate 7B

Plate 43A
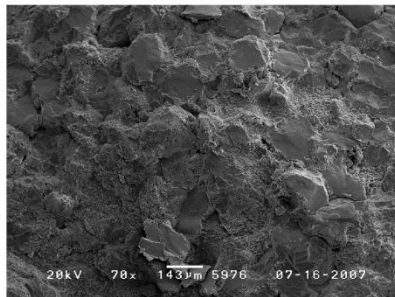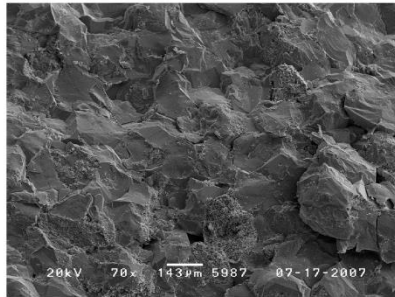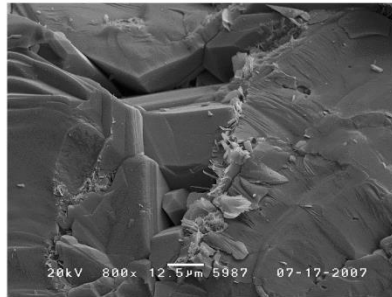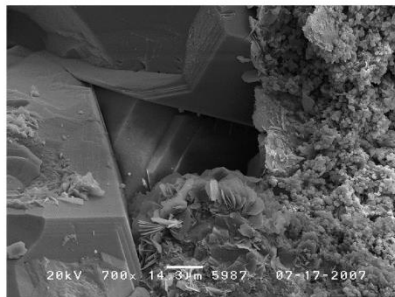
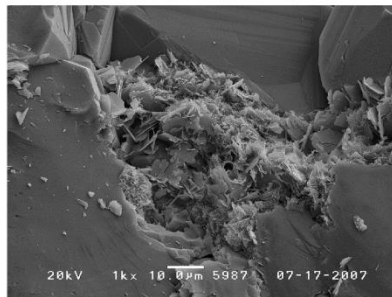

Plate 43B
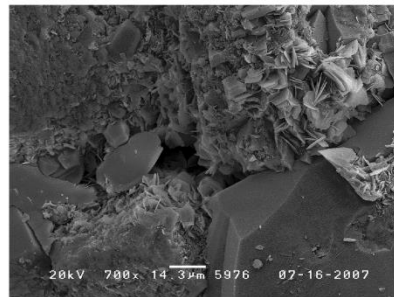
Plate 43C

Plate 43D

SAMPLE DEPTH: 5980.80 ft
SAMPLE NUMBER: 5-2

Measured Porosity*: 5.6%
Measured Permeability (air)*: 0.0089mD
(*Net Confining Stress: 800 psi)
Grain Density: 2.65gm/cc

PLATE 11A
General view is of medium-grained, moderately well sorted sandstone with a majority of
porosity being secondary intragranular pores. Only remnants of primary intergranular pores are
preserved due to extensive quartz overgrowth cements. Pockets of high detrital clay are probably
associated with burrows.
Magnification; 40X
Light: Plane Polarized

PLATE 11B
Detailed view shows remnants of intergranular pores and abundant quartz overgrowth cement
that fills or partially fills the intergranular pores. Compressed organic and pyrite rich detrital
clays infill pores. Fe-dolomite is replacing a grain. A large secondary intragranular pore is lined
with authigenic chlorite clays.
Magnification: 200X
Light: Plane Polarized

PLATE 47
Detrital grains in this moderately well sorted sandstone have an average size of 0.26 mm
(medium-grained sand). Quartz (Plate A, Plate C, and Plate D) is the primary grain type with
lesser lithic fragments (Plate A and Plate B) and feldspar (Plate B). The sample is classified as a
sublitharenite. Abundant coalescing quartz overgrowth cement (Plates A-D) reduces
intergranular pore volume. There is a minor amount of pore-filling chlorite clay (Plate B, Plate
C, and Plate D) that can locally inhibit the development of overgrowth cement. Pore types
consist of secondary intergranular pores (Plate A) associated with partially dissolved grains and
primary intergranular pores (Plate 8).
Magnification: 47A-100X
Magnification: 478 - 700X
Magnification: 47C - 1000X
Magnification: 47D -1500X
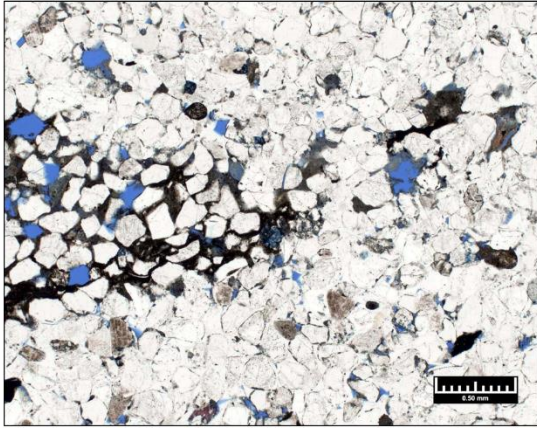
Plate 11A
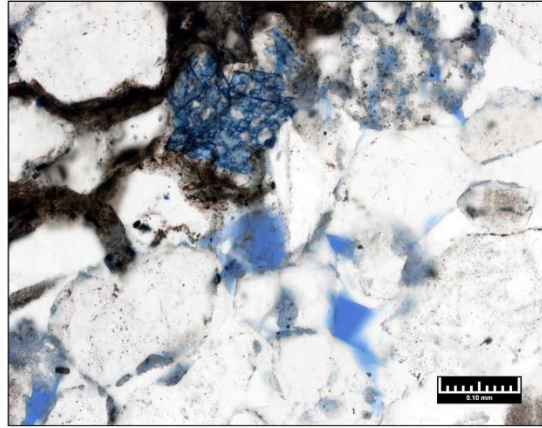
Plate 11B

Plate
47A
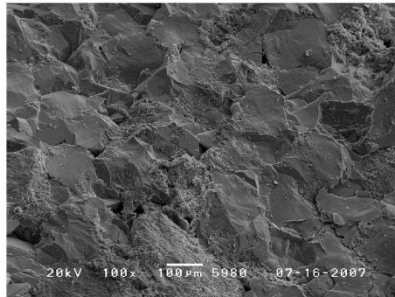
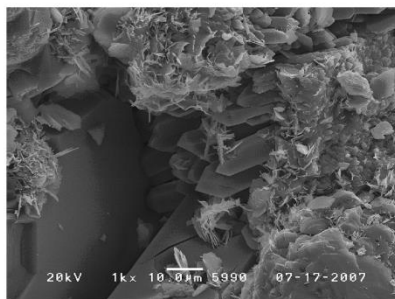

Plate
47B
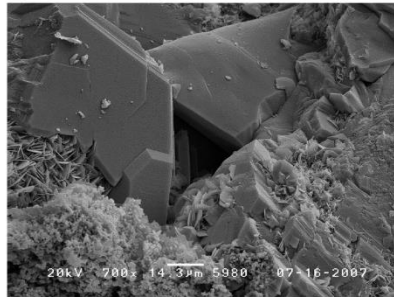
Plate
47C

Plate
47D

SAMPLE DEPTH: 5987.25 ft
SAMPLE NUMBER: 5-9

Measured Porosity*: 3.8%
Measured Permeability (air)*: 0.0075mD
(*Net Confining Stress: 800 psi)
Grain Density: 2.65gm/cc

PLATE 18A
General view is of a fine-grained, well sorted sandstone with a majority of porosity being secondary intergranular pores. Fe-rich dolomite is replacing grains and infilling pores. Only remnants of intergranular pores remain within pores partially infilled by quartz overgrowth cement.
Magnification: 40X
Light: Plane Polarized

PLATE 18B
In this detailed field of view the majority of porosity consists of remnants of primary intergranular pores. Quartz overgrowth cement is the most common cement. Fe-rich dolomite is replacing grains and infilling pores in some areas.
Magnification: 200X
Light: Plane Polarized

PLATE 54
Detrital grains in this moderately well sorted sandstone have an average size of 0.23 mm (fine sand). The sample is classified as a sublitharenite with quartz (Plates A-D) being the primary detrital grain type. Feldspar grains are partially replaced by chlorite (Plate C). Lithic fragment types include microporous chert fragments (Plate C). Compacted argillaceous rock fragments create pore-filling pseudomatrix (Plate D). Grain-coating clays are composed of intermixed illitic and chloritic clays (Plate B and Plate C). Quartz overgrowth cement (Plate C and Plate D) is abundant. Primary intergranular pores (Plate A and Plate C) are the dominant pore type.
Magnification: 54A - 70X
Magnification: 548 - 800X
Magnification: 54C - 700X
Magnification: 54D - 1000X
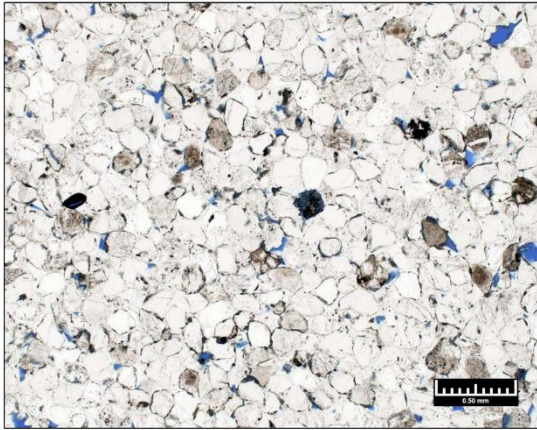
Plate 18A
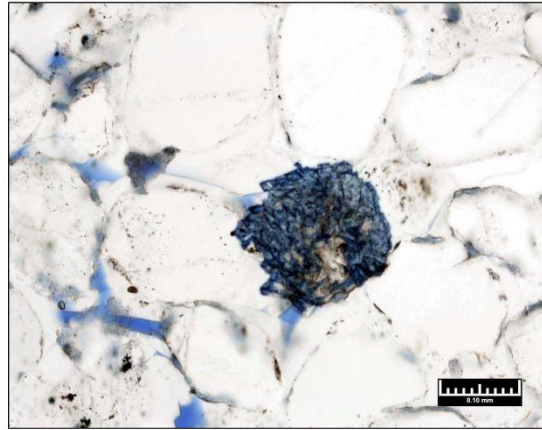
Plate 18B

Plate
54A

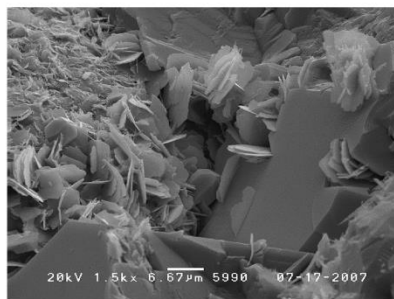
Plate
54B

Plate
54C

Plate
54D

SAMPLE DEPTH: 5990.60 ft
SAMPLE NUMBER: 5-12

Measured Porosity*: 6.9%
Measured Permeability (air)*: 0.046mD
(*Net Confining Stress: 800 psi)
Grain Density: 2.65gm/cc

PLATE 21A
General view shows multiple stylolites through a portion of this fine-grained, moderately
well sorted sandstone. Clays, micas, organics and other opaque material are concentrated along
the dissolution surfaces. Largest pores present are secondary intragranular pores. Some grains are
replaced by clays which are associated with microporosity. A slate fragment is present. Fe-rich
cement is replacing some grains. Fe-rich calcite is replacing a grain.
Magnification: 40X
Light: Plane Polarized

PLATE 21B
Detailed view of the crenulated stylolite surfaces shows opaques, clay, mica flakes, and organics
are concentrated along the dissolution surfaces. Also present along the stylolites are partially
dissolved lithic fragments and Fe-dolomite cements. Intergranular (possible secondary) pores are
present. Quartz overgrowth cement is common.
Magnification: 200X
Light: Plane Polarized

PLATE 57
Detrital grain types include abundant quartz (Plate A and Plate B) with common lithic fragments
(Plate A and Plate D) and feldspar (Plate A). There is a minor amount of intermixed chlorite and
illite clays bridging pore throats (Plate B) and coating grains (Plate C). Chlorite also occurs as
grain-replacing material (Plate B and Plate D). Quartz overgrowths (Plate B, Plate C, and Plate
D) reduce intergranular pore volume. Pore types include primary intergranular pores (Plate A),
secondary intragranular pores (Plate A) and micropores associated with clays.
Magnification: 57A - 70X
Magnification: 57B - 1000X
Magnification: 57C - 1000X
Magnification: 57D - 1500X
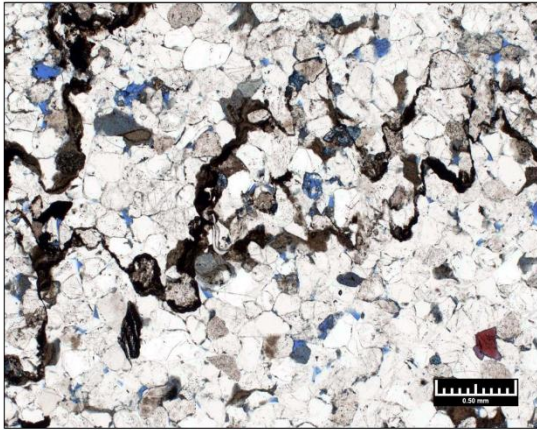
Plate 21A
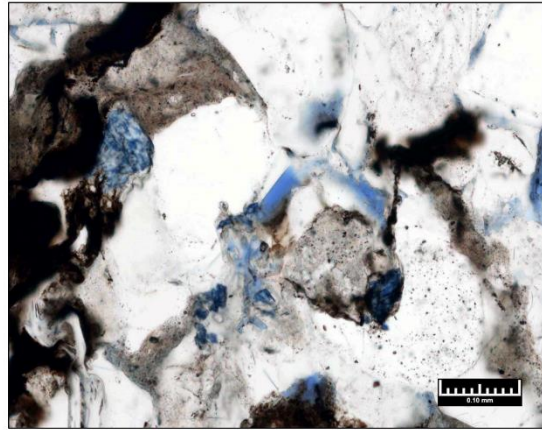
Plate 21B

Plate
57A
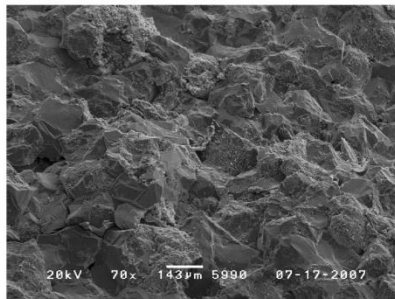
Plate
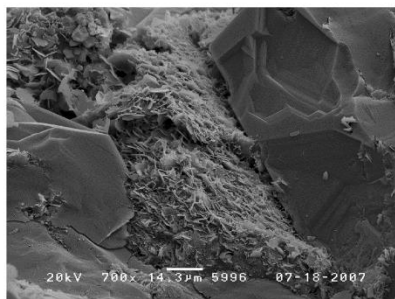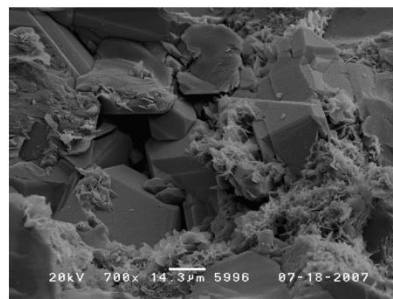57B
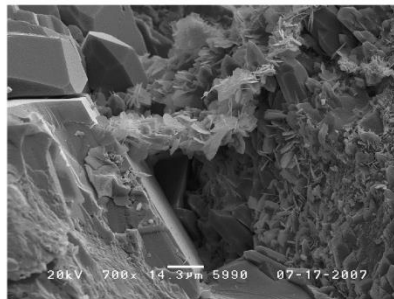
Plate
57C

Plate
57D

SAMPLE DEPTH: 5996.80 ft
SAMPLE NUMBER: 5-18

Measured Porosity*: 5.3%
Measured Permeability (air)*: 0.026mD
(*Net Confining Stress: 800 psi)
Grain Density: 2.65gm/cc

PLATE 27A
General view is of a medium-grained, moderately well sorted sandstone with a majority of the porosity being secondary intragranular pores (3% by volume based on modal analysis). Remnants of primary intergranular pores are isolated by pervasive quartz overgrowth cement. Some grains are replaced by clays which are associated with microporosity. Contorted mud lamination is apparent burrow lining.
Magnification: 40X
Light: Plane Polarized

PLATE 27B
Detailed view shows large pore, probably resulting from the complete dissolution of a framework grain. It is isolated from adjoining pores by infilling of pore throats with quartz overgrowth cement. Microporosity is present within clay rim (possibly chlorite) lining quartz grains. Quartz overgrowth cement makes up 18% of the total volume of this sample based on modal analysis.
Magnification: 200X
Light: Plane Polarized

PLATE 63
Detrital grains in this moderately well sorted sandstone have an average size of 0.26 mm (medium sand). The sample is classified as a sublitharenite with detrital grains consisting predominantly of quartz (Plate A and Plate C) with lesser amounts of lithic fragments (Plate A) and feldspar (Plate A and Plate C). Grains are coated with intermixed chlorite and illite clays (Plate B and Plate C). Quartz overgrowth cement (Plate B, Plate C, and Plate D) reduces pore volume. The presence of the clay inhibits the development of overgrowths (Plate B and Plate D). Effective pore types include primary intergranular pores (Plate D) and secondary intragranular pores (Plate A and Plate B).
Magnification: 63A - 100X
Magnification: 63B - 700X
Magnification: 63C - 700X
Magnification: 63D - 700X
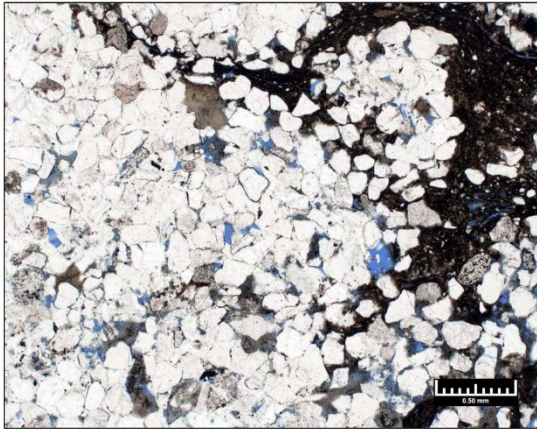
Plate 27A
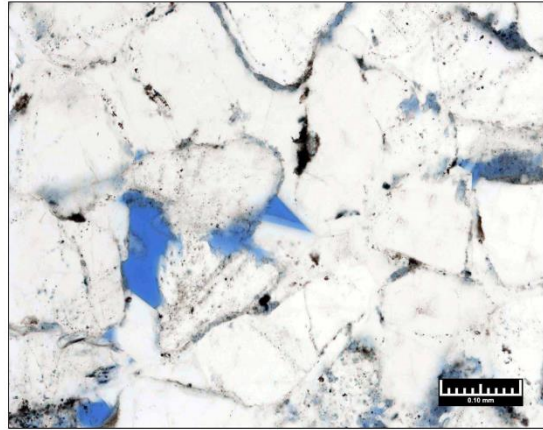
Plate 27B

Plate
63A
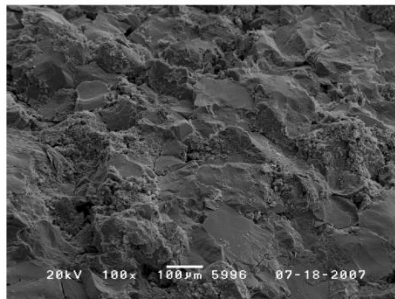
Plate
63B
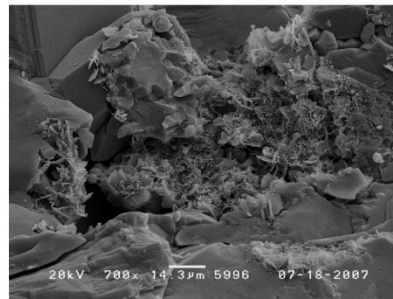
Plate
63C

Plate
63D

SAMPLE DEPTH: 5999.40 ft
SAMPLE NUMBER: 5-21

Measured Porosity*: 6.1%
Measured Permeability (air)*: 0.030mD
(*Net Confining Stress: 800 psi)
Grain Density: 2.66gm/cc

PLATE 30A
General view is of a fine-grained, moderately sorted sandstone with a majority of
porosity being secondary intragranular pores (3% by volume based on modal analysis).
Remnants of primary intergranular pores are isolated by pervasive quartz overgrowth cement
(9% by volume). Some grains are replaced by clays which are associated with microporosity.
Numerous labile grains or grains replaced by clays are compressed to form pseudomatrx.
Magnification: 40X
Light: Plane Polarized

PLATE 30B
Detailed view shows porosity consisting of both secondary intragranular macroporosity within
partially leached feldspar and primary intergranular. A majority of these pores are isolated due to
quartz overgrowth occluding pore throats.
Magnification: 200X
Light: Plane Polarized

PLATE 66
Detrital grains in this moderately sorted sandstone have an average size of 0.20 mm (fine sand).
The sample is classified as a litharenite and detrital grains consist predominantly of quartz
(Plates A-D) with lesser lithic fragments (Plate A and Plate C) and feldspar (Plate B and Plate
C). There is a moderate amount of grain-coating chlorite (Plate B and Plate C). Chlorite also
occurs as grain-replacing material (Plate C). Intermixed chlorite and illite clays bridge pore-
throats (Plate C). Quartz overgrowth cement (Plate B, Plate C, and Plate D) occludes
intergranular pores. Secondary intragranular pores (Plate A and Plate B) associated with partially
dissolved grains are the dominant pore type. Primary intergranular pores (Plate C) are present in
minor amounts due to the abundance of quartz overgrowth cement.
Magnification: 66A - 70X
Magnification: 66B - 500X
Magnification: 66C - 500X
Magnification: 66D - 1500X
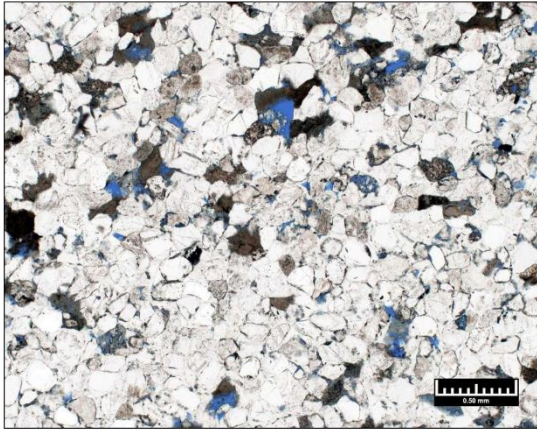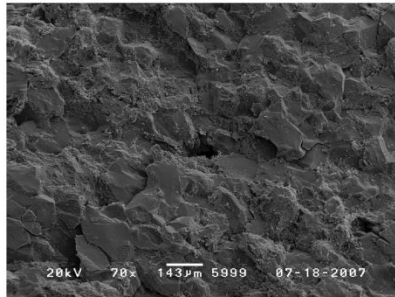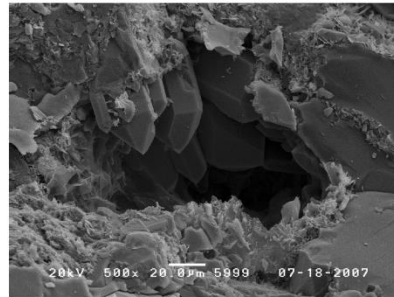
Plate 30A
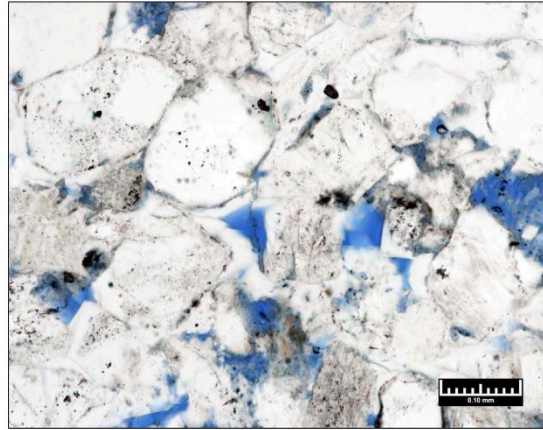
Plate 30B
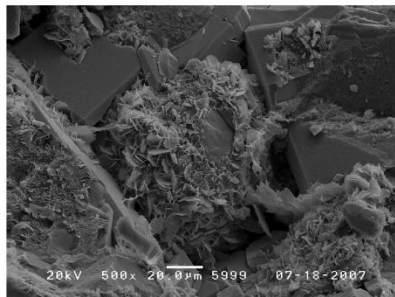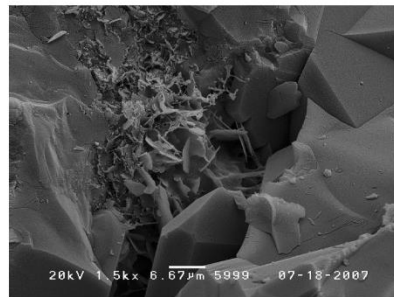
Plate
66A

Plate
66B

Plate
66C

Plate
66D

SAMPLE DEPTH: 6002.65 ft
SAMPLE NUMBER: 5-24

Measured Porosity*: 5.1%
Measured Permeability (air)*: 0.0095mD
(*Net Confining Stress: 800 psi)
Grain Density: 2.65gm/cc

PLATE 33A
General view is of a medium-grained, moderately well sorted sandstone with a majority of
porosity being secondary intragranular pores (3% by volume based on modal analysis). Some
grains are replaced by clays which are associated with microporosity. The majority of cement is
quartz overgrowth cement (20% by volume). Pyrite within pseudomatrix and replacing some
grains makes up 1% of the sample volume.
Magnification: 40X
Light: Plane Polarized

PLATE 33B
Detailed view shows secondary pore with remnants of grain and clay replacement within the
pore. Quartz overgrowth cement is partially infilling this pore and blocking pore throats. Fe-
dolomite is replacing part of a lithic fragment. Clay replaces some grains.
Magnification: 200X
Light: Plane Polarized

PLATE 69
Detrital grains in this moderately well sorted sandstone have an average size of 0.27 mm
(medium sand). The sample is classified as a sublitharenite. Detrital grains consist predominantly
of quartz (Plate A, Plate B, and Plate C) with lesser lithic fragments (Plate A) and feldspar (Plate
B and Plate C). Compacted argillaceous rock fragments (Plate B) form pore-filling
pseudomatrix. Chlorite coats the surface of detrital grains (Plate C and Plate D) Micropores
associated with the clays are likely to contain irreducible water. Quartz overgrowth cement (Plate
B, Plate C, and Plate D) reduces intergranular pore volume. Secondary intragranular pores
associated with partially dissolved grains (Plate A) are the dominant pore type.
Magnification: 69A - 70X
Magnification: 69B - 700X
Magnification: 69C - 800X
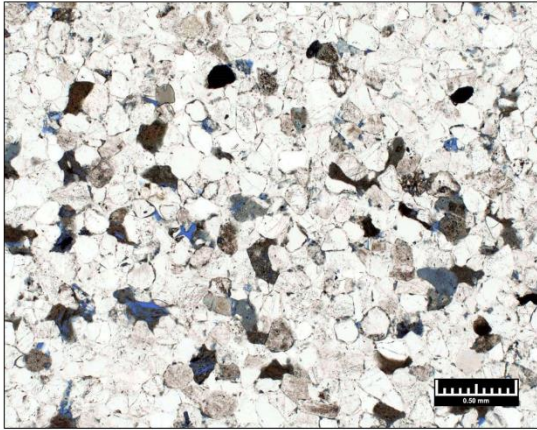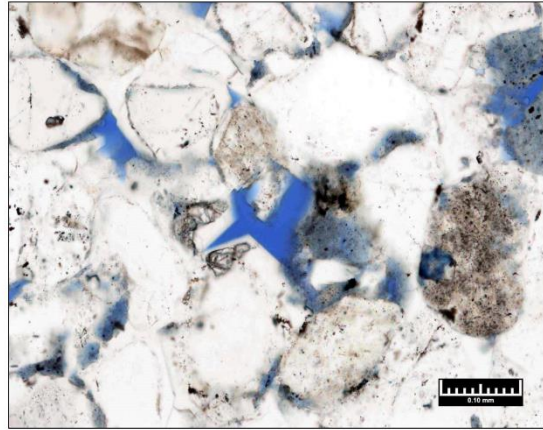Magnification: 69D - 1000X
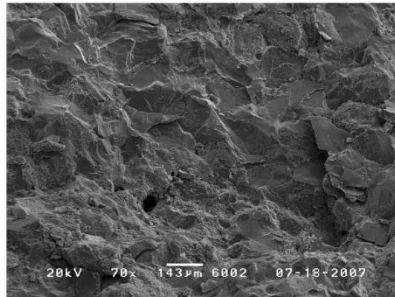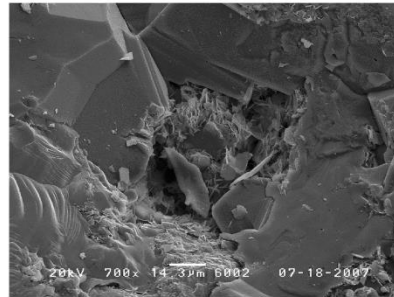
Plate 33A

Plate 33B

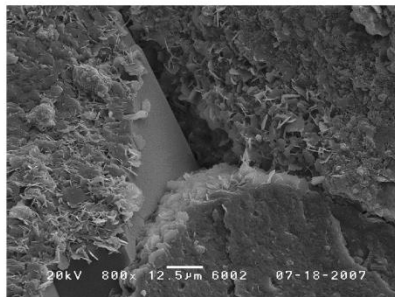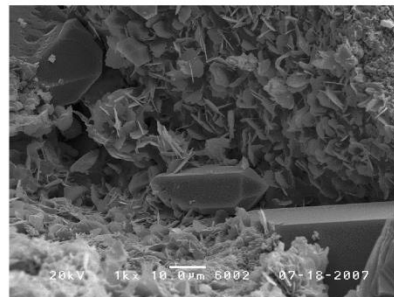Plate
69A

Plate
69B

Plate
69C

Plate
69D

SAMPLE DEPTH: 6005.00 ft
SAMPLE NUMBER: 6-1

Measured Porosity*: 6.2%
Measured Permeability (air)*: 0.051mD
(*Net Confining Stress: 800 psi)
Grain Density: 2.66gm/cc

PLATE 36A
General view is of fine-grained, moderately well sorted sandstone with a majority of porosity
being secondary intragranular pores. Some grains are replaced by clays which are associated
with microporosity. The majority of cement is quartz overgrowth cement but some small patches
of Fe-dolomite are present within intragranular pores. Pseudomatrix and residual clays are at the
base of the photomicrograph.
Magnification: 40X
Light: Plane Polarized

PLATE 36B
In this detailed view, one secondary intragranular pore contains Fe-dolomite cement. Secondary
intragranular pores make up the most abundant porosity type in this sample and accounts for 4%
by volume of the sample based on modal analysis. Quartz overgrowth cement accounts for 18%
of the total sample volume and separates the remnant primary, intergranular pores. Lithic
mudstone grain or clast present is compressed to form pseudomatrix.
Magnification: 200X
Light: Plane Polarized

PLATE 72
Quartz (Plate A, Plate B, and Plate D) is the primary detrital grain type in this sandstone. Lithic
fragments (Plate A) and feldspar (Plate A, Plate B, and Plate C) are present in lesser amounts and
the sample is classified as a sublitharenite. Detrital grains have an average size of 0.23 mm (fine
sand) and are moderately well sorted. Chlorite clay occurs as grain-replacing material (Plate D).
Pore-filling quartz overgrowth cement is abundant. Secondary intragranular pores associated
with partially dissolved grains (Plate A and Plate D) are the dominant grain type.
Magnification: 72A - 100X
Magnification: 72B - 800X
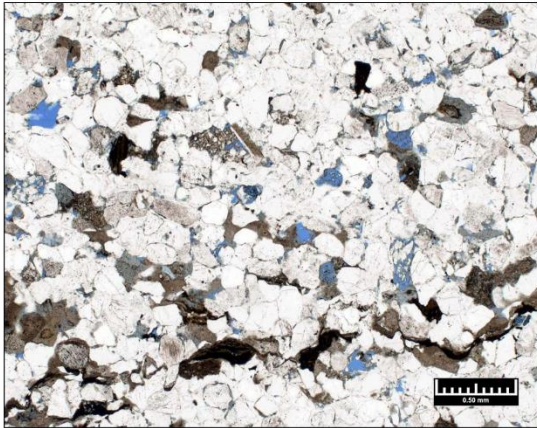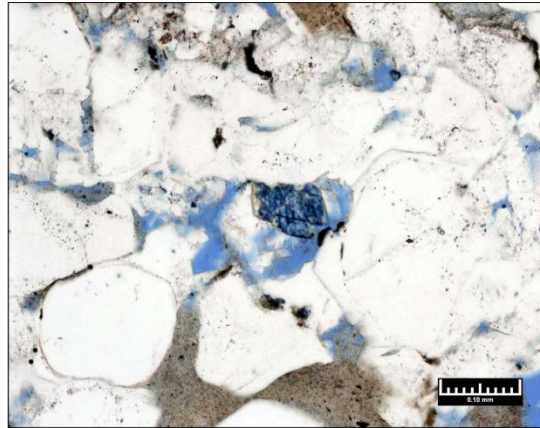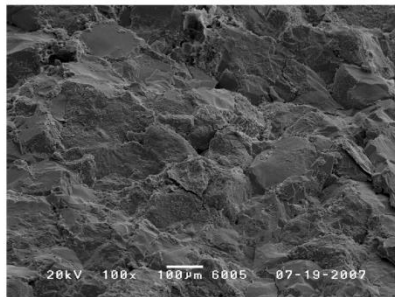Magnification: 72C - 1000X
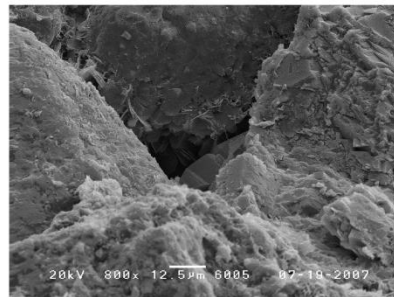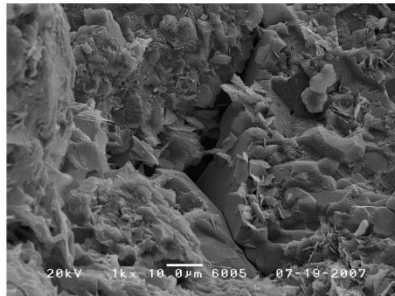Magnification: 72D - 1500X

Plate 36A

Plate 36B

Plate
72A

Plate
72B

Plate
72C

Plate
72D